DESIGN AND DEVELOPMENT OF OUT-OF-PILE VERSION OF INSTRUMENTED CAPSULE FOR ONLINE DETERMINATION OF UNIAXIAL CREEP BEHAVIOR IN STRUCTURAL SPECIMEN

By

SADU VENKATESU

(ENGG02201004006)

INDIRA GANDHI CENTRE FOR ATOMIC RESEARCH, KALPAKKAM

A thesis submitted to the

Board of Studies in Engineering Sciences

In partial fulfilment of requirements

For the Degree of

DOCTOR OF PHILOSOPHY

of

HOMI BHABHA NATIONAL INSTITUTE

MARCH, 2016

Homi Bhabha National Institute

Recommendations of the Viva Voce Committee

As members of the Viva Voce Committee, we certify that we have read the dissertation prepared by **Sadu Venkatesu** entitled "**Design and Development of Out-of-pile version of Instrumented Capsule for Online Determination of Uniaxial Creep behavior in Structural Specimen**" and recommend that it may be accepted as fulfilling the thesis requirement for the award of Degree of Doctor of Philosophy.

Chairman – Dr. K. Velusamy		**Date:** 26/8/2016
Guide / Convener – Dr. S. Venugopal		**Date:** 26/8/16
Examiner – Prof. Satish Vasu Kailas		**Date:** 26/08/16
Member 1 – Dr. Saroja Saibaba		**Date:** 26/08/2016
Member 2- Dr. S. Murugan		**Date:** 26/08/2016

Final approval and acceptance of this thesis is contingent upon the candidate's submission of the final copies of the thesis to HBNI.

I hereby certify that I have read this thesis prepared under my direction and recommend that it may be accepted as fulfilling the thesis requirement.

Date: 26/08/16

Place: Kalpakkam

Dr. S. Venugopal
(Guide)

STATEMENT BY AUTHOR

This dissertation has been submitted in partial fulfillment of requirements for an advanced degree at Homi Bhabha National Institute (HBNI) and is deposited in the library to be made available to borrowers under rules of the HBNI.

Brief quotations from this dissertation are allowable without special permission, provided that accurate acknowledgement of source is made. Requests for permission for extended quotation from or reproduction of this manuscript in whole or in part may be granted by the Competent Authority of HBNI when in his or her judgment the proposed use of the material is in the interests of scholarship. In all other instances, however, permission must be obtained from the author.

(Sadu Venkatesu)

DECLARATION

I, hereby declare that the investigation presented in this thesis has been carried out by me. The work is original and has not been submitted earlier as a whole or in part for a degree /diploma at this or any other Institution/ University.

(Sadu Venkatesu)

List of Publications arising from the Thesis

Journals

1) "Determination of Temperature of Structural Material Specimens in an Irradiation Capsule by Analytical and Simulation Techniques", **Sadu Venkatesu**, S.Murugan and S.Venugopal, Springer Transactions of the Indian Institute of Metals, **2016,** *DOI 10.1007/s12666-015-0610-0.*

2) "Development of out-of-pile version of instrumented irradiation capsule for determination of online creep deformation", **Sadu Venkatesu**, Rajesh Saxena, M. Muthuganesh, P. K. Chaurasia, S. Murugan and S. Venugopal, Springer Transactions of the Indian Institute of Metals, Vol.69 (2), 283-287, **2016,** *DOI: 10.1007/s12666-015-0808-1.*

3) "Development of High-temperature Nicrobrazed joints using Induction Heating in an Argon gas Environment", **Sadu Venkatesu**, P.K.Chaurasia, S.Murugan and S.Venugopal, Springer Transactions of the Indian Institute of Metals, **2015,** *DOI 10.1007/s12666-015-0696-4*.

To Be Communicated

4) "A Comparative Study of Pulsed laser, GTAW and High Temperature nicrobrazing Processes on Microstructural and Mechanical Properties of AISI type 316 L Stainless Steel", **Sadu Venkatesu**, Rajesh Saxena, R. Ravikumar, P. K. Chaurasia, S. Murugan and S. Venugopal, **(Manuscript under review).**

5) "Comparison of Instrumented Irradiation Capsule Out-of-pile Test Results with Available Literature Results of Uniaxial Creep behavior in Structural Specimen" **Sadu Venkatesu**, Rajesh Saxena, M. Muthuganesh, P. K. Chaurasia, S. Murugan and S. Venugopal, **(Manuscript under review).**

- **Conference Presentations:**

1) "Development of out-of-pile version of instrumented irradiation capsule for determination of online creep deformation", **Sadu Venkatesu**, Rajesh Saxena, M. Muthuganesh, P. K. Chaurasia, S. Murugan and S. Venugopal, Presented in Creep - Fatigue 7 (CF-7 International conference) at IGCAR Kalpakkam, Jan 19-22, **2016**.

2) "Development of High-Temperature brazed joints and its Compatibility test with High Temperature Sodium", P.K. Chaurasia, K. Chandran, **Sadu Venkatesu**, S. Murugan, S. Anthonysamy, S. Venugopal and T. Jayakumar, Presented in National Welding Seminar at Jamshedpur , Jan 22- 24, **2015**.

3) "Design and Analysis of Instrumented Irradiation Capsule for Online Determination of Uniaxial Creep behavior in Structural specimen", **Sadu Venkatesu**, K.A. Gopal, M. Muthuganesh, R. Saxena, S. Murugan, S. Venugopal and T. Jayakumar, Presented in International Symposium for Research Scholars at IIT Madras, Dec 11-13, **2014**.

4) "Development of High-temperature Nicrobrazed joints using Induction Heating in an Argon gas Environment", **Sadu Venkatesu**, P. K.Chaurasia, S.Murugan, S.Venugopal and T. Jayakumar, Presented in National Weld Meet at Mohammed Satak College of Engineering, Keelankarai, Sep 02-03, **2014**.

5) "Determination of Temperature of Structural Material Specimens in an Irradiation Capsule", **Sadu.Venkatesu**, S. Murugan and S.Venugopal, Presented in 5th International Symposium for Research Scholars at IIT Madras, Dec 13-15, **2012.**

S. Venkatesu

(SaduVenkatesu)

DEDICATED TO

MY **PARENTS**

Shri. Subbaiah and Smt. Varalakshmi

ACKNOWLEDGMENT

This research work could not have been realized without the support of many people. At the outset, I am very much indebted to Department of Atomic Energy, Government of India for providing the prestigious PhD fellowship to carry out the work at the Indira Gandhi Centre for Atomic Research (IGCAR), Kalpakkam, India in association with the Homi Bhabha National Institute (HBNI), Mumbai, India.

I express my sincere indebtedness to my guide ***Dr. S. Venugopal***, Senior Professor/ Former Director, Metallurgy and Materials Group for his guidance, valuable suggestions and encouragement during the research work.

I am thankful to ***Dr. S. Murugan*** (Head, RIRD) for being my advisor. His well-built opinions, questions, and suggestions have significantly improved my work at every stage.

I am grateful to my other doctoral committee members – ***Dr. K. Velusamy*** (Chairman), Head, MHD, Dr. Saroja Siababa (Member), Head, MTPD and Dr. S. Murugan (Member), Head, RIRD for their valuable suggestions, reviewing the work progress and proof reading the synopsis. I am thankful to ***Dr. G. Sasikala***, Dean, Academic, Engineering Sciences, IGCAR for valuable guidelines in the completion of thesis work.

I express my gratitude towards ***Dr. S.A.V Satyamurty*** (Director, IGCAR) and former Directors, IGCAR Dr. Baldev Raj, Sri S.C. Chetal and Dr. P.R. Vasudeva Rao for their support to the research scholars. I am thankful to Dr. T. Jayakumar (former Director, MMG, IGCAR), for introducing and motivating me to take up the research topic.

I would like to thank ***Sri. K.A. Gopal*** (former Scientific Officer-F, IDEAS/MMG) and ***Sri. P.K. Chaurasia*** (Programme Leader, IDEAS/MMG) for motivation and support.

I am thankful to ***Dr. M. Sai Baba*** (Associate Director, RMG) for all his support and encouragement during the tenure.

I would like to thank Sri. M. Muthuganesh, Sri. R. Ravikumar, Sri. M.S. Rao, Sri. Mahendra Prabhu, Sri. Rajesh Saxena, Sri. R. Ramesh and other colleagues of IDEAS for their valuable support.

I appreciate the timely help of Mr. Palani and Mr. Kalaichelvan.

I would like to thank Sri. Saji jacob (RIRD), Sri. Praveen (EIG) and Sri. Arun (EIG) for their valuable support.

I am grateful to my father Sri. Subbaiah and mother Smt. Varalakshmi for their moral support and numerous blessings.

I am thankful to my friends, Mahendra, Srihari, Sowmya, Yadagiri, Kalyan, Deepak, Dhanashekaran, Shashwat, Ramana, Prasanna, Masilamani, Aditya, Chandan, Veerendra, Vikas, Nagendra, Jagapathi and Balaji for making my stay wonderful.

(Sadu Venkatesu)

Table of Contents

SYNOPSIS.....**i**

LIST OF FIGURES.....**v**

LIST OF TABLES……..……**viii**

CHAPTER - 1 INTRODUCTION..... **1**

1.1 INTRODUCTION TO NUCLEAR REACTORS 1

1.1.1 THERMAL REACTORS……2

1.1.2 FAST REACTORS.....2

1.2 INTRODUCTION TO THE FAST REACTOR DEVELOPMENTS IN INDIA..... 3

1.2.1 FAST BREEDER TEST REACTOR (FBTR).....3

1.2.2 PROTOTYPE FAST BREEDER REACTOR (PFBR).....5

1.3 FBTR AS AN IRRADIATION FACILITY 6

1.4 EFFECT OF RADIATION ON MATERIALS 7

1.5 INTRODUCTION TO THE CREEP..... 7

1.6 INTRODUCTION TO IRRADIATION CAPSULES..... 9

1.7 OBJECTIVE OF THE PRESENT WORK..... 10

1.8 OVERVIEW OF THE THESIS..... 11

Summary.....15

CHAPTER-2 LITERATURE REVIEW 16

2.1 INTRODUCTION 16

2.2 BELGIUM (IN-PILE TENSILE TESTING IN BR2) 16

2.3 FRANCE (IMPROVEMENT OF LVDT DEVELOPED BY IFE-HRP)..... 18

2.4 NORWAY (IFE-HRP).....20

2.5 JAPAN (JMTR)..... 21

2.6 NETHERLANDS (HFR)..... 23

2.7 KOREA (KAERI) 23

2.8 DEVELOPMENT OF INSTRUMENTED CREEP TEST RIG IN IDAHO NATIONAL LABORATORY 24

2.9 OAK RIDGE NATIONAL LABORATORY (ORNL) 27

2.10 OVERVIEW OF LITERATURE REVIEW AND OBJECTIVE OF THE PRESENT WORK 30

Summary 32

CHAPTER - 3 HEAT TRANSFER ANALYSIS OF AN IRRADIATION CAPSULE 33

3.1 INTRODUCTION 33

3.2 DETAILS OF IRRADIATION CAPSULE AND CALCULATION METHODOLOGY 34

3.3 METHODOLOGY 36

3.3.1 TEMPERATURE DISTRIBUTION USING ANALYTICAL METHOD (ITERATIVE TECHNIQUE) 36

3.3.2 TEMPERATURE DISTRIBUTION DETERMINED BY COMPUTER CODE COMSOL 41

3.4 RESULTS AND DISCUSSION 44

Summary 49

CHAPTER - 4 ESTABLISHMENT OF HIGH TEMPERATURE NICROBRAZING PROCEDURE UNDER ARGON GAS ENVIRONMENT AND QUALIFICATION OF BRAZED JOINTS 50

4.1 INTRODUCTION 50

4.2 DEVELOPMENT OF JOINTS BY BRAZING METHOD 52

4.3 ELEMENTS OF THE BRAZING PROCESS 53

4.3.1 FILLER-METAL FLOW 54

4.3.2 BASE-METAL CHARACTERISTICS 54

4.3.3 FILLER-METAL CHARACTERISTICS 55

4.3.4 BRAZING TEMPERATURE 55

4.3.5 LARGE-SCALE MECHANICAL PROPERTIES 56

4.3.6 THE PLACEMENT 56

4.3.7 SURFACE PREPARATION 56

4.3.8 JOINT DESIGN AND CLEARANCE 57

4.3.9 HEAT SOURCES FOR BRAZING 59
4.4 AVAILABLE FORMS OF BRAZE FILLER METALS 60
4.5 LOW AND HIGH ENERGY TEMPERATURE BRAZING 61
4.6 INDUCTION HEATING USED IN HIGH TEMPERATURE BRAZING 62
4.6.1 PROTECTIVE ATMOSPHERES 63
4.7 EXPERIMENTAL DETAILS 63
4.8 QUALIFICATION OF NICROBRAZED JOINTS 67
4.8.1 HELIUM LEAK TEST 68
4.8.2 METALLOGRAPHIC ANALYSIS 68
4.8.3 MICRO HARDNESS TEST 69
4.8.4 EFFECT OF BRAZING TEMPERATURE ON EMF OF THERMOCOUPLE 70
4.8.5 SODIUM COMPATIBILITY TEST 70
4.9 COMPARATIVE STUDY ON JOINTS DEVELOPED BY HIGH TEMPERATURE NICROBRAZING, LASER AND GTAW JOINING PROCESSES 72
4.9.1 CHEMICAL COMPOSITION OF MATERIALS 73
4.9.2 HIGH TEMPERATURE NICROBRAZING 73
4.9.3 GAS TUNGSTEN ARC WELDING (GTAW) 75
4.9.4 PULSED ND: YAG LASER WELDING 78
4.9.5 RESULTS AND DISCUSSION 81
Summary 84
CHAPTER - 5 DESIGN AND DEVELOPMENT OF OUT-OF-PILE VERSION OF INSTRUMENTED CAPSULE FOR ONLINE DETERMINATION OF UNIAXIAL CREEP BEHAVIOR IN STRUCTURAL SPECIMEN 86
5.1 INTRODUCTION 86
5.2 SELECTION OF BELLOWS 87
5.2.1 SPECIFICATIONS OF BELLOWS 88
5.2.2 CHEMICAL COMPOSITION OF MATERIALS USED IN BELLOWS 89
5.2.3 TESTS PERFORMED ON BELLOWS AFTER FABRICATION 89

5.3 COMPONENTS OF INSTRUMENTED IRRADIATION CAPSULE.....90
5.3.1 DESIGN AND ASSEMBLY OF AN INSTRUMENTED CAPSULE.....92
5.3.2 STEPS IN ASSEMBLY OF AN INSTRUMENTED CAPSULE.....96
5.3.3 OUT-OF-PILE EXPERIMENTAL SET UP.....98
5.3.4 EXPERIMENTAL ANALYSIS.....99
5.4 OUT- OF- PILE EXPERIMENT FOR ONLINE DETERMINATION OF UNIAXIAL CREEP BEHAVIOR IN STRUCTURAL SPECIMEN.....101
5.4.1 MODIFICATIONS CARRIED OUT.....102
5.4.2 ASSEMBLY OF EXPERIMENTAL SET UP.....103
5.4.3 OUT-OF-PILE EXPERIMENT.....104
5.4.4 RESULTS AND DISCUSSION.....105
5.4.4.1 DETAILED ANALYSIS.....106
5.4.4.2 COMPARISON OF RESULTS.....112
Summary.....115
CHAPTER - 6 SUMMARY AND SUGGESTIONS FOR FUTURE WORK..... 117
References.....*122*

SYNOPSIS

1. Introduction

Irradiation affects the physical and mechanical properties of structural materials. Tensile strength, impact properties and creep strength are affected by radiation. Creep is the slow, time-dependent strain that occurs in a material under a constant stress (or load) at high temperature. The steady state creep rate is enhanced due to the presence of radiation. Irradiation creep is the additional strain that occurs as a result of the combined effect of irradiation and stress in the materials. The strain occurring in the absence of irradiation is generally called as thermal creep. Performance of fuel, cladding tubes, reactor pressure vessel, and other in-core components of nuclear reactors can be affected by the dimensional changes associated with creep. Hence, it becomes necessary to determine the amount of creep expected to be suffered by a component during its lifetime in a reactor. This will enable the designer to assess the useful life of the component in the reactor and design suitable components after taking irradiation creep into consideration. Irradiation capsules are designed to expose the structural materials specimens to the operating environment of a nuclear reactor in order to obtain data on the changes in properties due to radiation. Irradiation capsule is a device designed to carry out irradiation of any fuel, structural material, and shielding material specimens in a reactor.

2. Motivation

As discussed in the literature, several MTRs (for instance Belgian Reactor-2 [BR2], Belgium, OSIRIS reactor, France, Halden Boiling Water Reactor [HBWR], Norway, Japan Materials Testing Reactor [JMTR], Japan, High-Flux Advanced Neutron Application Reactor [HANARO], Korea have deployed creep test rigs to detect the growth of tensile and creep specimens using a bellows system to apply a variable load on the specimen and LVDTs to measure the growth of the specimen. The literature review reveals that there are worldwide developments of irradiation facilities in nuclear reactors to determine the various changes in the material properties by using irradiation vehicle/ capsules. It has been found that there are certain limitations in the irradiation capsules presently being used, and an attempt has been made to

design and develop an instrumented capsule for determining in-pile creep behaviour of materials overcoming these limitations.

1. In many of the instrumented capsules for in-reactor creep experiments, the loading of the specimen is done using pressurized gas supplied through a connecting tube from an external source outside the reactor. While this method is good for controlling the pressure of gas as desired, it is having a disadvantage of need to accommodate a long connecting line where space constraints are there. In the present design the connecting line is dispensed with. Instead, the irradiation capsule with bellows is filled with a pressurised gas and the capsule is sealed. At the irradiation temperature, the gas will exert the required load on the specimen.
2. The overall diameter of capsule has been reduced and kept as 22 mm in the present design to use it even in fast reactors where the core is compact and irradiation space available is limited. Most of the irradiation capsules found in literature have larger overall diameters.
3. The LVDT to be used in irradiation capsule should withstand high temperatures of the order of 400 to 500°C, and special high temperature LVDTs have been used by a few of the experimenters. High temperature LVDTs are scarcely available commercially and there are restrictions in procuring them. Hence in our study, LVDT with a working temperature of 200°C has been used and it is placed outside the high temperature zone of the capsule. The core of the LVDT has been connected to the specimen through a stiff ceramic rod to transfer the elongation of specimen to the core of LVDT. The irradiation capsule has been developed and tested successfully in furnace with the above mentioned modifications/ features.

3. Objective and scope of the work

The main aim of this research work is to develop an out-of-pile version of instrumented irradiation capsule for online determination of uniaxial creep behavior in structural specimen.
The work has been divided into different parts as given below:

1. Analysis of temperature of structural material specimens in an irradiation capsule surrounded by different compositions of mixtures of helium and argon during irradiation in a reactor.
2. Establishment of high temperature nicrobrazing procedure under argon gas atmosphere and qualification of brazed joints.
3. Comparison of high-temperature nicrobrazed joints with Gas tungsten arc welding and Laser weld joints to determine the relative merits and demerits.
4. Analysis and design of instrumented capsule for determination of uniaxial creep behaviour in structural specimen; fabrication of an out-of-pile version of instrumented capsule and testing in electrical furnace and validating the design concepts.

4. Structure of Thesis and description of the work

The thesis is structured as follows:

The first chapter begins with the general introduction. Chapter 2 describes the literature review on irradiation creep measurement techniques in in-pile and out-of-pile tests. This chapter includes the status of international developments on design and analysis of tests for irradiation creep measurements. The motivation drawn out of the literature review and scope of the present work are also discussed in this chapter.

In chapter 3, heat transfer analysis of an irradiation capsule by analytical and simulation techniques has been presented. The results have been compared with the results obtained through the use of computer code COMSOL.

In chapter 4, establishment of high temperature nicrobrazing procedure under argon gas atmosphere which is required in the fabrication of instrumented irradiation capsule is presented. High-temperature nicrobrazed joints under argon atmosphere have been produced as part of the research work. An induction heating and furnace heating techniques have been used for this development. Helium leak test, metallographic, micro hardness tests, and sodium compatibility test have been carried out on the brazed samples to qualify the joints. Optimization of the process parameters of available joining methods for tube to end plug configuration have been presented in this chapter. Helium leak test, metallographic and micro hardness tests have been carried out

on the joints made by laser, GTAW and high temperature nicrobrazing joining processes to measure and compare the merits and demerits of each joint.

In chapter 5, design and analysis of instrumented capsule for online determination of uniaxial creep behaviour in structural specimen has been presented. Fabrication of an out-of-pile version of instrumented capsule and testing of it in a vertical electrical furnace for validation of design concepts has been carried out. The overall diameter of this instrumented capsule is 22 mm and operative portion is 170 mm. The experiment has been carried out by using the set up arranged in the laboratory to perform the uniaxial creep experiments. The experiment has been carried out at three different stresses and temperatures (269 MPa at 450°C , 287 MPa at 500°C and 306 MPa at 550°C). Electric furnace temperature was set at 450°C in the specimen and at this temperature 269 MPa of stress would apply on the specimen. This condition has been kept constant for 200 hours to get the secondary creep data in the specimen. The same procedure has been followed for the remaining temperatures and stresses. The elongation of the tensile specimen due to deformation was measured by LVDT. The experimental results have been compared with those reported in literature and found to be matching.

In chapter 6, the important conclusions drawn from the results of the research work have been presented. This chapter also provides suggestions for future work to be carried out.

List of Figures

Figure 1-1 Flow Sheet of Fast Breeder Test Reactor 4

Figure 1-2 Core of FBTR 4

Figure 1-3 Flow Sheet of Prototype Fast Breeder Reactor 6

Figure 1-4 A typical creep curve 8

Figure 2-1 Tensile test rig for BR-2 irradiations 17

Figure 2-2 Principle of LVDT 18

Figure 2-3 Proposed sensor for detecting elongation and diameter changes in OSIRIS testing 19

Figure 2-4 Illustration of instrumented tensile specimen used in stress relaxation study. 20

Figure 2-5 Schematic diagram of irradiation creep capsule (94M-2A) under a high thermal neutron flux condition in JMTR 22

Figure 2-6 Creep test rig positioned in autoclave for testing 25

Figure 2-7 Representative test of specimen in elastic region 26

Figure 2-8 Schematics of bellows-loaded rabbit capsules for irradiation creep testing 28

Figure 2-9. A bellows-loaded tensile frame before and after in-furnace testing 29

Figure 3-1 (a) Schematic of an irradiation capsule that has five compartments (b) single compartment of the irradiation capsule filled with gas mixture around the specimen 34

Figure 3-2 Compartment of Irradiation capsule in 2D 35

Figure 3-3 Temperature of specimens by analytical method 41

Figure 3-4 Capsule design using simulation software 42

Figure 3-5 Insulated at top and bottom portions 43

Figure 3-6 Constant liquid sodium temperature at wall of capsule 43

Figure 3-7 Temperature of specimens by simulation software 44

Figure 3-8 Simulation results at Q = 1.5W/gm 45

Figure 3-9 Simulation results at Q = 1.8W/gm 46

Figure 3-10 Simulation results at Q = 2.0W/gm 47

Figure 3-11 Comparison of results at Q = 1.5 W/gm.....48

Figure 3-12 Comparison of results at Q = 1.8 W/gm.....48

Figure 3-13 Comparison of results at Q = 2.0 W/gm.....48

Figure 4-1 Principle of Brazing 52

Figure 4-2 Torch Brazing.....59

Figure 4-3 Induction Brazing.....59

Figure 4-4 Induction Heating System for Brazing Application 62

Figure 4-5 Drawing of the sample (as end plug) used for high-temperature brazing 64

Figure 4-6 (a) Photograph of the arrangement for the development of high-temperature brazed joints using induction heating in an argon gas environment, (b) Sketch.....65

Figure 4-7 One of the high-temperature brazed joint (sample).....68

Figure 4-8 Microstructure observed in metallurgical microscope. 69

Figure 4-9 Results of micro hardness test.....70

Figure 4-10 Schematic of parent metal geometry.....72

Figure 4-11 Arrangement for the development of high-temperature brazed joints using furnace heating in an argon gas environment.....74

Figure 4-12 GTAW setup arrangement 76

Figure 4-13 GTAW operation.....77

Figure 4-14 CNC Laser work stage 78

Figure 4-15 Samples of all the joining processes 81

Figure 4-16 Micro structures of weld joints at its centre 82

Figure 4-17 Micro structures of weld joints at higher magnification 83

Figure 4-18 Micro hardness values obtained by all the three joining processes.....84

Figure 5-1 Special bellow assembly 87

Figure 5-2 Schematic of instrumented irradiation capsule.....90

Figure 5-3 (a) Inner tubular part (b) Outer tubular part.. 91

Figure 5-4 Top specimen plug with EDM slot.....91

Figure 5-5 Outer top plug 91

Figure 5-6 (a) Tensile specimen (b) Ceramic tube..... 91

Figure 5-7 Out-of-pile version of instrumented capsule 93

Figure 5-8 Components of instrumented capsule. 97

Figure 5-9 (a) Schematic diagram (b) Out-of-pile experimental set up arrangement with capsule loaded in electric furnace 98

Figure 5-10 (a) Temperature and elongation of the specimen with time up to 130°C (b) Component of elongation..... 99

Figure 5-11 (a) Temperature and elongation of the specimen with time up to 330°C (b) Component of elongation..... 100

Figure 5-12 Comparison of results (a) at temperature 130°C (b) at temperature 330°C 100

Figure 5-13 Schematic of instrumented capsule with thermocouple attachment:..... 102

Figure 5-14 Steps involved in instrumented capsule experimental set up assembly 103

Figure 5-15 Out-of-Pile experimental set up..... 105

Figure 5-16 Out-of-pile experimental results 106

Figure 5-17 (a) Temperature Vs Young's modulus (b) Temperature Vs Stiffness of Inconel 625 and SS 316L……109

Figure 5-18 Thrust force Vs Stress and Temperature 110

Figure 5-19 Pressure Vs Total load, specimen load and load on bellow……...……...110

Figure 5-20 (a) Temperature Vs Pressure and Specimen load (b) Stress Vs Strain..... 111

Figure 5-21 Comparison of strain rates..... 115

List of Tables

Table 3-1 Variation of thermal conductivity of SS 316 with temperature 37

Table 3-2 Thermal conductivity of Argon 39

Table 3-3 Thermal conductivity of Helium……..…..39

Table 4-1 Comparison of joining processes 53

Table 4-2 Composition of selected filler metals used for brazing applications 58

Table 4-3 Composition of Base and Filler metals, (Wt. %) 61

Table 4-4 Parameters recorded during heating and cooling 66

Table 4-5 Observed change in weight due to exposure of sodium 71

Table 4-6 Chemical composition of materials used,(Wt. %) 73

Table 4-7 Optimized parameters for high temperature furnace brazing 74

Table 4-8 Process Parameters of Pulsed Laser, GTAW and Nicrobrazing Processes 80

Table5-1Specifications of bellows..... 88

Table5-2Chemical composition of materials used,(Wt. %) 89

Table 5-3 Tests performed on bellows after fabrication 89

Table 5-4 Comparison of results 114

CHAPTER - 1
INTRODUCTION

1

This chapter begins with an introduction of nuclear reactors and briefly covers the Fast Breeder Test Reactor (FBTR) and Prototype Fast Breeder Reactor (PFBR) flow systems and their core configurations. General background of irradiation effects on materials and irradiation capsules is given. A detailed explanation of the creep mechanism is given. Overview of the thesis has been discussed.

1.1 INTRODUCTION TO NUCLEAR REACTORS

Even though a nuclear reactor can be defined in different ways, almost all reactors except fusion reactor (commercially nonexistent) can be defined as: "A nuclear reactor is a device, designed to produce and sustain a long term, controlled fission chain reaction, and made with carefully selected and strategically placed collection of various materials." The nuclear reactors are classified as research/ test reactors and power reactors.

- Research/ test reactors : Designed for neutron production for research purposes, usually low power range (1-10MWt). These reactors provide steady and accurate neutron flux for nuclear and solid-state physics research.
- Power reactors : Main aim is to generate large amount of energy, transformation of the kinetic energy from the fission fragments into heat and electricity in the most efficiently method possible. Typical output is 500-1000 MW. Depending on the average energy of the neutrons, the reactors can also be classified as thermal reactors and fast reactors.

1.1.1 THERMAL REACTORS

Thermal reactors utilize slow neutrons to sustain the nuclear chain reaction. The speed at which the neutrons are released by the fission reaction is too fast to be fully absorbed by fissile atoms. In order to slow down the neutrons the fuel is surrounded by a "moderator" so that a continuous chain reaction can be maintained. The moderator is usually water, heavy water (water whose hydrogen atoms contain both proton and neutron as opposed to just one proton) and graphite. In addition to being used as the moderator, water in thermal reactors also serves as the coolant, to remove the heat generated in fission reactions and get converted into steam to rotate the turbine to produce electricity. Both thermal and fast reactors must constantly be cooled, even when shutdown, because of the heat generated by the radioactive decay of the fission products. Thermal reactors are the ones that are currently being used for commercial operations since the technology to make fast reactors economically viable is still under progress.

1.1.2 FAST REACTORS

As opposed to thermal reactors, fast reactors can sustain a nuclear chain reaction using the fast neutrons, thus they do not need a moderator. However in order to maintain the nuclear chain reaction using fast neutrons, a fuel that is richer in fissile materials is needed. Fast reactors can use either a fuel that has a higher concentration of U- 235 (20 percent or higher as opposed to 0.75-5 percent for thermal reactors) or plutonium-239 (Pu-239). Pu-239 is more suitable for fast reactors because it releases 25 percent more neutrons per fission than U-235. Even though there is less neutron absorption because of the higher speed of the neutrons, this is compensated by the higher amount of neutrons released and higher enrichment of fuel and the nuclear reaction is able to be maintained. Since fast reactors depend on fast neutrons, in order to avoid any type of moderation, a

liquid metal (usually sodium) is used as the coolant instead of water. A liquid metal is also a more efficient medium for transferring heat. Fast reactors that are able to produce (breed) more Pu-239 than they consume are known as Fast Breeder Reactors (FBRs) [1-3].

1.2 INTRODUCTION TO THE FAST REACTOR DEVELOPMENTS IN INDIA

In India, Fast Breeder Test Reactor is in operation at Indira Gandhi Centre for Atomic Research, Kalpakkam. Prototype Fast Breeder Reactor designed by IGCAR is under construction at Kalpakkam under the public enterprise, "BHAVINI". A brief description of these reactors is given below.

1.2.1 FAST BREEDER TEST REACTOR (FBTR)

Fast Reactor programme constitutes the second stage of India's three stage nuclear energy program. FBTR is a 13.2 Megawatt electrical, sodium cooled, loop type, mixed carbide fuelled reactor. The main purpose of FBTR is to acquire experience in the design, development and operation of the fast reactors. It serves as a test bed for irradiation of fuel and structural materials and provides experience in large scale sodium handling and reactor operation. The reactor started operating with Mark I Core (70% PuC-30% UC) which is indigenously developed. It has two primary and secondary loops and a common steam water circuit with once through steam generator (SG) supplying super heated steam to the turbine. There are two steam generators per loop and are located in the common casing. The heat transportation circuit has been divided into two loops so that incase of non availability of one loop, the other loop is available for removing the decay heat from the core. Heat generated by the reactor is removed by these two primary sodium loops, and transferred to corresponding secondary sodium loops through intermediate heat exchangers. Flow sheet of FBTR is shown in Figure 1-1 [1-3].

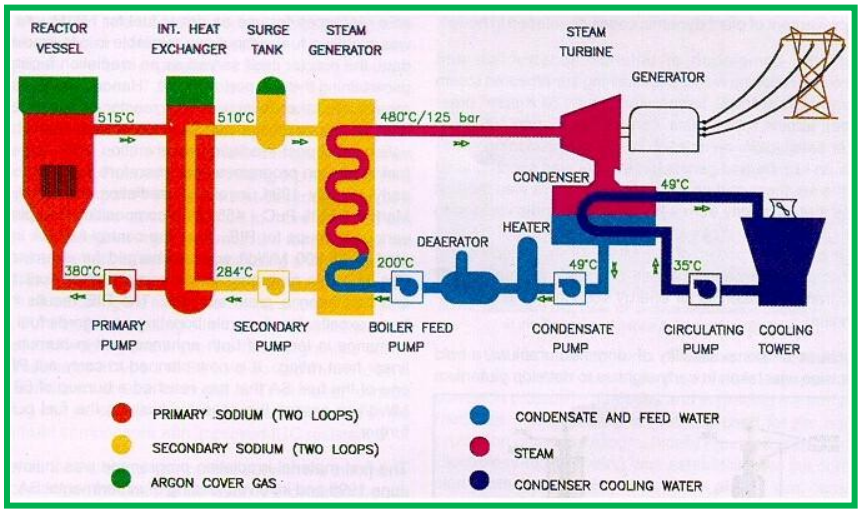

Figure 1-1 Flow Sheet of Fast Breeder Test Reactor

Though FBTR is designed and developed based on the French reactor Rapsodie, more than 80% of the components were indigenously developed. The excellent performance of the components and structures during the past 30 years bears the testimony to the caliber of Indian industries.

1.2.1.1 CORE OF FBTR

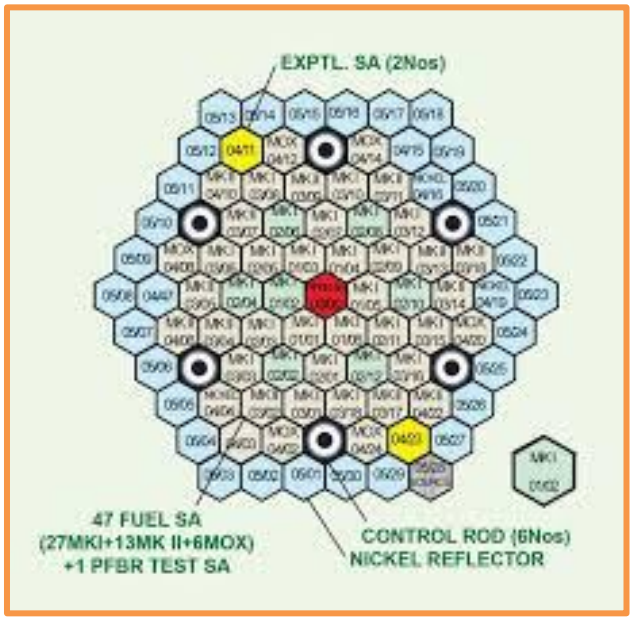

Figure 1-2 Core of FBTR

Figure 1-2 shows the core of the reactor constituting fuel subassemblies at the centre, surrounded by nickel reflectors, thorium blankets and steel reflectors. The core is vertical and freestanding, with the subassemblies supported at the bottom by the grid plate. The reactor vessel houses the core and serves as a conduit for the primary sodium coolant flow through the core. The sodium inlet pipe joins the reactor vessel at the bottom and two sodium outlet pipes radially branch out of the vessel above the core. The reactor is closed at the top by large and small rotatable plugs serving as top shields. Thermal shields are provided inside the reactor vessel to minimize the thermal stresses due to cold and hot shocks. A steel vessel with thermal insulation surrounds the reactor vessel [3].

1.2.2 PROTOTYPE FAST BREEDER REACTOR (PFBR)

PFBR is a 500 Megawatt electrical (MWe), sodium cooled, pool type, mixed oxide (MOX) fuelled reactor, with two secondary loops. The primary objective of PFBR is to demonstrate techno-economic viability of Fast Breeder Reactors on an industrial scale. PFBR being a commercial demonstration plant, mixed oxide fuel is selected on account of its proven capability for safe operation, high burn up, ease of fabrication and proven reprocessing. Pool type concept is adopted due to its inherently high thermal inertia of the large mass of sodium in the pool which eases the removal of decay heat. Two loop designs have been adopted from economic and safety point of view. The flow sheet of PFBR having all the components is shown in Figure 1-3. The main components of PFBR are reactor core, reactor assembly, heat transport system and steam water system shown in the flow sheet given in Figure 1-3. PFBR has been designed and constructed based on the experience gained from FBTR.

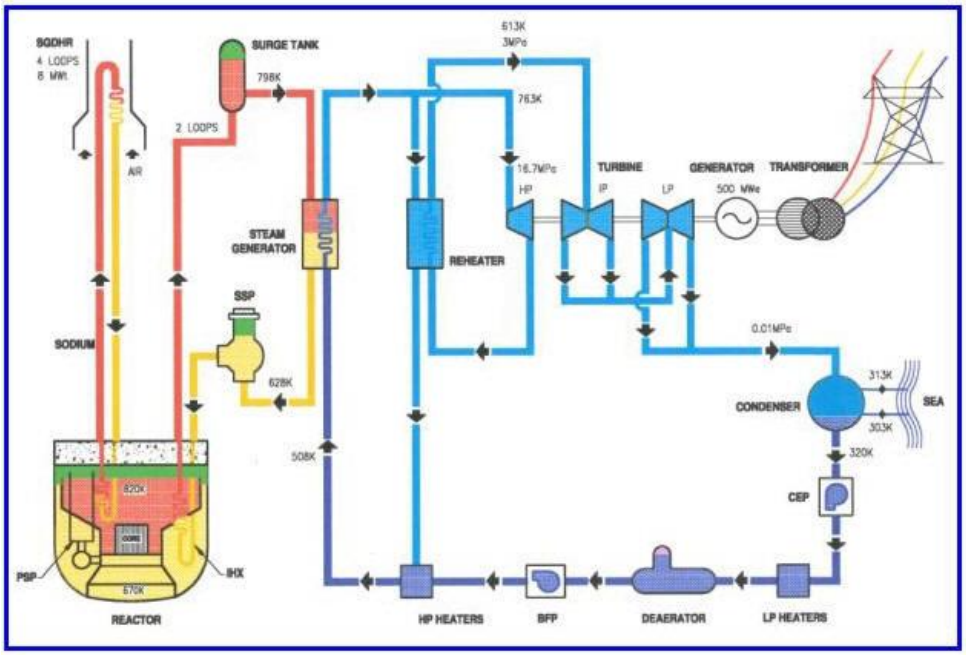

Figure 1-3 Flow Sheet of Prototype Fast Breeder Reactor

A homogeneous core concept with two fissile enrichment zones is adopted for power flattening in PFBR. The active core where most of the nuclear heat is generated consists of 181 fuel subassemblies. There are 12 absorber rods viz. 9 control and safety rods and three diverse safety rods arranged in two rings. Two independent and diverse shutdown systems are provided for ensuring safe shutdown of reactor even when one system is unavailable [4-5]. This reactor is under construction in Kalpakkam.

1.3 FBTR AS AN IRRADIATION FACILITY

Fast Breeder Test Reactor (FBTR) is used for carrying out the irradiation experiments on fuel and structural materials under intense neutron environment to determine their performance and the changes in properties including creep. Irradiation capsules are mainly used for carrying out irradiation experiments in FBTR. The creep data of core structural material specimens is of importance to designers for the design of the reactor components and determine the safe working

limits under various conditions in the reactor. A special plug called "Central Irradiation Plug for Testing and Experiments (CIPTEX)" offers a leak tight access to the central location of FBTR core (0-0 position) to carry out irradiation experiments using an instrumented device. The equipment holder well of CIPTEX will be introduced into a special fuel subassembly with a housing in the form of a channelled guide tube. CIPTEX offers the advantage of online monitoring for the irradiation experiments.

1.4 EFFECT OF RADIATION ON MATERIALS

Due to intense neutron flux and high temperature in a nuclear reactor, there will be degradation in the mechanical properties of materials such as ductility, impact strength and in-pile reactor creep strength. The impingement of neutrons on the structural material in the reactor causes extensive displacement of lattice atoms from their normal position and a variety of defect structures gets produced affecting the mechanical properties of materials.

1.5 INTRODUCTION TO THE CREEP

Creep is the slow, time-dependent strain that occurs in a material under a constant stress (or load) at high temperature. High temperature is a relative term, dependent on the materials being evaluated. A typical creep curve is shown in Figure 1-4 [6]. In a creep test, a constant load is applied to a tensile specimen maintained at a constant temperature. Strain is then measured over a period of time. The slope of the curve, identified in the figure 1-4, is the strain rate of the test during Stage II is the steady state creep rate of the material. Primary creep, Stage I, is a period of decreasing creep rate due to work hardening of the material. Primary creep is primarily of transient in nature. During this period, deformation takes place and the resistance to creep increases until Stage II, secondary stage creep. Stage II creep is a period with a roughly constant creep rate. Stage II is referred to as steady-

state creep because a balance is achieved between the work hardening and annealing (thermal softening) processes. Tertiary creep, Stage III, occurs when there is a reduction in cross sectional area due to necking or internal void formation; that is, the creep rate increases due to necking of the specimen and the associated increase in local stress.

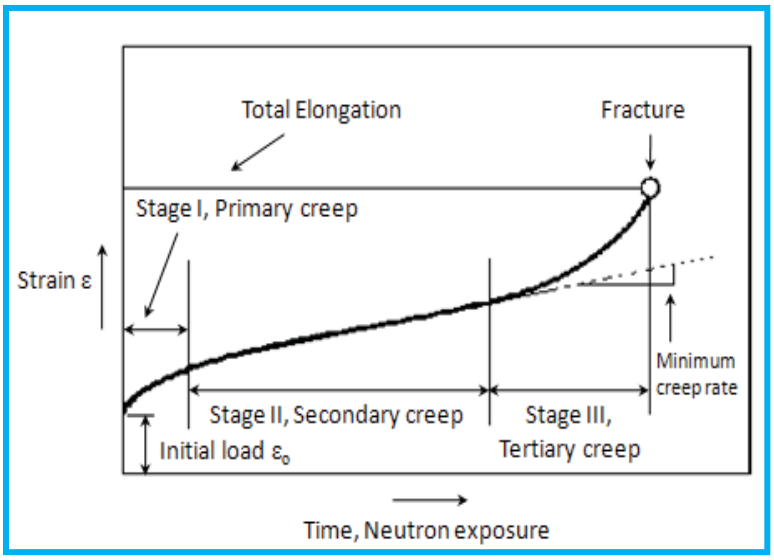

Figure 1-4 A typical creep curve

Irradiation creep is the additional strain that occurs as a result of the combined effect of irradiation and stress in materials. The strain occurring in the absence of irradiation is generally called thermal creep. Performance of fuel, cladding tubes, reactor pressure vessel, and other in-core components of nuclear power reactors will be affected by dimensional changes associated with creep. Hence, it becomes necessary to determine the amount of creep expected to be suffered by a component during its lifetime in a reactor. This will enable the designer to assess the useful life of the component in the reactor and design suitably the components after taking irradiation creep into consideration. Often, radiation-induced creep is measured using a 'cook and look' approach [6-7] where samples are irradiated in-situ for a period of time, removed from

the reactor, measured for dimensional changes, and then returned to the reactor. Repetition of this process can be expensive and time-consuming. Furthermore, it has the potential to disturb the phenomena of interest.

1.6 INTRODUCTION TO IRRADIATION CAPSULES

Irradiation capsule is a device designed to carry out irradiation of fuel, structural material, and shielding material specimens in a reactor. In-reactor creep behavior of structural specimens is determined by two methods: by using instrumented or non-instrumented irradiation capsules. In non-instrumented method, the material specimens are pre-stressed and loaded in the irradiation capsule, and after irradiation the samples are taken out of reactor and tested in hot cells for changes in dimensions. In case of instrumented capsule, the creep deformation of specimens can be recorded online, during reactor operation. Instrumented experiments are complicated to design and expensive but will give more accurate results. Non-instrumented experiments are comparatively simple in design, enable larger numbers of specimens to be tested at a time, and less expensive to manufacture. In instrumented capsule, the loading of tensile specimen can be done through a system of bellows by applying pressure in the bellows using a high pressure gas. The specimen elongation is, in turn, measured using the Linear Variable Differential Transducer (LVDT). Experimental parameters such as temperature can be monitored in these capsules. The central 0-0 position of the core of FBTR can be used for instrumented irradiation experiments. The instrumented capsule experiments can be done in two ways: In-pile and Out-of-pile. In-pile experiments are carried out under intense neutron environment inside the reactor core. Out-of-pile experiments are carried out with simulated experimental conditions which are similar to the in-pile testing but in a laboratory condition without neutron environment. Before carrying out in-pile testing, it is always preferred to do out-of pile

experiment to verify the design and experimental concepts and ensure satisfactory performance of all the subsystems involved.

Generally, the effects of irradiation on mechanical properties of materials are evaluated by carrying out irradiation tests in MTRs (Material Test Reactors) followed by PIE (Post Irradiation Examination). During the last 50 years, a large number of these tests have been performed to analyze the degradation of mechanical properties as a function of fluence (or dpa-displacement per atom) and temperature. These results are used to assess the safety and useful lifetime of materials used in structural components of operating nuclear power plants. Recently, it is increasingly emphasized that the research on neutron irradiation effects of materials is necessary in order to assess the integrity, and for lifetime extension of operating Nuclear Power Plants (NPPs), and to develop fuels and materials supporting advanced reactor systems. During irradiation tests of materials in MTRs, it is desirable to measure characteristic changes in a variety of ways, including remote sensing and in situ observations. Effort is currently progressing to measure dimensional changes (elongation) of materials during in-pile creep tests in MTRs [7].

1.7 OBJECTIVE OF THE PRESENT WORK

The instrumented experiments offer control over the experimental variables and provide improved accuracy of data than possible in non-instrumented experiments. The space available in a fast test reactor for loading the instrumented capsule for creep measurement is off the order of 22 mm diameter X 1000 mm long. It is a challenge to design and develop an instrumented capsule for creep determination in this limited space. Hence, the primary objective of this work is to design, develop an out-of-pile version of instrumented capsule for online determination of

uni-axial creep behavior in structural specimen meeting the space available in a fast test teactor and experimentally verify the performance of this capsule in electrical furnace for the intended purpose. Design of an instrumented capsule, development of high temperature brazing technique and comparison of different materials joining processes have been carried out prior to successful development of instrumented capsules for out of pile experiments.

1.8 OVERVIEW OF THE THESIS

An overview of this thesis is presented in this section:

Chapter 1 begins with the general background and introduction about the irradiation capsules and experimental methods. An explanation to creep phenomenon has been given. This chapter briefly covers the Fast Breeder Test Reactor (FBTR) and Prototype Fast Breeder Reactor (PFBR) flow systems and their core configurations.

Chapter 2 describes the literature review on various topics of irradiation creep measurements. The chapter includes the international developments of design and analysis of irradiation capsules. The motivation drawn out of the literature review and scope of the research work are also discussed.

Chapter 3 starts with a brief discussion on heat transfer analysis of irradiation capsule by analytical and simulation techniques. In a nuclear reactor, structural material specimens are subjected to irradiation to determine the changes in their mechanical properties due to exposure to radiation. In one of the types of irradiation capsules, the specimens are kept in four to five separate sealed compartments of the capsule located one over the other. Helium/ Argon gas or mixture of these gases will be filled around the specimens in these compartments. Liquid

sodium, which is the coolant in the fast reactor, will be flowing around the irradiation capsule. The temperature of specimens has been determined with various types of gases (helium/ argon/ helium-argon mixture) filled in the compartment and the results are presented in this chapter. Variable properties of gases have been used and iterative method has been employed to calculate the temperatures. Using the results obtained, one can select the type of gas mixture required to attain a specific higher temperature in the specimens during irradiation. The results have been compared with the results obtained through the use of a computer code COMSOL.

Chapter 4 discusses about the establishment of high temperature nicrobrazing procedure under argon gas atmosphere which is required in the fabrication of instrumented irradiation capsule. Brazing is a metal-joining process whereby a filler-metal is heated above the melting point and distributed between two or more close-fitting parts by capillary action. The filler metal is brought slightly above its melting (liquidus) temperature while protected by a suitable atmosphere, usually a flux. It then flows over the base metal (known as wetting) and is then cooled to join the work pieces together.

Fabrication of instrumented capsule requires the development of thin-walled joints capable of withstanding high temperatures. High-temperature brazing method has an advantage of joining multiple metal-sheathed cables such as thermocouples through a solid stainless steel plug in a single operation. High-temperature nicrobrazed joints under argon atmosphere have been produced as part of the research work. An induction heating technique has been used for this development. Protective atmosphere is required for high-temperature brazing to prevent oxidation of the base metal and the filler metal during the brazing operation. Commercial grade argon gas (99.996% pure) has been used and brazed joints have been developed. Brazing procedure has been established and development of high temperature nicrobrazed joints using

induction heating system in an argon gas environment has been carried out. Helium leak test, metallographic, micro hardness tests, and sodium compatibility test have been carried out on the brazed samples to qualify the joints.

The fabrication of an instrumented capsule also requires joints with tube-to-tube and tube-to-end plug configurations. Optimization of the parameters of available joining methods and qualification of the joints according to the standards have been presented in this chapter. Helium leak test, metallographic and micro hardness tests have been carried out on the joints made by laser, GTAW(Gas Tungsten Arc Welding) and high temperature nicrobrazing joining processes. Common joint area has been provided for all the joining processes to measure and compare the merits and demerits of each joint.

In Chapter 5 design and analysis of instrumented capsule for online determination of uniaxial creep behaviour in structural specimen has been presented. Fabrication of an out-of-pile version of instrumented capsule and testing of it in a vertical electrical furnace for validation of design concepts has been carried out. The overall diameter of this instrumented capsule is 22 mm and operative portion is 170 mm. This capsule has three different zones located one over the other. In the bottom zone of the capsule the tensile specimen (40 mm length x 8 mm shoulder width x 1 mm thick) is located, with one end fixed to the bottom portion of capsule and the other end connected to a central tube through a connecting plug; in the middle zone two bellows are arranged back to back by circumferential welding, with the tube passing through the centre of the bellows. The middle portion of the central tube is welded to the bellows circumferentially. In the top zone a LVDT is placed and its core is passing through the central tube. The end point of the LVDT core touches the plug connected to the specimen to measure the elongation of the structural specimen. In this capsule setup, bellows are used to apply a load on the structural

specimen with the use of pressurized argon gas. With the application of pressure, the bottom bellow will expand and the top bellow will get compressed. Since the central tube is welded to the bellows, during this expansion of the bottom bellow, tensile load will be applied on the specimen, and the elongation of the structural specimen will be measured by the movement of the core of the LVDT. Bellows setup has been fabricated through the industry. These bellows have been tested under cyclic load and found to be performing satisfactorily. In the experimental setup, pressurization has been done in the bottom bellow using argon gas at room temperature filled at a pressure of 6 MPa. At the temperature of testing of 550 °C, the pressure increases to about 16 MPa resulting in a tensile stress of ~306 MPa in the gauge portion of the tensile specimen. The fabricated instrumented capsule has been placed in the electric furnace with two thermocouples, one positioned at middle of the specimen and other one positioned on the capsule at nearly the same plane to measure the temperatures at these two points. The LVDT has been positioned out of the furnace using an vertical stand arrangement. The LVDT cables are connected to the displacement indicator and YOKOGAWA make data logger to measure and record the data.

The experiment has been carried out by using the set up arranged in our laboratory to perform the uniaxial creep experiments. The experiment has been carried out at three different stresses and temperatures (269 MPa at 450°C, 287 MPa at 500°C and 306 MPa at 550°C). Electric furnace temperature was set at 450°C in the specimen and at this temperature 269 MPa of stress would apply on the specimen. This condition has been kept constant for 200 hours to get the secondary creep data in the specimen. The same procedure has been followed for the remaining temperatures and stresses. The elongation of the tensile specimen due to deformation was

measured by LVDT. The experimental results have been compared with those reported in literature.

Chapter 6 important conclusions drawn from the results of the research work have been presented. This chapter also provides suggestions for future work to be carried out.

- **Summary**

In the present chapter, a brief introduction to nuclear reactors, fast reactors of india, degradation of material properties due to radiation creep phenomena, and irradiation capsules have been given. The primary objective of this thesis is discussed. Chapter wise organisation of thesis is presented.

CHAPTER-2

LITERATURE REVIEW

2

This chapter describes the literature review on various topics of irradiation creep measurement by in-pile and out-of-pile tests. Briefly discusses the worldwide developments on design and analysis of irradiation capsule. The motivation drawn out of the literature review and scope of the research work are also presented.

2.1 INTRODUCTION

In Chapter-1, it was mentioned that the irradiation capsules are designed to expose the structural materials specimens to the operating environment of a nuclear reactor in order to obtain data on the changes in properties due to radiation. In the present chapter, a brief explanation on in-pile (in the core of the reactor) and out-of-pile (out of core of reactor in the laboratory environment) tests have been given and the world wide developments of irradiation capsules and high temperature sensors being used in the irradiation capsules have been explained in detail.

2.2 BELGIUM (IN-PILE TENSILE TESTING IN BR2)

In-reactor uniaxial tensile tests at a constant strain rate were performed in the BR2 reactor at Mol, Belgium [8-9]. Design, construction and calibration of tensile loading module for instrumented tensile tests were carried out in the BR2. The materials used in this test were thin (0.3 mm) sheets of oxygen free high conductivity (OFHC) copper and CuCrZr alloy because these materials are expected to be exposed to thermal and mechanical loads in ITER (International Thermonuclear

Experimental Reactor). This work has shown that it is technically feasible to carry out well-defined, controlled dynamic in-reactor tensile tests, making it possible to investigate the intrinsic role of applied stress and displacement damage acting concurrently in determining the global deformation behavior of the material under dynamic irradiation conditions. Figure 2-1 shows the actual tensile test rig for BR-2, and this test rig is assembled with a combination of bellow, LVDT and tensile specimen at center, and this set up has been placed in a high temperature pneumatic loading unit.

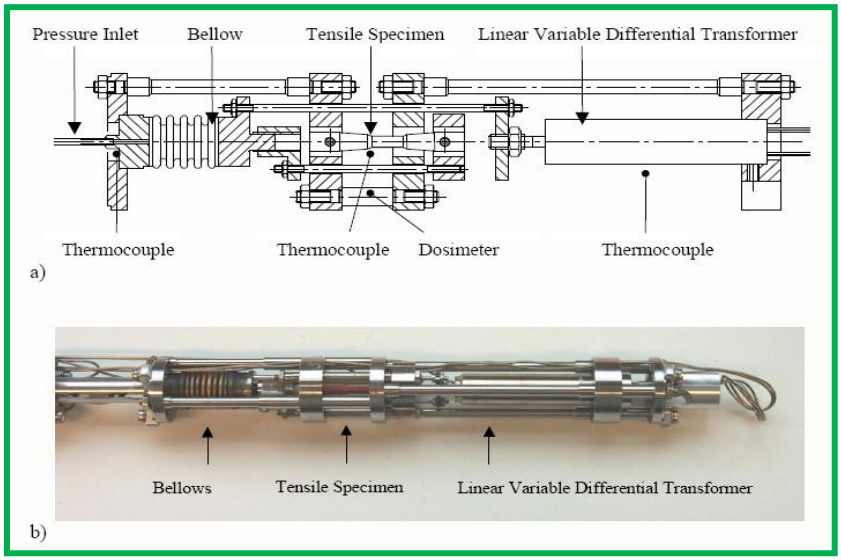

Figure 2-1 Tensile test rig for BR-2 irradiations: (a) simplified layout and instrumentation; and (b) final assembly of test module prior to installation in the test rig.

A two step calibration procedure was implemented. In the first step, the characteristic stiffness of the bellows together with friction forces of the moving parts of the module was determined. The pressure loss (arising from the metal bellows stiffness and internal parts) and the friction fall of the pneumatic loading unit can be determined over its working range. In the second step, the load induced on the tensile specimen by the applied gas was measured directly by a load cell. The interaction of pressure and load was determined by performing constant displacement rate tests with

demonstration specimens. The results of load arrived from the load sensor and the load calculations from pressure at test environment of 23°C have been compared. Both the methods gave the similar load values of maximum 310N at 1.3 mm displacement.

2. 3 FRANCE (IMPROVEMENT OF LVDT DEVELOPED BY IFE-HRP)

The Institute for Energy Technology/ Halden Reactor Project (IFE/HRP) has developed a wide range of specialized sensors, equipments and techniques to perform in-core measurements during irradiation tests in the HBWR (Halden Boiling Water Reactor). The intension of IFE-HRP is to improve the LVDT performance for detecting elongation and diameter changes in OSIRIS reactor. IFE/HRP in-core sensors for fuel and material performance can detect fuel temperature, fission gas release, fuel swelling/densification, cladding creep, corrosion/crud buildup, and crack-growth rates [10-13]. The LVDTs are designed to operate under PWR conditions (350 °C and 150 bar), but they can also be operated for shorter periods up to 500°C. Figure 2-2 shows the principle design of an LVDT.

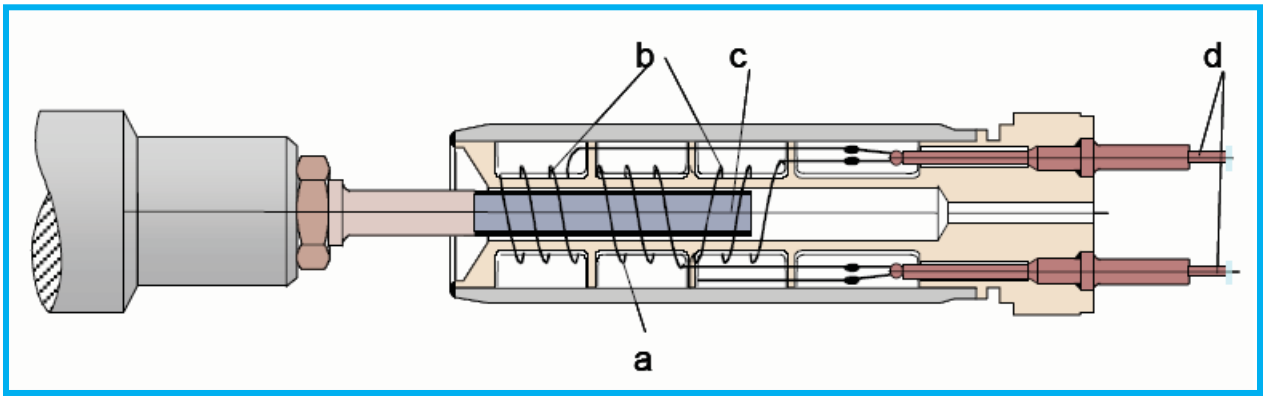

Figure 2-2 Principle of LVDT (a: primary coil; b: secondary coils; c: magnetically permeable core; d: signal cables)

CEA (Commissariat à l' Energy Atomique) has used LVDTs fabricated by the IFE/HRP in the OSIRIS reactor with accuracies of ± 4 µm and displacements up to ± 15 mm (total range) and ±

6 mm (linear range). CEA performed a series of out-of-pile tests to characterize and try to improve the performance of these LVDTs and diameter gauges based on LVDT sensors. Tests were conducted at room temperature and at higher temperatures (up to 380 °C) in inert gas, water, and sodium potassium conditions. As part of this effort, CEA proposed several improvements to LVDT designs manufactured by IFE/HRP. As long as the LVDT is at a uniform temperature, the signal should be more accurate (because it is no longer susceptible to Curie temperature effects if all components are simultaneously subjected to the same temperature). It was planned to evaluate the performance of these improved designs in the OSIRIS reactor. Figure 2-3 shows the MELODIE test configuration to provide real-time elongation and diameter change data from an in-core irradiation of a PWR fuel cladding tube (90 mm) at 350 °C. The test capsule includes controlled mechanical loading ranging from 60 to 180 MPa (with stress steps) and variable bi-axial stress ratio: ranging from 0 (hoop stress) to infinity (axial stress).

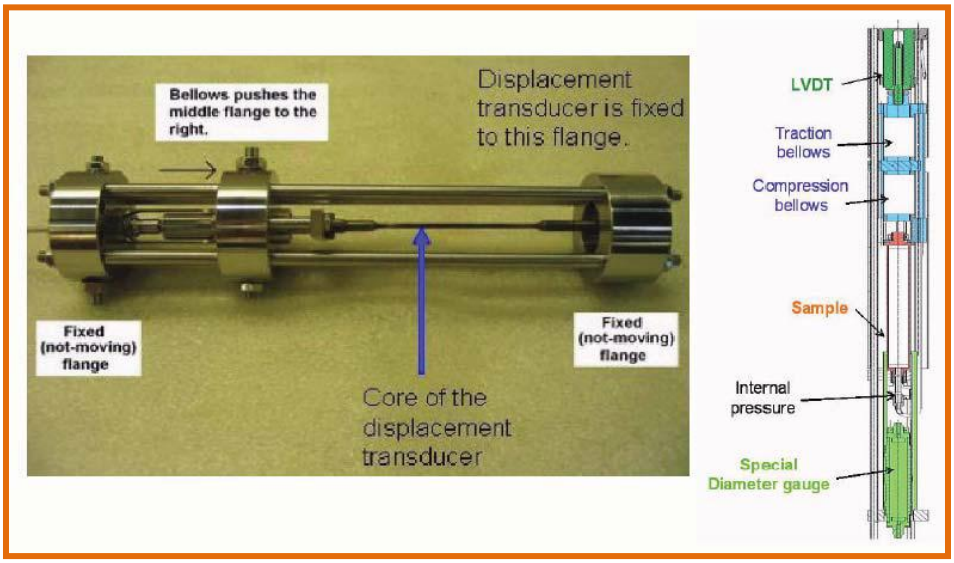

Figure 2-3 Proposed sensor for detecting elongation and diameter changes in OSIRIS testing

As described in [11,15 and 16], even if these sensors (LVDTs) are now reliable and accurate, their use can be limited because of their size and mass, which can imply high gamma heating that may affect the thermal homogeneity of the sample.

2.4 NORWAY (IFE-HRP)

IFE-HRP's instrumentations are primarily based on the LVDT measuring principle. Figure 2-4 shows the IFE-HRP developed instrumented capsule with a gas-gap for controlling the specimen temperature to be varied in the range from 240-400°C , by alternating the composition of helium-argon gas mixture surrounding the specimens. Load (stress) is applied to the specimens via bellows that are compressed by means of gas pressure that is introduced into the chamber housing the bellows (Figure 2-4). Constant displacement of the tensile specimens is maintained by monitoring sample elongation by means of LVDTs and adjusting (reducing) the applied load (stress) on the specimens online, by decreasing the pressure in the bellows housing units.

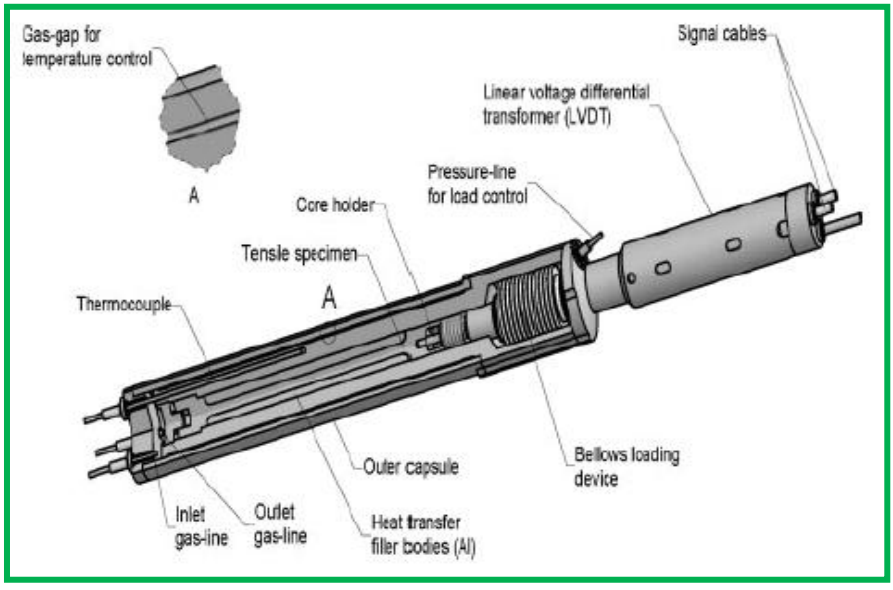

Figure 2-4 Illustration of instrumented tensile specimen used in stress relaxation study; Instrumentation includes bellows that allows online variation of applied load (stress), temperature control through gas lines and monitoring of specimen elongation by means of LVDT.

The standard Halden LVDTs can withstand Boiling Water Reactor (BWR) and Pressurized Water Reactor (PWR) conditions. However, for operation in liquid metal (NaK), as used in fast reactors, or for operation under super-critical water conditions [17], the maximum pressure can be up 250 bar and the required operating temperature can be as high as 600°C, which is above the maximum-recommended temperature for the IFE/HRP LVDTs. In addition, international research into Gen-IV reactors has led to the High Performance Light Water Reactor (HPLWR) concept, which will operate at ~250 bar and ~500°C. Tests by INL determined that standard Halden LVDT operate at temperatures above 500°C for a limited time (up to approximately 700 hours) prior to signal degradation [18]. Standard LVDTs have two-wire mineral insulated (Al_2O_3) cables with an Inconel 600 sheath. In these developmental LVDTs, the wires are either anodized aluminum or ceramic insulated silver alloy wire. Different wire materials are being tested for these LVDT's. Successful operation of these LVDTs has been demonstrated by IFE/HRP at 600 °C and 250 bar [19].

2.5 JAPAN (JMTR)

A study on in-pile/post-irradiation creep under different neutron spectra has been performed using uni-axial tensile specimens in the Japan Materials Testing Reactor (JMTR), Japan. The objective of this creep experiment was to contribute to the understanding of the neutron spectral effect on creep behavior. For this purpose, in-pile creep capsules with uni-axial creep specimens for irradiating under different neutron spectra were developed for JMTR testing. Irradiation temperatures of specimens ranged between 485 and 556°C. In-pile creep tests with high thermal neutron flux were performed at 550°C using stress levels of 245 and 284 MPa. Under the thermal neutron shield condition, the in-pile creep test of the lower specimen was performed at 550 °C and 245 MPa because the temperature of the upper specimen could not reach 550°C. Figure 2-5

[20] shows a schematic diagram of one of the creep irradiation capsules (94M-2A). Different levels of stress can be applied to two creep specimens using bellows pressurized by helium gas. The elongation of each creep specimen was measured using an LVDT.

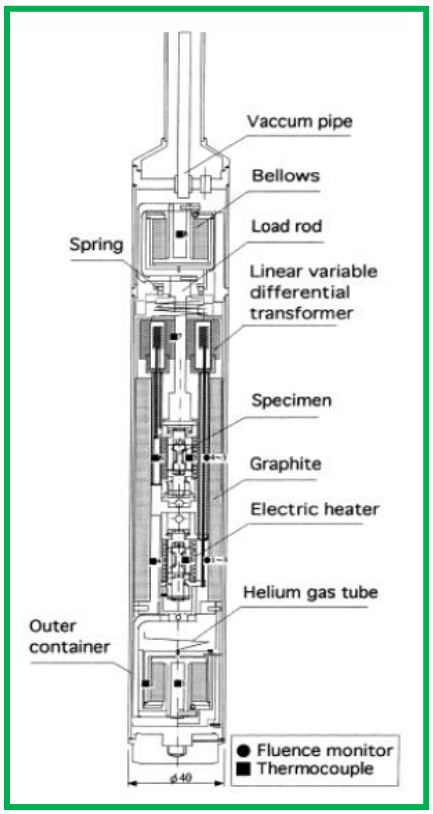

Figure 2-5 Schematic diagram of irradiation creep capsule (94M-2A) under a high thermal neutron flux condition in JMTR

In-pile creep properties at 550 °C appear to depend on the neutron spectrum, but a spectral effect on post-irradiation creep properties is not exhibited. The steady-state creep rate of in-pile creep under a thermal neutron shield condition is slightly larger than observed for the un-irradiated material. The steady-state in-pile creep rate under a high thermal neutron flux condition and post-irradiation creep increases in comparison with that of the un-irradiated material. It is suspected that the cause of the accelerated creep deformation and fracture observed in irradiation creep tests may be related to enhancement of thermal creep in terms of freely migrating defects

(FMD) [21] formed under a high thermal neutron flux in addition to increased helium embrittlement.

2.6 NETHERLANDS (HFR)

Irradiation creep elongation has been investigated in the High Flux Reactor (HFR) at Petten using two types of irradiation creep facilities for uniaxial stresses [22]. In the Trieste facility, 49 specimens can be irradiated simultaneously at various stresses and temperatures. Then, creep elongations are measured out-of-pile at ambient temperatures in a hot cell using a photoelectric incremental linear measuring system. The typical neutron flux density in the Trieste irradiation position in the HFR is 2×10^{18} m^{-2} s^{-1} corresponding to a displacement rate of 1.7×10^{-7} dpa s^{-1} for AMCR alloys (AMCR-0033, -7758, and -7763) and US stainless steels (CE-316, US-316 and US-PCA). In order to check whether the ε-phase, which is formed in the manganese-containing steels during cooling, disturbs creep elongations measurements, CRISP, a second type of irradiation creep facility was developed. In this facility, the in-situ creep elongation of three specimens can be measured during irradiation.

2.7 KOREA (KAERI)

KAERI has developed specialized capsules for creep and fatigue testing [23-25]. These capsules often include thermocouples, fluence monitors, and heaters. In these capsules, stresses on specimens can be loaded using bellows that are internally pressurized with Helium gas. The temperatures of the specimen can be controlled by varying gap sizes among the internal parts of capsules and using small electric heaters installed in the capsule. Temperatures are measured using thermocouples near the specimen. Real-time changes in specimen length are measured

using LVDTs. Test objectives included confirming the design of the creep capsule and to compare the performance of IFE-HRP's LVDT and commercial LVDTs. Creep tests in HANARO were performed with specimens in an inert atmosphere. The HANARO creep test capsule contains four tensile specimens. The first HANARO creep test investigated four stainless steel 316L tensile specimens that were 1.8 mm in diameter and 30 mm in gauge length. This creep test, which was performed with specimens subjected to temperatures of up to 600°C and stresses as high as 253 MPa for 23 full power days (the 45th cycle) of HANARO operation. During this creep test, the temperatures and the displacements were measured real-time for the four specimens. The temperatures of the specimens varied from 367 to 555°C when subjected to 1 bar (internal pressure in the capsule) of Helium gas at a power of 30 MW. These temperatures depended on the specimen position in the HANARO irradiation location. During the irradiation test, the temperatures of the specimens were measured by controlling Helium gas pressure and heater power. The displacement of the specimen was measured with the IFE/ HRP's LVDT without any failures. Results were within the range of displacements estimated in out-pile performance test, but specimen property data were not compared with literature data to assess accuracy of estimated loads applied by the test rig. Displacements from the commercial LVDTs were not detected due to failures that occurred at the beginning of the test. Due to budget limitations, the program was terminated.

2.8 DEVELOPMENT OF INSTRUMENTED CREEP TEST RIG IN IDAHO NATIONAL LABORATORY

An instrumented creep test rig has been developed to complete specimen creep testing under PWR coolant conditions in the ATR (Advanced Test Reactor). A prototype of this creep test rig

was initially designed, fabricated and evaluated in an autoclave at INL's High Temperature Test Laboratory (HTTL). Results from this autoclave evaluation have been used to finalize a design for deployment in an ATR PWR loop. As shown in figure 2-6, major components of the INL creep test rig include a tensile specimen, a bellows, an LVDT and fixturing to connect these components. IFE/HRP provided the LVDT and welded it to the bellows and connected fixtures using e-beam and seal welding techniques. The accuracy of the creep test rig shown in figure 2-6 was evaluated using the autoclave at INL's HTTL. The autoclave was designed for operation at a maximum allowable working pressure of 22.75 MPa at 454 °C.

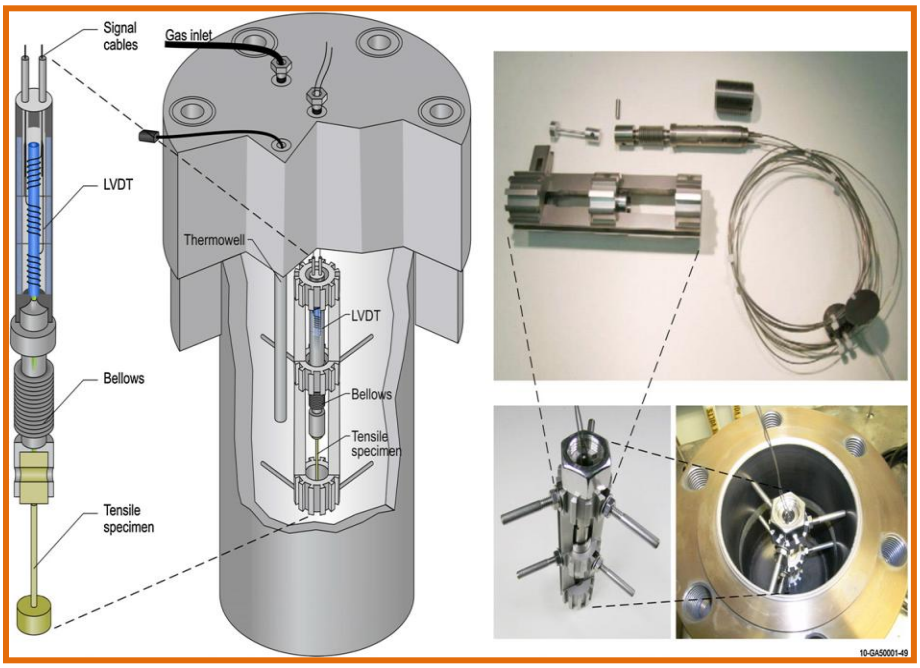

Figure 2-6 Creep test rig positioned in autoclave for testing

Test rig evaluations were completed at elevated pressure and temperatures that bound PWR loop conditions (e.g. pressures ranging from 10.0 to 20.0 MPa and temperatures ranging from 200 to 350 °C) with stainless steel tensile specimens in the elastic region yielded data that are consistent with results obtained from a load frame for this material [28]. Specifically, data shown in figure

2-7 indicate the measurement of Young's Modulus at 206 GPa, which compares favorably with load frame measurements of 200 GPa. In addition, key insights were gained relative to test rig performance during this initial testing. Most notably, the lack of response from the test rig when initial strains were applied emphasized the need to minimize 'compliance' tolerances. As shown in figure 2-7, sample elongation is essentially linear (as expected) after test rig 'compliance' is exceeded.

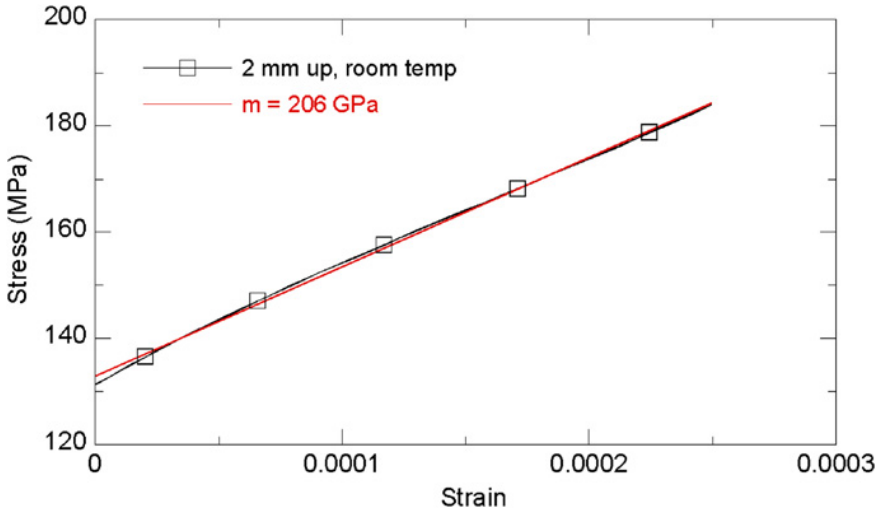

Figure 2-7 Representative test of specimen in elastic region (SS02 stainless steel sample)

Based on results from creep test rig evaluations, an enhanced test rig design was developed, key modifications to the test rig are as follows.

- LVDT coil wires are made from silver alloy wires rather than copper–nickel alloy to eliminate Curie temperature instabilities.
- Connecting design of fixturing has been substantially modified. First, to minimize gamma heating and make it compatible with typical ATR PWR loop fixturing, less

stainless steel was deployed and it has a hexagonal shape. Second, a screw connection is used to minimize compliance issues observed with the initial design. Finally, specimen-to-fixture interfaces were designed to minimize mating mismatch while promoting easier assembly/ disassembly.

2.9 OAK RIDGE NATIONAL LABORATORY (ORNL)

The principles and conceptual designs of gas bellows-loading in-capsule frames to apply tensile and compressive stresses to specimens used in ORNL are discussed here. Theoretical models for the bellows- loading scheme had been set up based on the designs, and detailed calculation was carried out to evaluate the nominal stresses applied to specimens. The calculation results include the stress applied to specimens as a function of internal gas pressure and temperature, which also provide reference data to determine experimental conditions in application as well as a confirmation on the viability of the bellows-based loading technology. The net thrust force exerted to the specimen can be calculated by [30-31]

$$F = A_{eff} \cdot p(T) \cdot f(\delta) \cdot E(T) - F_f \qquad (2.1)$$

where the parameters are defined by Aeff (effective cross-sectional area), p (gas pressure at T), $f(\delta)$ (volume factor =1), T is the test temperature (K), E(T) is the bellows spring rate at T and F_f is the friction of load frame.

From the load–displacement responses of the IN718 and 316 SS bellows pressurized up to a gas pressure of 12 MPa at room temperature and at 400°C. In the same condition the 316 SS bellows generates slightly higher (~15%) force than the IN718 bellows and the difference increases with internal pressure. This difference is caused mainly by the difference in the effective cross-sectional areas of the two bellows. Since the sizes of bellows and capsule internals were chosen to induce stress levels needed in most practical applications, i.e., the irradiation creep

experiments for metallic specimens in tensile mode and for graphite rod specimens in compressive mode. To apply a stress of 10 MPa to the 6 mm diameter graphite specimen at 400°C, for example, the IN718 bellows needs to be pressurized to about 5.8 MPa at room temperature. The same configuration can apply about 220 MPa to a SS-3 tensile specimen with gage section dimensions of 0.76 *1.52 *7.62 mm. As these stresses and samples geometries are consistent with current studies of creep in nuclear-grade materials it is concluded that the creep bellows, in principal, are conceptually viable.

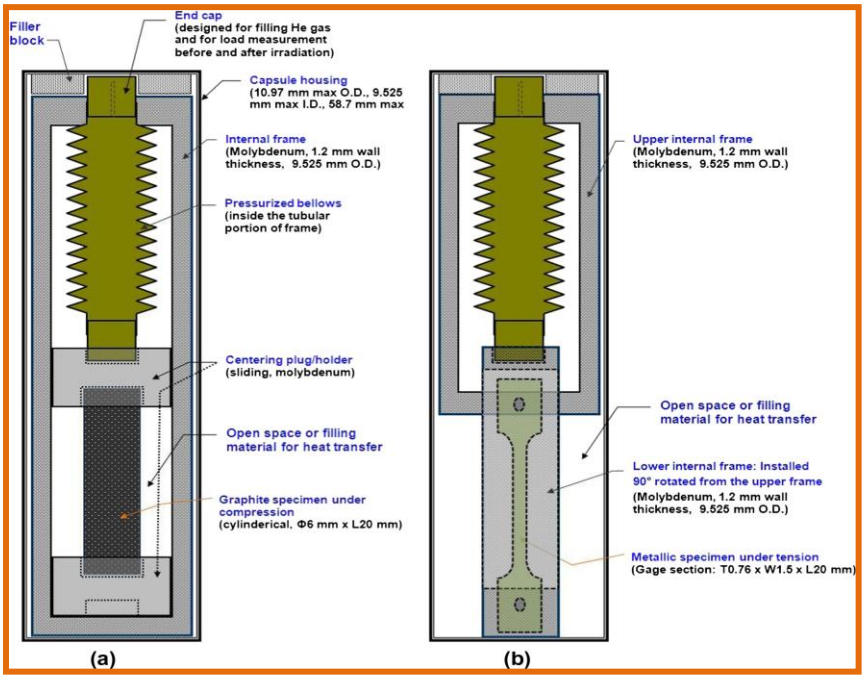

Figure 2-8 Schematics of bellows-loaded rabbit capsules for irradiation creep testing (a) of a graphite specimen under compression load and (b) of a metallic specimen under tensile load

In Figure 2-8(a) the compression load generated by the pressurized bellows is directly transmitted to the graphite specimen through the centering plug that can slide axially as the specimen contracts and bellows expands. In assembly these specimen-bellows pair is set in a rigid internal frame before the bellows is pressurized through a very small hole in the top end cap

(or end plug) and sealed by electron or laser beam welding. The capsule housing holds the load frame-specimen assembly while allowing lateral motion of the sample and bellows. The empty spaces or gas gaps within capsule housing are determined based on thermal calculation to appropriately achieve sample target temperature and to ensure load train motion. In Figure 2-8(b), the pressurized bellows pushes down the lower internal frame with the specimen pinned at its lower end, while the specimen is held up by a pin at the bottom end of the upper internal frame.

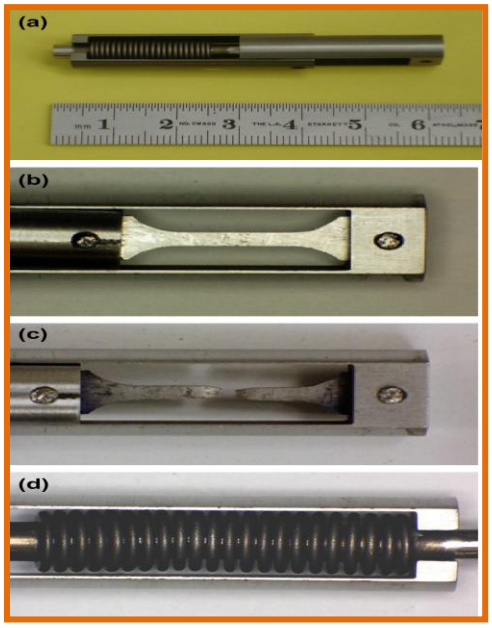

Figure 2-9. A bellows-loaded tensile frame before and after in-furnace testing: (a) the as-assembled frame, (b) crept specimen after 1.3 h at 700°C, (c) failed specimen after 19.5 hrs, and (d) bellows after exposure to 700°C for 19.5 h. The IN 718 bellows were pressurized by helium gas to 3.5 MPa at room temperature

As a preliminary test prior to in-reactor experiment, a bellows loaded tensile frame was tested in vacuum furnace to confirm (i) the capability of bellows-produced load for inducing creep strain and failure in metallic tensile specimen and (ii) the integrity of gas-loaded bellows at high temperature. Figure 2-9 displays the internal frame assembled with an Inconel 718 bellows and

an SS-3 specimen with gage section with dimension of 0.76 *1.52 *7.62 mm. The bellows was pressurized to 3.5 MPa at room temperature. The tensile specimen was made of the modified 9Cr-1Mo ferritic - martensitic steel, whose tensile yield stress is about 500 MPa at room temperature and about 150 MPa at 700°C. Figure 2-9(b) shows the tensile specimen after maintaining in furnace for 1.3 h at 700 °C. The specimen might be crept but no neck was formed, indicating that the creep is still in the uniform deformation mode. It has failed before 19.5 h at 700°C as seen in Figure 2-9(c). The specimen shapes in Figure 2-9(b) and (c) indicate that it has experienced uniform and necking deformation before the final failure. It is notable that such a small IN718 bellows pressurized by helium gas can cause such rapid deformation and failure of a metallic tensile specimen through thermal creep mechanism only. Figure 2-9(d) also confirms that no significant buckling or squirming has occurred in the mini IN718 bellows for 19.5 hrs. The clear gap between the bellows and frame wall indicates that no measurable radial swelling by thermal creep in the bellows wall has occurred. These observations confirm that the gas bellows can provide load to the specimen without any contribution of friction. The gap closed by swelling induced by creep in bellows wall is a major concern for the validity of the applied load measured [32].

2.10 OVERVIEW OF LITERATURE REVIEW AND OBJECTIVE OF THE PRESENT WORK

As discussed in the literature [26-29], several MTRs, for instance Belgian Reactor-2 [BR2], Belgium, OSIRIS reactor, France, Halden Boiling Water Reactor [HBWR], Norway, Japan Materials Testing Reactor [JMTR], Japan, High-Flux Advanced Neutron Application Reactor [HANARO], Korea have deployed creep test rigs to detect the growth of tensile and creep

specimens using a bellows system to apply a variable load to a specimen and LVDTs to detect the growth of the specimen. The literature review reveals that there are worldwide developments of irradiation facilities in nuclear reactors to determine the various changes in the material properties by using irradiation vehicles/capsules. The irradiation capsule experiments are carried out in in-pile/ neutron environment with online application of loading and controlling by pressurized inert gas. It can be observed that for applying load on the specimen, bellows are the most important components in the design of irradiation capsules. It has been found that there are certain limitations in the irradiation capsules presently being used, and an attempt has been made in the present research work, to design and develop an instrumented capsule for determining in-pile creep behavior of materials overcoming these limitations.

1. In many of the instrumented capsules for in-reactor creep experiments, the loading of the specimen is done using pressurized gas supplied through a connecting tube from an external source outside the reactor. While this method is good for controlling the pressure of gas as desired, it is having a disadvantage of need to accommodate a long connecting line where space constraints are there. In the present design the connecting line is dispensed with. Instead, the irradiation capsule with bellows is filled with a pressurized gas and the capsule is sealed. At the irradiation temperature, the gas will exert the required load on the specimen.
2. The overall diameter of capsule has been reduced and kept as 22 mm in the present design to use it even in fast reactors where the core is compact and irradiation space available is highly restricted. Most of the irradiation capsules found in literature have larger overall diameters.

3. The LVDT to be used in irradiation capsule should withstand high temperatures of the order of 400 to 500°C, and special high temperature LVDTs have been used by a few of experimenters. High temperature LVDTs are scarcely available commercially and there are restrictions in procuring them. Hence in our study, LVDT with a working temperature of 200°C has been used and it is placed outside the high temperature zone of the capsule. The core of the LVDT has been connected to the specimen through a stiff ceramic rod to transfer the elongation of specimen to the core of LVDT. The irradiation capsule has been developed and tested successfully in furnace with the above mentioned modifications/ features.

- **Summary**

In this chapter, major test facilities available worldwide for irradiation creep experiments have been discussed. The limitations of these facilities/ irradiation capsules have been identified. The motivation for carrying out the present research work has been brought out.

CHAPTER - 3

3

HEAT TRANSFER ANALYSIS OF AN IRRADIATION CAPSULE

This chapter describes the heat transfer analysis of an irradiation capsule with heat generated in the solid specimens kept in the compartment of irradiation capsule by neutron and gamma heating as heat source, and with constant temperature liquid sodium around it. The composition of He-Ar gas mixture is varied in the compartment. The heat transfer calculations have been carried out analytically and compared with the simulation results.

3.1 INTRODUCTION

In a nuclear reactor, structural material specimens are subjected to irradiation to determine the changes in their mechanical properties due to exposure to radiation. Figure 3-1 (a) shows one of the type of irradiation capsule, in which the specimens are kept in five separate sealed compartments of the capsule located one over the other. Figure 3-1 (b) shows a single compartment of the irradiation capsule, in which helium/ argon gas or mixture of these gases is filled around the specimens. Liquid sodium, which is the coolant in the reactor will be flowing around the irradiation capsule. During irradiation, due to attenuation of gamma rays and neutrons on the specimens, heat will be generated in the specimens. Due to surrounding He-Ar gas mixture around the specimens, the temperature of the specimens will be more than the temperature of the sodium flowing over the capsule and we can obtain an irradiation temperature in the specimens which is higher than the sodium temperature. In the present analysis, the temperature of specimens has been determined with various types of gases (helium/ argon/ helium-argon mixture) filled in the compartment, in order to design a capsule to expose

structural material specimens at a desired temperature that is higher than the temperature of sodium flowing around the irradiation capsule.

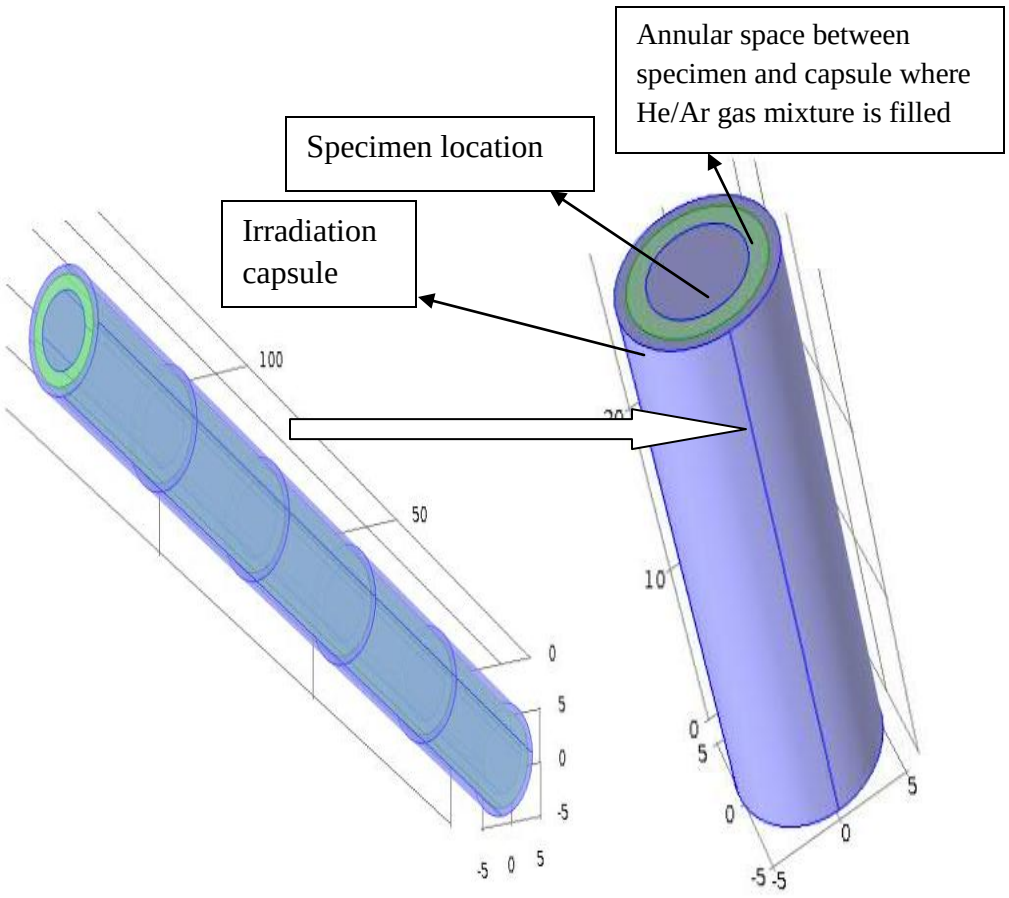

(a) (b)

Figure 3-1 (a) Schematic of an irradiation capsule that has five compartments (b) single compartment of the irradiation capsule filled with gas mixture around the specimen

3.2 DETAILS OF IRRADIATION CAPSULE AND CALCULATION METHODOLOGY

The sketch of a capsule compartment is shown in Figure 3-2. This compartment is made from a stainless steel tube (type 316 SS) of OD 10.5 mm and ID 9 mm with a length 29 mm. The

specimens kept in the compartment can be approximated as a solid stainless steel cylinder of 6.5 mm diameter and of 29 mm long.

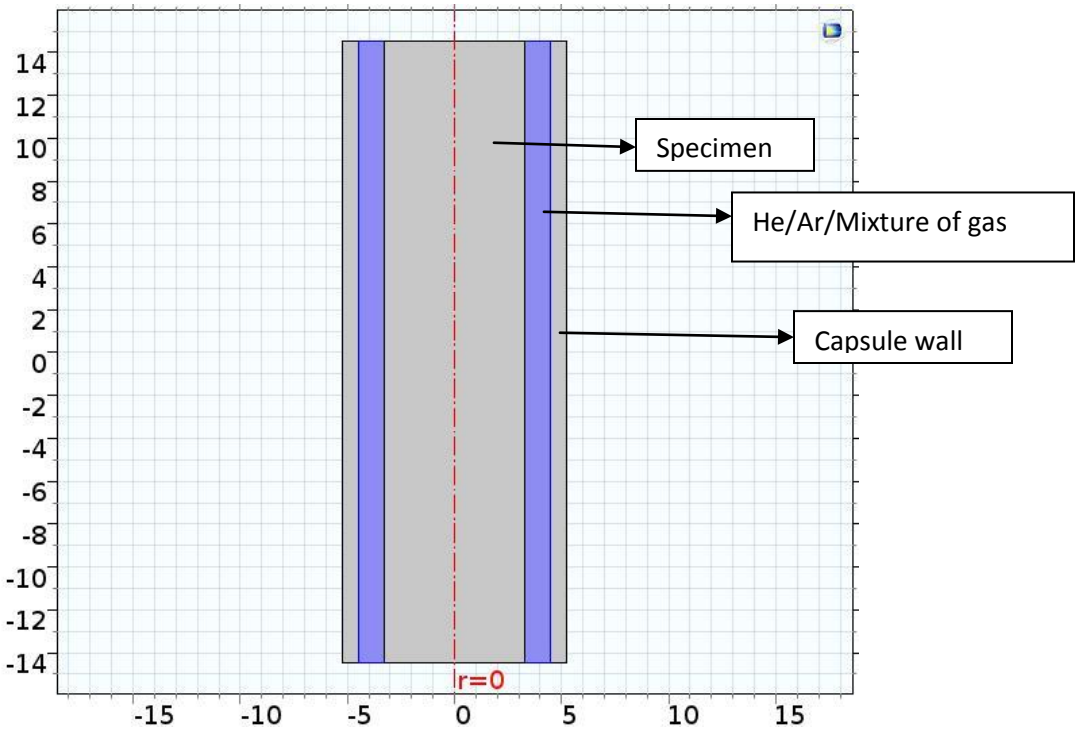

Figure 3-2 Compartment of Irradiation capsule in 2D

The temperature of the outer surface of the compartment is same as the temperature of flowing sodium (420°C). The heat generation rate in stainless steel due to nuclear heating depends on the location of irradiation in the core of the reactor and three different rates as 1.5 W/gm, 1.8 W/gm and 2 W/gm are considered in this work. Different compositions of the gases are considered to be filled in the annular space around the specimens in the compartment (100% He, 100% Ar, and mixtures of these gases with different fractions). The calculations to determine the temperature of specimens have been done by two different methods: (i) by the analytical method, and (ii) by using computer code. Both conduction and radiation are considered. Variable properties of gases have been used in the calculations and an iterative method has been employed to calculate the

temperatures. The problem has been considered as 1-D axisymmetric model with top and bottom surfaces as insulated.

3.3 METHODOLOGY

The calculations to determine the temperature of specimens have been done by two different methods:

(i) By Analytical method and

(ii) By using Computer code COMSOL (V4.3a).

COMSOL is a widely used multiphysics simulation software & using this software, we can simulate different types of problems. Presently our problem is related to the Heat Transfer module, 1-D and static condition.

3.3.1 TEMPERATURE DISTRIBUTION USING ANALYTICAL METHOD (ITERATIVE TECHNIQUE)

Temperature distribution is calculated assuming steady state heat transfer from the specimens to the sodium present outside the compartment.

The temperature rise across the wall of the capsule (compartment) can be determined by the equation-(3.1) [33].

$$Q = \frac{2.0 * \pi * K * L * (T_2 - T_1)}{\ln\left(\frac{r_1}{r_2}\right)} \quad \text{…….. (3.1)}$$

Where

Q - Rate of heat flow (W)

L - Length of tube (m)

K - Thermal conductivity of SS 316 (W/mK)

T_1 - Capsule tube – outer temperature (or) liquid sodium temperature (K)

T_2 - Capsule tube – inner temperature (K)

r_1 - Capsule tube – outer radius (m)

r_2 - Capsule tube – inner radius (m)

The variable thermal conductivity of SS 316 with temperature [34] as shown in Table 3-1 has been considered in the calculations.

Table 3-1 Variation of thermal conductivity of SS 316 with temperature [34]

Temperature (K)	Thermal conductivity (W/mK)
300	13.40
400	15.20
500	16.75
600	18.30
700	19.80
800	21.30
900	22.75
1000	24.70

The temperature rise across the annular gap filled with He/ Ar/ mixture of these gases can be found out by equation-(3.2).

$$Q = \frac{2.0 * \pi * L * K_{mix} * (T_3 - T_2)}{\ln\left(\frac{r_2}{r_3}\right)} + \frac{\sigma * A_3 * (T_3^4 - T_2^4)}{\left(\frac{1}{\varepsilon} + \frac{A_3}{A_2}\left(\frac{1}{\varepsilon} - 1\right)\right)} \quad \text{.....(3.2)}$$

Where,

K_{mix} - Thermal conductivity of gas mixture (W/mk)

T_3 - Specimen temperature (K)

T_2 - Capsule tube – inner temperature (K)

r_2 - Capsule tube – inner radius (m)

r_3 - Radius of Specimen cylinder (m)

σ - Stefan- Boltzmann constant = $5.67*10^{-8}$ W/m^2K^4

A_2 - Capsule tube – inner surface area (m^2)

A_3 - Surface area of a specimen cylinder (m^2)

ε - Emissivity

Thermal conductivity of helium – argon gas mixture is determined using the following relation-(3.3) [35].

$$K_{mix} = \frac{K_{Helium}}{1+2*\left(\frac{x_2}{x_1}\right)} + \frac{K_{Argon}}{1+2.2*\left(\frac{x_1}{x_2}\right)} \text{.....(3.3)}$$

Where,

K_{mix} - Thermal conductivity of gas mixture (W/mk)

K_{Helium} - Thermal conductivity of helium (W/mk)

K_{Argon} - Thermal conductivity of argon (W/mk)

x_1 - Volume fraction of helium in gas mixture

x_2 - Volume fraction of argon gas mixture

Variable thermal conductivities of argon and helium with temperature [36 and 37] are considered as shown in Tables 3-2 and 3-3.

Table 3-2 Thermal conductivity of Argon[36]

Temperature (K)	Thermal conductivity (W/mK)
300	0.018
350	0.020
500	0.026
1000	0.043
1500	0.055

Table 3-3 Thermal conductivity of Helium[37]

Temperature (K)	Thermal conductivity (W/mK)
723.16	0.2875
750.00	0.2950
773.16	0.3014
800.00	0.3088

3.3.1.1 ITERATIVE TECHNIQUE

Thermal conductivity is a function of temperature, and this implies that as temperature changes the thermal conductivity also changes.

In the calculation T_2 - capsule tube inner temperature can be found by conduction equation. T_3 depends on the temperature drop across the gas mixture, but gas mixture temperature cannot be determined without knowing thermal conductivity of gas mixture (K_{mix}), which again depends on the temperature of mixture. Hence an iterative technique was used. Initially T_3 was assumed and T_{avg} was found out from equation-(3.4), K_{mix} is calculated using equation-(3.3) for T_{avg}. Substituting this K_{mix} value in the heat transfer equation-(3.2), a new specimen temperature value (T_3) is found out.

Using new T_3 and T_2, T_{avg} is again found out. The above procedure is repeated till the T_3 becomes same and does not change with an iteration.

$$K_{Mix} = f(T)$$

$$T_{avg} = \frac{T_2 + T_3}{2} \quad \text{.....(3.4)}$$

The calculations are done by an iterative technique with above formulations. The results obtained are shown in Figure 3-3 at different heating values with different gas mixtures. The temperature of liquid sodium surrounding the outer surface of the capsule is considered as 420 °C. The film drop is neglected.

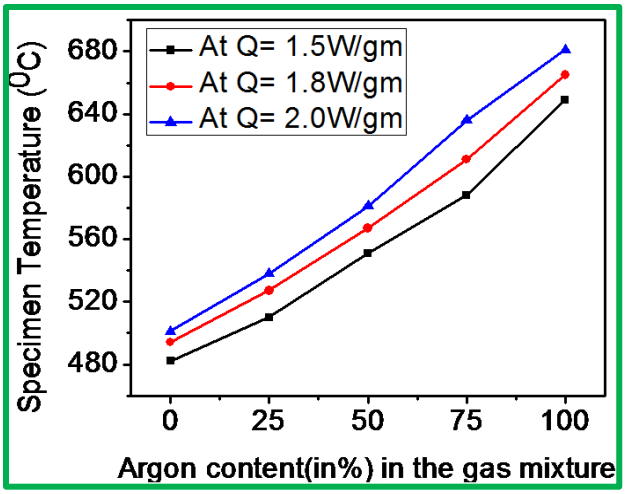

Figure 3-3 Temperature of specimens by analytical method

Figure 3-3 shows the variation of temperature of the specimen while changing the proportion of He + Ar gas mixture in the gas gap region provided between the inner surface of irradiation capsule and solid specimen.

In this graph, the argon content in the gas mixture has been taken along X- coordinate and the specimen temperature has been taken along the Y- coordinate. It can be seen that specimen temperature is increased with the increase of Ar gas in the gas mixture. The temperature is higher at higher value of Ar in the mixture. The specimen temperature depends on the rate of heat generation also. Hence the temperature of specimens depends on both nuclear heat rating and the composition of the gas mixture.

3.3.2 TEMPERATURE DISTRIBUTION DETERMINED BY COMPUTER CODE COMSOL

The computer code COMSOL is a multi-physics simulation software and can be used to solve problems of heat transfer. The dimensions of the capsule, conductivity data of stainless steel, helium and argon, and thermal conductivity relation of gas mixtures are given as input to the

code. The 1-D model was considered by insulating the top and bottom portions of the compartment. The details and method of approach of using this computer code is explained below.

3.3.2.1 APPROACH USING COMSOL

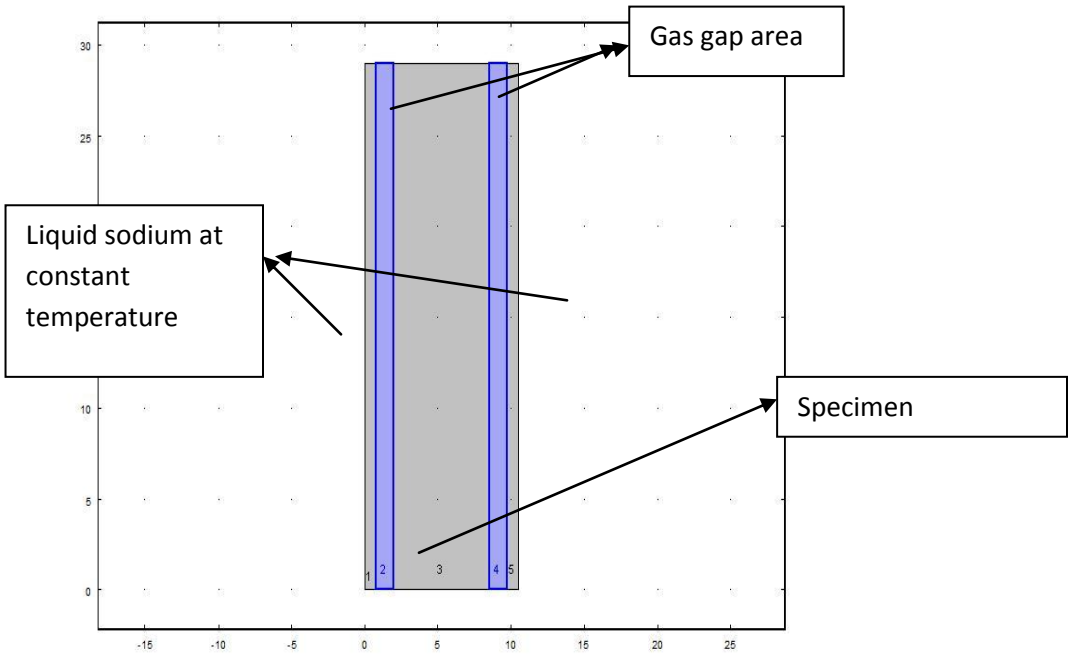

Figure 3-4 Capsule design using simulation software

Figure 3-4 shows the irradiation capsule setup in COMSOL. In this figure 1,3,5 are the SS 316 materials and 3 is the specimen. 2,4 is the gap between the specimen and capsule tube and in this gap only the gas mixture will be filled. This gas mixture will be varied (Helium and Argon gas mixture). Due to this change in composition of gas, the specimen temperature will differ, and the aim is to find the temperature of specimen by using the code COMSOL.

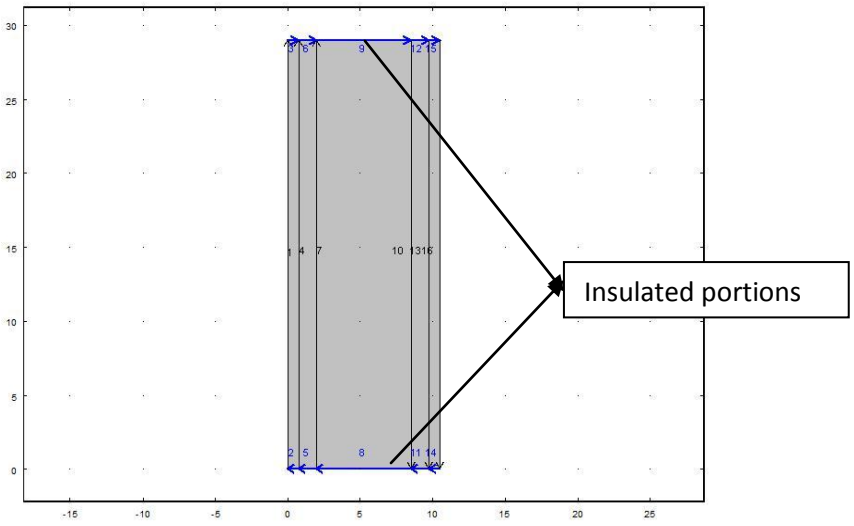

Figure 3-5 Insulated at top and bottom portions

The problem is considered as 1-D/ Axisymmetric. Top and bottom faces are considered as insulted shown in Figure 3-5. Sodium temperature is taken as constant. The temperature of the specimen is calculated for various values of He-Ar gas mixtures surrounding the specimen using the COMSOL code. Figure 3-6 shows the outer temperature of irradiation capsule (1,16). The results obtained from this simulation software are shown in Figure 3-7.

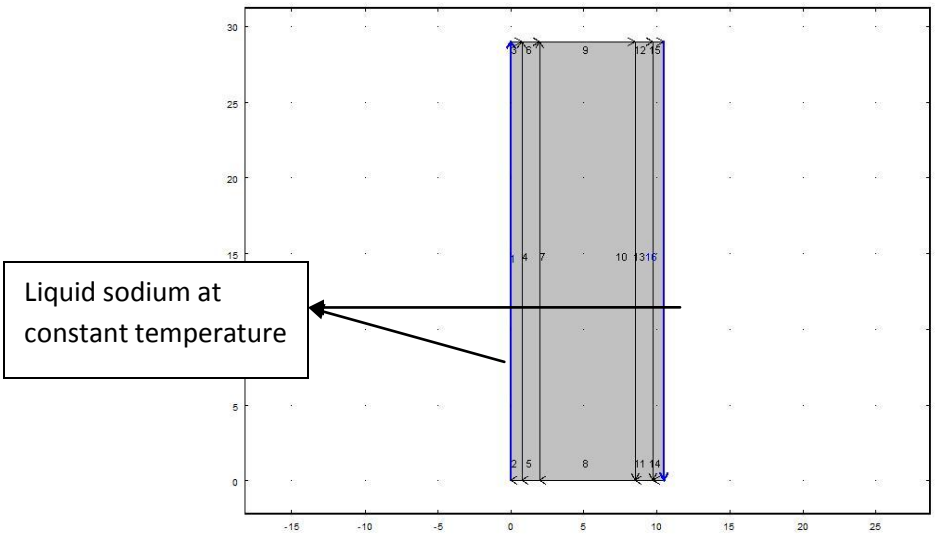

Figure 3-6 Constant liquid sodium temperature at wall of capsule

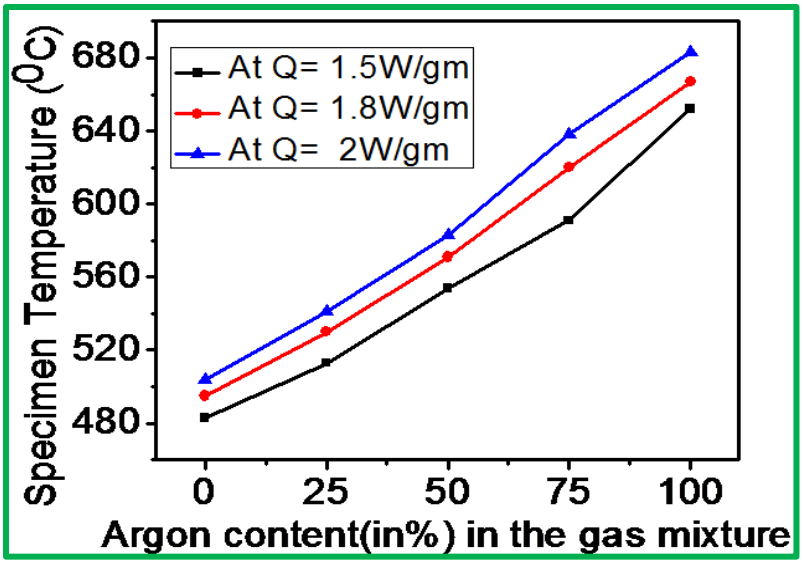

Figure 3-7 Temperature of specimens by simulation software

Figure 3-7 shows the temperature changes in the specimen with variation in the proportion of He+Ar gas mixture in the gas gap region between irradiation capsule inner surface and solid specimen.

In this graph the He+Ar gas mixture has been taken on X-coordinate and the specimen temperature has been taken on the Y-coordinate. It can be seen that in all the heating rates, specimen temperature increases with the increase of argon proportion in the gas mixture.

3.4 RESULTS AND DISCUSSION

Figure 3-8, 3-9 and 3-10 show the simulation results by COMSOL. The argon gas proportion has been varied in the Helium and Argon gas mixture. We observes that, the specimen temperature has increased with a higher percentage of argon in He-Ar gas mixture, and with increasing the heat generation rate. Here two parameters are influencing the specimen temperature, one is heat source and the other one is percentage of argon. Figure 3-10(d) shows the higher specimen temperature at Q= 2.0 W/gm and 100% argon in the He-Ar gas mixture.

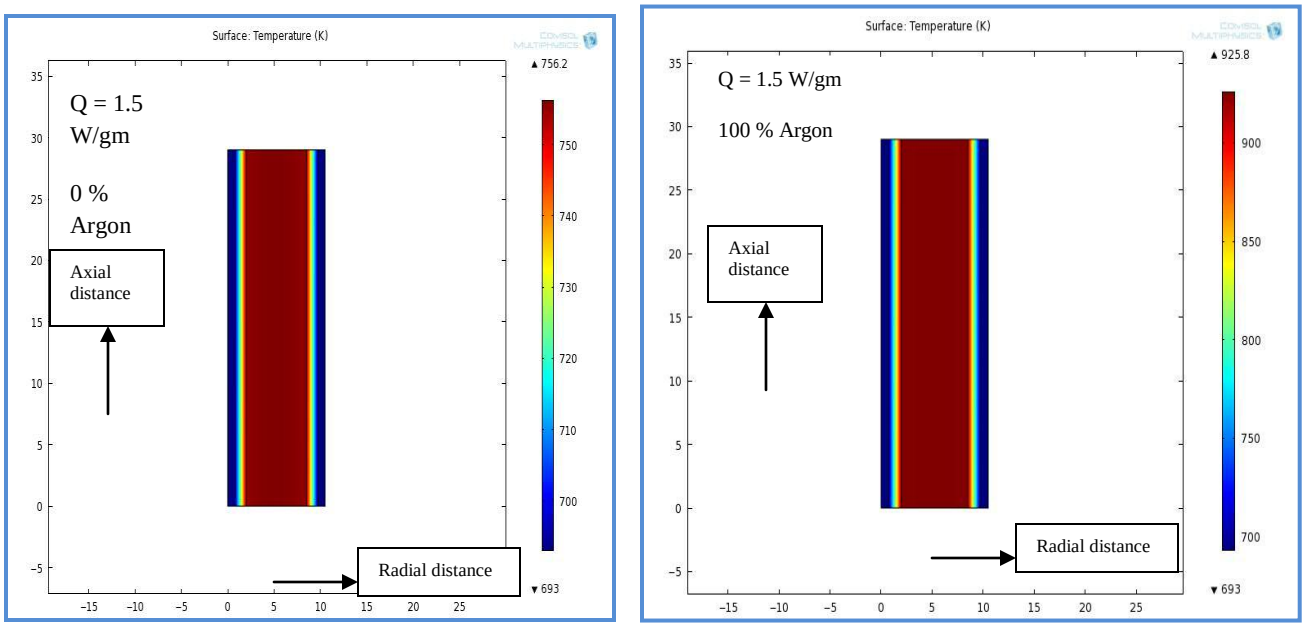

(a) (b)

Figure 3-8 Simulation results at Q = 1.5W/gm : (a) 0% of Argon gas (b) 100% of Argon gas

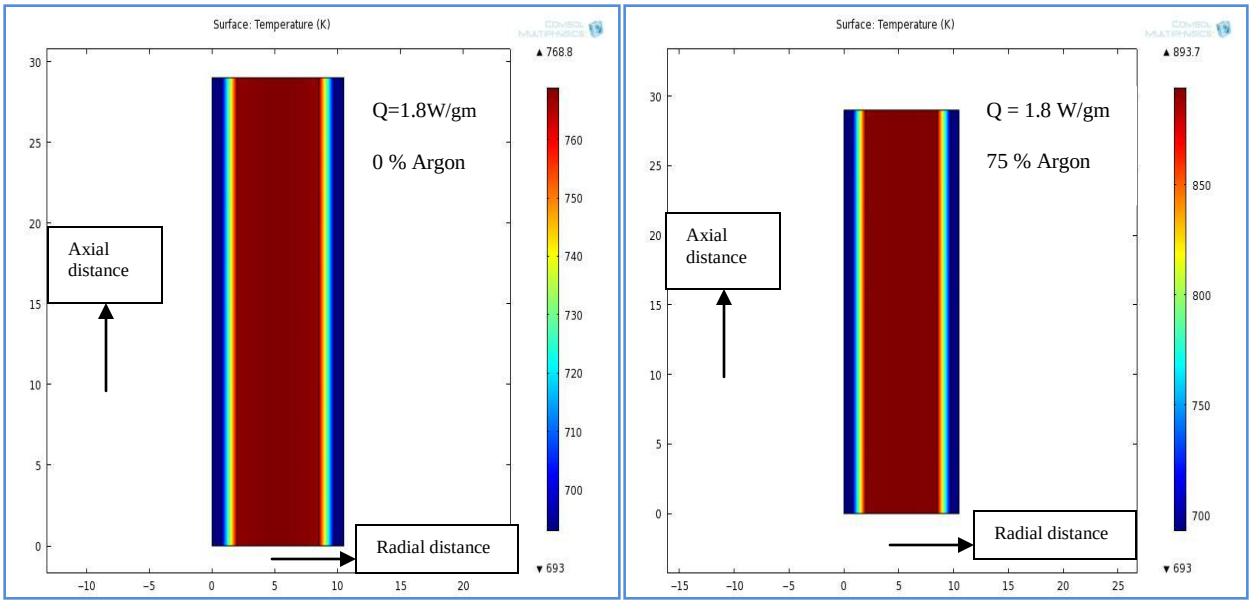

(a) (b)

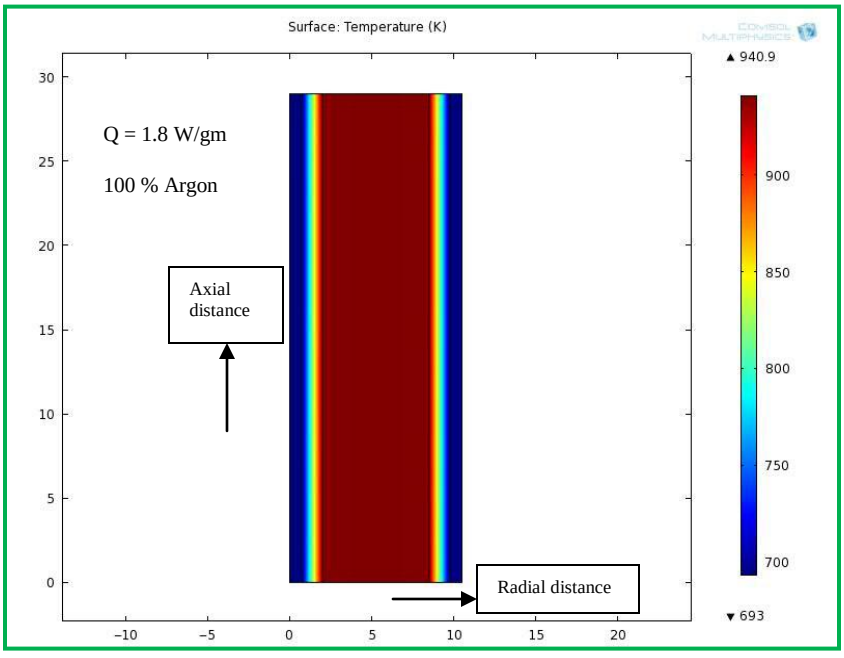

(c)

Figure 3-9 Simulation results at Q = 1.8W/gm : (a) 0% of Argon gas (b) 75% of Argon gas (c) 100% of Argon gas

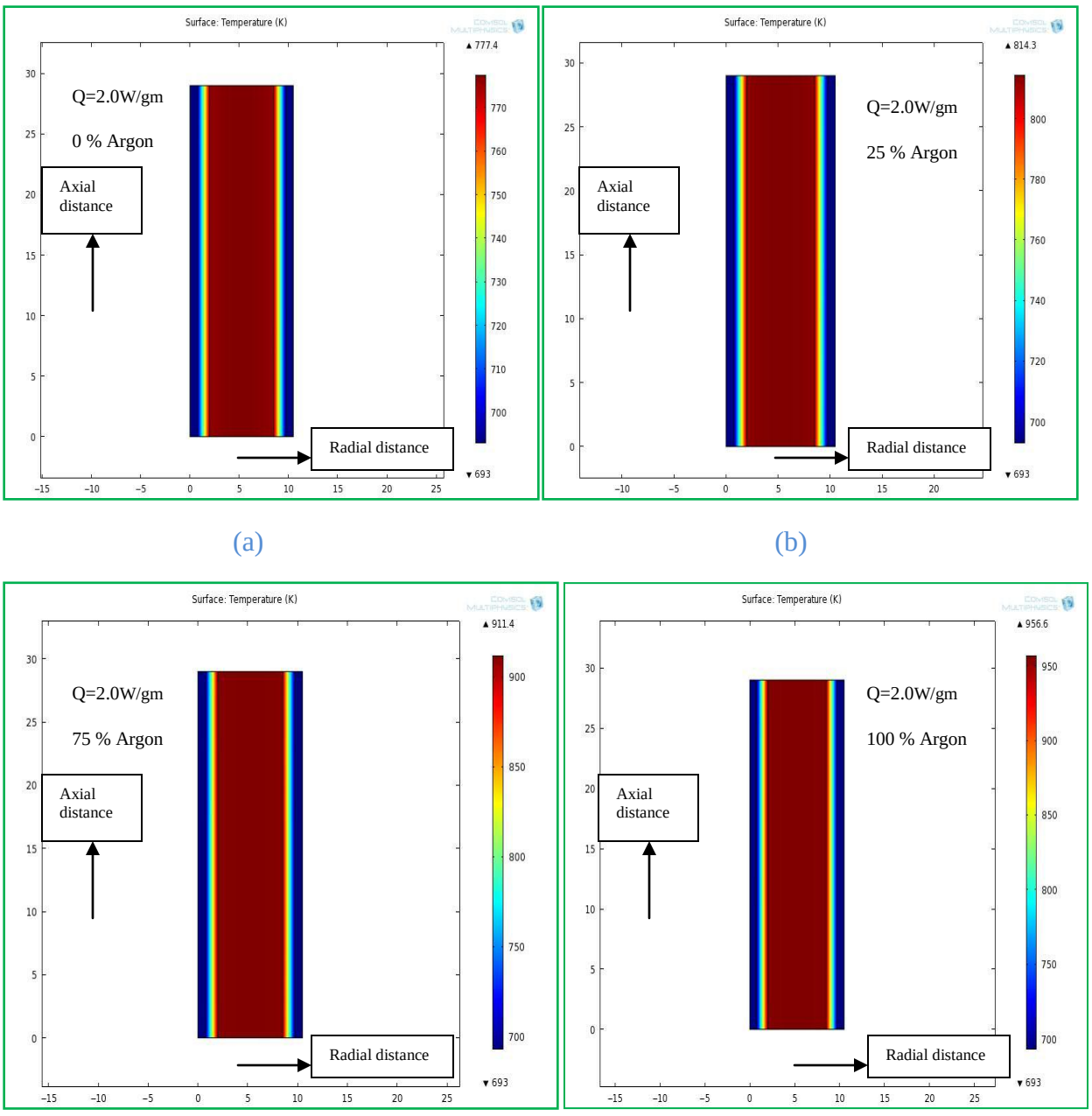

Figure 3-10 Simulation results at Q = 2.0W/gm : (a) 0% of Argon gas (b) 25% of Argon gas (c) 75% of Argon gas (d) 100% of Argon gas

The results obtained from both analytical method and COMSOL software are compared in Figures 3-11 to 3-13 for different heat generation rates. It can be seen that there is good match between these two results.

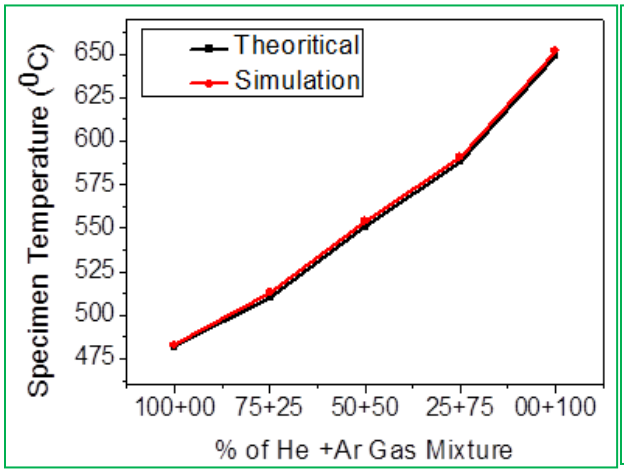

Figure 3-11 Comparison of results at Q = 1.5 W/gm

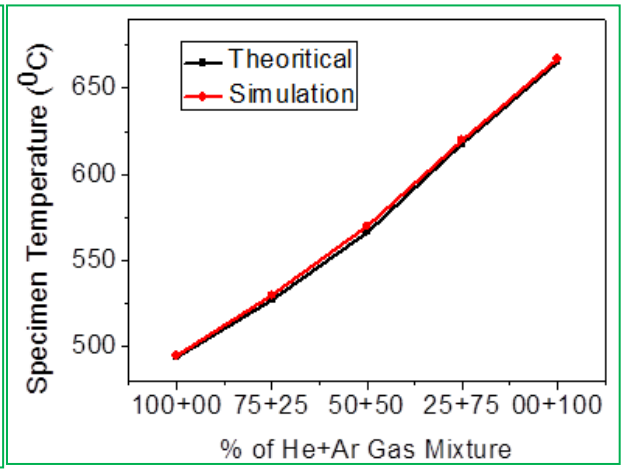

Figure 3-12 Comparison of results at Q = 1.8 W/gm

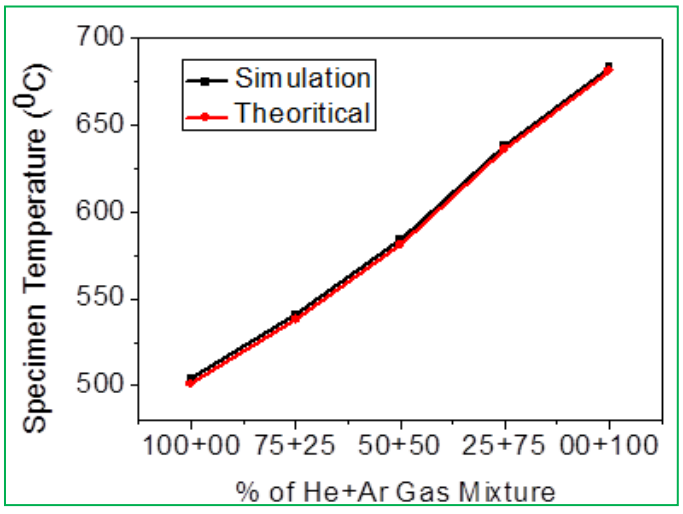

Figure 3-13 Comparison of results at Q = 2.0 W/gm

- **Summary**

In one of the type of irradiation capsule, the specimens are kept in five separate sealed compartments of the capsule located one over the other. Helium/ Argon gas or mixture of these gases will be present around the specimens in these compartments. Liquid sodium, which is the coolant in the reactor, will be flowing around the irradiation capsule. During irradiation, due to attenuation of gamma rays and neutrons on the specimens, heat will be generated in the specimens. Due to this, the temperature of the specimens will be more than the temperature of the sodium around the capsule and we can obtain the irradiation temperature in the specimens which is higher than the sodium temperature. Using the calculation methodology presented in this chapter, the appropriate He-Ar gas mixture can be selected to obtain a desired irradiation temperature in the specimens.

4

CHAPTER - 4

ESTABLISHMENT OF HIGH TEMPERATURE NICROBRAZING PROCEDURE UNDER ARGON GAS ENVIRONMENT AND QUALIFICATION OF BRAZED JOINTS

This chapter includes the details about establishment of high temperature nicrobrazing procedure, qualification of brazed joints and optimization of process parameters of weld joints developed by laser, GTAW and high temperature nicrobrazing joining processes. High-temperature nicrobrazed joints under argon atmosphere have been developed as part of the project work. Helium leak, metallographic, micro hardness tests, and sodium compatibility test have been carried out on the brazed samples to qualify them. Fabrication of instrumented capsules requires the development of thin-walled joints capable of withstanding high temperatures. High-temperature brazing method has an advantage of joining multiple metal-sheathed cables such as thermocouples through a solid stainless steel plug in a single operation. During assembly of an instrumented capsule, weld joints of tube- to- tube and tube- to- end plug configurations are required and, there is a need to optimize the parameters of available joining methods and qualify the joints according to the standards. Helium leak test, metallographic and micro hardness tests have been carried out on all the types of joints to measure and compare their performance. The geometry was maintained as same in all three joints.

4.1 INTRODUCTION

Fabrication of instrumented irradiation capsules involves development of thin walled joints. Brazing, Gas Tungsten Arc Welding(GTAW) and Laser welding processes have been considered for this purpose. Brazing is a metal-joining process whereby a filler-metal is heated above

melting point and distributed between two or more close-fitting parts by capillary action. The filler metal is brought slightly above its melting (liquidus) temperature while protected by a suitable atmosphere, usually a flux. It then flows over the base metal (known as wetting) and is then cooled to join the work pieces together [38]. It is similar to soldering, except the temperatures used to melt the filler metal are higher. In order to obtain high-quality brazed joints, parts must be closely fitted, and the base metals must be exceptionally clean and free of oxides. In most cases, joint clearances of 0.03 to 0.08 mm are recommended for the best capillary action and joint strength.

Capillary flow is the dominant physical phenomenon that ensures good brazements when both surfaces to be joined are wet by the molten filler metal. The joint must be properly spaced to permit efficient capillary action and coalescence. More specifically, capillarity is a result of the relative attraction of the molecules of the liquid to each other and to those of the solid. In actual practice, brazing filler metal flow characteristics are also influenced by dynamic considerations involving fluidity, viscosity, vapor pressure, gravity, and especially by the effects of any metallurgical reactions between the filler metal and the base metal. Capillary attraction makes the brazing of leak tight joints a simple proposition.

Fig. 4-1 [38] schematically shows the principle of capillary attraction for selected liquids when the liquid is sandwiched between two clean glass plates: (a) When immersed in water or ink, a column will rise between the plates because of wetting, (b) When the plates are immersed in mercury, no wetting occurs and the column is depressed. If paraffin plates are used in place of the glass plates, immersion of the plates in mercury will produce wetting. In welding processes, the joint temperature is raised above the melting temperature and a strong metallurgical bond is formed at the joint.

Experimental work was carried out using all the three joining methods(brazing, GTAW and laser welding) to select the suitable joining method. This chapter discusses the comparison of the above three different methods of joining.

4.2 DEVELOPMENT OF JOINTS BY BRAZING METHOD

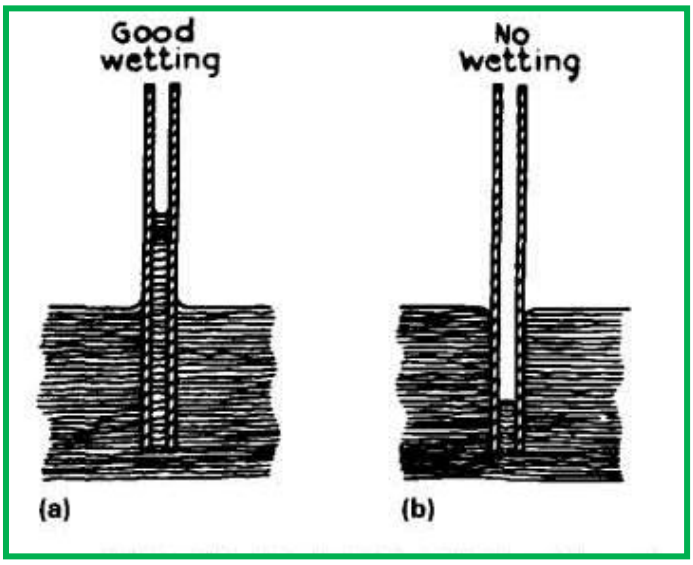

Figure 4-1 Principle of Brazing [38]

Brazing and Soldering requires the application of a number of scientific and engineering skills to produce joints of satisfactory quality and reliability. Brazing employs highest temperatures than soldering, but the fundamental concepts are similar, particularly with respect to metallurgy and surface chemistry (Table 4-1). However, joint design, materials to be joined, filler metal and flux selection, heating methods and joint preparation can vary widely between the two processes. Economic considerations involving filler metal and process technology are also varied, particularly in relation to automated techniques and inspection and testing. Brazing and soldering are performed in many industries, from exotic applications in the electronics and aerospace field to everyday plumbing applications.

Table 4-1 Comparison of joining processes [39]

Parameter	Soldering	Brazing	Welding
Joint formed	Mechanical	Metallurgical	Metallurgical
Filler metal melt temperature ^{O}C	<450	>450	>450
Base metal	Does not melt	Does not melt	Melts
Fluxes	Required	Optional	Optional
Typical heat sources	Soldering iron; ultrasonic's; resistance; oven	Furnace; chemical reaction; induction; torch; infrared	Plasma; electron beam; tungsten and submerged arc; resistance; laser
Tendency to wrap or burn	Atypical	Atypical	Potential distortion and warpage of base-metal likely
Residual stresses	.....	.....	Likely around weld area

4.3 ELEMENTS OF THE BRAZING PROCESS

An engineer must consider reliability and cost when designing the brazed joint. Joint strength, fatigue resistance, corrosion susceptibility, and high-temperature stability are additional concerns that determine the selection of joint design, braze filler materials, and processing parameters. A careful and intelligent appraisal of the following elements is required in order to produce satisfactory brazed joints [38-40]:

- Filler-metal flow
- Base-metal characteristics
- Filler-metal characteristics
- Temperature and time

- Large scale mechanical properties
- Placement of filler-metal
- Surface preparation
- Joint design and clearance
- Source of heating
- Protection by an atmosphere or flux.

4.3.1 FILLER-METAL FLOW

As mentioned previously, wetting is only one important facet of the brazing process. A low contact angle, which implies wetting, is also necessary, but is not a sufficient condition itself for flow. Viscosity is also important. Brazing filler metals with narrow melting ranges that are close to the eutectic composition generally have lower viscosities than those with wide melting ranges. Thus, a high surface tension of liquid filler metal, a low contact angle, and low viscosity are all desirable. Flowability is the property of a brazing filler metal that determines the distance it will travel away from its original position, because of the action of capillary forces. To flow well, a filler metal must not gain an appreciable increase in its liquidus temperature even though its composition is altered by the addition of the metal it has dissolved. This is important because the brazing operation is carried out at temperatures just above the liquidus of the filler metal. The composition and surface energy of liquids and solids are assumed to remain constant. In real systems, however, these interactions occur [38-40].

4.3.2 BASE-METAL CHARACTERISTICS

The base metal has a prime effect on joint strength. A high strength base metal produces joints of greater strength than those made with softer base metals(other factors being equal). When hardenable metals are brazed, joint strength becomes less predictable. This is because more-

complex metallurgical reactions between hardenable base metals and the brazing filler metals are involved. These reactions can cause changes in the base metal hardenability and can create residual stresses. In cases where different materials make up the assembly, and gaps may open or close as heating proceeds to the joining temperature, the coefficient of thermal expansion becomes vitally important. Several metallurgical phenomena influence the behavior of brazed joints and, in some instances, necessitate special procedures [38-40].

4.3.3 FILLER-METAL CHARACTERISTICS

Proper fluidity at brazing temperatures to ensure flow by capillary action and to provide full alloy distribution. Stability to avoid premature release of low melting point elements in the brazing filler metal. Ability to wet the base-metal joint surfaces, low volatilization of alloying elements of the brazing filler metal at brazing temperatures. Ability to alloy or combine with the base metal to form an alloy with a higher melting temperature. Control of washing or control of erosion between the brazing filler metal and the base metal within the limits required for the brazing operation.

4.3.4 BRAZING TEMPERATURE

When choosing a brazing filler metal, the first selection criterion is the brazing temperature. Some brazing-temperature ranges are given in Table 4-2. Very few brazing filler metals possess narrow melting ranges. Brazing filler metals in which the solidus and liquidus temperatures are close together do not usually exhibit a strong tendency to coexist as a mixture of liquid and solid phases or to liquate. They flow readily and should be used with small joint clearances. As the solidus and liquidus temperatures diverge, the tendency to liquate increases, requiring greater precautions in brazing filler metal application. The mixture of solid and liquid metal can aid gap filling. The necessity for the brazing filler metal to melt below the solidus of the base metal is

just one of several factors that affect its selection. It may be necessary for the brazing filler metal to melt below the temperature at which parts to be brazed [38-40].

4.3.5 LARGE-SCALE MECHANICAL PROPERTIES

Large scale mechanical properties of brazing filler metals can be a guideline for their suitability(in terms of strength, oxidation resistance, and so on) for use in different capillary joining applications. However, designers cannot use the mechanical properties of brazed assemblies that are related to different joint configurations brazed at given cycles of time and temperatures.

4.3.6 PLACEMENT OF FILLER METAL

The placement of the brazing filler metal is an important design consideration, not only because the joint must be accessible to the method chosen, but because, in automatic heating setups, the filler metal must be retained in its location until molten. Brazing filler metals are available in different forms and filler-metal selection may depend on which form is suitable for a particular joint design. Several general rules apply in the filler-metal placement. Wherever possible, the filler metal should be placed on the most slowly heated part of the assembly in order to ensure complete melting. Although brazing is independent of gravity, gravity can be used to assist filler-metal flow, particularly for those filler metals having wide ranges between their solidus and liquidus temperatures.

4.3.7 SURFACE PREPARATION

A clean, oxide-free surface is imperative to ensure uniform quality and sound brazed joints. All grease, oil, dirt, and oxides must be carefully removed from the base and filler metals before

brazing, because only then can uniform capillary attraction be obtained. Brazing should be done as soon as possible after the material has been cleaned. The length of time that the cleaning remains effective depends on the methods involved, atmospheric conditions, storage and handling practices, and other factors. Cleaning operations are commonly categorized as being either chemical or mechanical. Chemical cleaning is the most effective means of removing all traces of oil or grease. Trichloroethylene and tri sodium phosphate are the usual cleaning agents employed. Oxides and scale that cannot be eliminated by these cleaners should be removed by other chemical means. The selection of the chemical cleaning agent depends on the nature of the contaminant, the base metal, the surface condition, and the joint design. Regardless of the nature of the cleaning agent or the cleaning method used, it is important that all residue or surface film be adequately rinsed from the cleaned parts to prevent the formation of other equally undesirable films on the faying surfaces. Objectionable surface conditions can be removed by mechanical means, such as grinding, filing, wire brushing, or any form of machining, provided that joint clearances are not disturbed [38-40].

4.3.8 JOINT DESIGN AND CLEARANCE

A brazed joint is not a homogeneous body. Rather, it is a heterogeneous area that is composed of different phases with different physical and chemical properties. In the simplest case, it consists of the base-metal parts to be joined and the added brazing filler metal. However, dissimilar materials must also be considered. Small clearances are used because the smaller the clearance, the easier it is for capillarity to distribute the brazing filler metal throughout the joint area and the less likely it is that voids or shrinkage cavities will form as the brazing filler metal solidifies. The optimum joints are those in which the entire joint area is wetted and filled by the brazing filler metal. Typically, brazing clearances that range from 0.03 to 0.08 mm resulting in strong capillary

action and greatest joint strength. Because brazing relies on capillary attraction, the design of a joint must provide an un obstructed and unbroken capillary path to enable the escape of flux, if used, as well as allow the brazing filler metal into the joint [38-40].

Table 4-2 Composition of selected filler metals used for brazing applications [40 and 41]

		Liquidus		Solidus	
Filler metal	Composition	°C	°F	°C	°F
Silver	99.99Ag	961	1762	961	1762
Cusil	72Ag-28Cu	780	1436	780	1436
Palcusil 5	68Ag-27Cu-5Pd	810	1490	807	1485
Palcusil 10	58Ag-32Cu-10Pd	852	1566	824	1515
Palcusil 15	65Ag-20Cu-15Pd	900	1650	850	1560
Palcusil 25	54Ag-21Cu-25Pd	950	1740	900	1650
Capsil 9	82Ag-9Ga-9Pd	880	1615	845	1555
Nicusil 3	71.5Ag-28.1Cu-0.75Ni	795	1465	780	1435
Nicusil 8	56Ag-42Cu-2Ni	893	1639	771	1420
T50	62.5Ag-32.5Cu-5Ni	866	1591	780	1435
T51	75Ag-24.5Cu-0.5Ni	802	1476	780	1435
T52	77Ag-21Cu-2Ni	830	1525	780	1435
Cusiltin 5	68Ag-27Cu-5Sn	760	1400	743	1369
Cusiltin 10	60Ag-30Cu-10Sn	718	1324	602	1116
Braze 630	63Ag-28Cu-6Sn-3Ni	800	1472	690	1275
Braze 580	57Ag-33Cu-7Sn-3Mn	730	1345	605	1120
Braze 655	65Ag-28Cu-5Mn-2Ni	850	1560	750	1380
Silcoro 60	60Au-20Ag-20Cu	845	1550	835	1535
Nioro	82Au-18Ni	950	1740	950	1740
Palnioro 7	70Au-22Ni-8Pd	1037	1899	1005	1840
Incuro 60	60Au-37Cu-3In	900	1650	860	1580
Silcoro 75	75Au-20Cu-5Ag	895	1645	885	1625
Nicoro 80	81.5Au-16.5Cu-2Ni	925	1695	910	1670
Palcusil 20	52Au-28Cu-20Pd	925	1695	875	1605
Goid	99.99Au	1064	1947	1064	1947
Palniro 4	30Au-36Ni-34Pd	1169	2136	1135	2075
Palniro 1	50Au-25Ni-25Pd	1121	2050	1102	2016
Ticusil	68.8Ag-26.7Cu-4.5Ti	850	1560	830	1525
Painicusil	48Ag-18.9Cu-10Ni-22.5Pd	1179	2154	910	1670
Palco	65Pd-35Co	1235	2255	1230	2245
Incusil15	62Ag-24Cu-15In	705	1300	630	1165
Incusil 10	63Ag-27Cu-10In	730	1345	685	1265
BAg-8a	71.8Ag-28Cu-0.2Li	760	1400	760	1400
BAg-19	92.5Ag-7.3Cu-0.2Li	890	1635	760	1400
Braze 071	85Cu-7Ag-8Sn	986	1807	665	1230
Braze 852	85Ag-15Mn	970	1780	960	1760
Nioroni	73.8Au-26.2Ni	1010	1850	980	1795
Nicuman 23	67.5Cu-23.5Mn-9Ni	955	1750	925	1695
Palsil 10	90Ag-10Pd	1065	1950	1002	1836
Palni	60Pd-40Ni	1238	2260	1238	2260

4.3.9 HEAT SOURCES FOR BRAZING [42]

4.3.9.1 TORCH BRAZING

Torch brazing is a heating source supplied by a fuel gas flame. Gases include acetylene, hydrogen or propane. A typical application is to braze a tube into a fitting using copper or silver brazing filler metals.

Figure 4-2 Torch Brazing

4.3.9.2 INDUCTION BRAZING

Electric coils, which are designed for specific joint geometries, are used to heat the part and the brazing filler metal until the liquid metal flows via capillary attraction into the joint. This process is primarily used for brazing with copper and silver alloys.

Figure 4-3 Induction Brazing

4.3.9.3 CONTINUOUS FURNACE

Conveyor belts transport the pre-alloyed components through preheating, heating and post-heating zones where the braze alloy reaches temperature, then re-solidifies during cooling. Silver and copper based brazing filler metals are most commonly used in these processes.

4.3.9.4 RETORT OR BATCH FURNACE

The furnace used can be refractory lined and heated by gas, oil or electricity. Atmospheres can be either a generated gas (endothermic or exothermic) or an inert gas such as argon or nitrogen. Hydrogen gas is also used for brazing filler metals that oxidize in other atmospheres. Copper, silver, nickel and gold based brazing filler metals can be brazed successfully in these types of furnaces.

4.3.9.5 VACUUM FURNACE

A furnace with electrically heated elements that surround the workload and heat the brazing filler metal to the liquidus state so that flow and capillary attraction are achieved. To permit brazing of alloys that are sensitive to oxidation at high temperatures, a pumping system is employed that removes oxygen. Gold, copper, nickel, cobalt, titanium and ceramic based filler metals are successfully vacuum brazed.

4.4 AVAILABLE FORMS OF BRAZE FILLER METALS [41 AND 42]

- Braze Powder
- Braze Paste
- Braze Tape
- Braze Foil
- Braze Rod

4.5 LOW AND HIGH ENERGY TEMPERATURE BRAZING

The filler metals used for low-temperature brazing are based on aluminum, silver, copper and other metals with relatively low melting temperatures. On the other hand, for high-temperature brazing, it is based on heat-resistant metals such as nickel, cobalt, iron, the noble metals other than silver, refractory metals etc. The filler metals containing nickel as their principal alloying element are most important for high-temperature service. In our case, a nickel based filler metal (AWS, BNi-7) has been used and its chemical composition along with the chemical composition of base metal (SS-316L) is given in Table 4-3 [43]. This high temperature brazing process is commonly known as Nicro-brazing.

Table 4-3 Composition of Base and Filler metals, (Wt. %)

Material	C	Si	P	B	Cr	Ni	Mo	Mn	Fe
Filler metal (BNi-7)	0.03	-	10	-	14	Balance	-	-	-
Base metal (SS 316L)	0.03	0.4	0.03	0.001	17	13	2.36	1.27	Balance

High temperature brazing is a subset of brazing operations and it can be defined as the brazing in which brazing operations are conducted at temperatures generally in excess of 927°C [44]. High temperature service requirements are stringent and many factors must be considered to obtain consistently sound brazed joints. High temperature brazed joints are strong in nature. Nickel based filler metals are mainly used in High Temperature Brazing and this method is commonly

known as nicrobarzing method. Experiments were carried out in laboratory, to develop Nicrobrazed joints, both by induction heating method and furnace exposure method.

4.6 INDUCTION HEATING USED IN HIGH TEMPERATURE BRAZING

For high-temperature brazing, because of the need to protect the work-pieces from oxidation, it is done exclusively in chambers or enclosures that can be either evacuated or filled with a reducing or inert gas atmosphere during heating [45]. Induction heating system as shown in Figure 4-4 is a very good heat source for this purpose, because it provides a reliable, compact solution for heating the parts with a quick, clean source of heat, ideal for repeatable, non-contact heating of parts. Heating is very well controlled and can be extremely rapid. Chambers for controlled atmosphere brazing can be fabricated from quartz tube; in our case, heating coil of the induction heating system fits around the quartz tube in which work piece is kept. Heating power is made available using the principle of induction. When an alternating current is passed through a conductor such as a wire or copper tube, a magnetic field is generated and if this field passes through another conductor (work piece) in the vicinity, current will circulate through the object. If enough current circulates through it, the object will get heated. The high-frequency induction heating method for brazing is a clean and rapid process and it requires little operator skill. The work piece is placed inside a heating coil carrying alternating current, which induces the heating current in the desired area.

Figure 4-4 Induction Heating System for Brazing Application

The coils, which are water cooled, are designed specifically for each part. Therefore, heating efficiency relies on establishing the best coil design and power frequency for each application. The magnitudes of the induced currents decrease continuously from the surface of the specimen, and this phenomenon is known as "Skin effect". The temperature of the brazing filler metal has an important effect on the wetting and alloying action, which increases with increasing temperature. The temperature must be above the melting point of the brazing filler metal and below the melting point of the parent metal.

4.6.1 PROTECTIVE ATMOSPHERES

The primary function of a flux or a controlled atmosphere is to protect the base metal and filler metal from oxidation during brazing operation. Inert gas atmospheres can be used to braze most metals. Although both argon and helium can be used for controlled atmosphere brazing, argon is most frequently used as in our experiments. The parts to be brazed must be cleaned and handled carefully, because the primary purpose of the inert gas atmosphere is to prevent formation of oxides during brazing.

4.7 EXPERIMENTAL DETAILS

In the instrumented capsules, normally thermocouples of around 1.0 mm dia will be attached to measure the temperature of specimens. It will be attached with intermediate or closure plugs in a leak tight manner to know the temperature of specimens undergoing irradiation. The thermocouples can be joined to the closure plugs by nicrobrazing method. Drawing of the sample used for high-temperature brazing for above purpose is shown in Figure. 4-5.

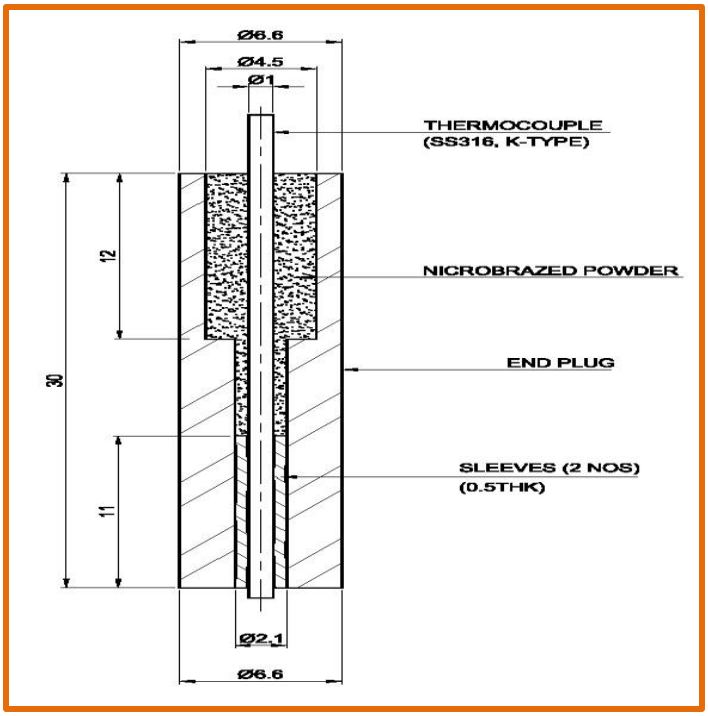

Figure 4-5 Drawing of the sample (as end plug) used for high-temperature brazing

Prior to the implementation of induction heating process, the details of the actual heating requirements must be considered. Such considerations include type of heating, heating time, material of the component, peak temperature etc. Type of heating may be surface heating or through (volume) heating. In the present application, volumetric heating is required. It is important to measure the temperature of the component during induction heating and control it by increasing/ decreasing the current of the induction heating system. Current is the only parameter which can be controlled and depending on that, power, frequency and, in turn, the temperature of component varies.

Two numbers of K-type thermocouples of diameter 1.5 mm were attached on the outer surface of the component to measure the temperature during induction heating. Hot junction of the thermocouple was kept in the middle zone of heating coil so that peak temperature faced by the component can be monitored and controlled.

Specimen was kept inside the quartz tube, which in turn, was placed inside the induction heating coil. Specimen was positioned inside the quartz tube in such a way that it was within the range of the induction heating coil to ensure the uniform heating in it. Argon gas flow was directed on the specimen inside the quartz tube so that at brazing temperature (eg. 1303 K), oxidation can be avoided, and at the same time brazing alloy which is in the form of powder is not disturbed. Arrangement for the development of high-temperature brazed joints using induction heating in an argon gas environment is shown in Figure 4-6.

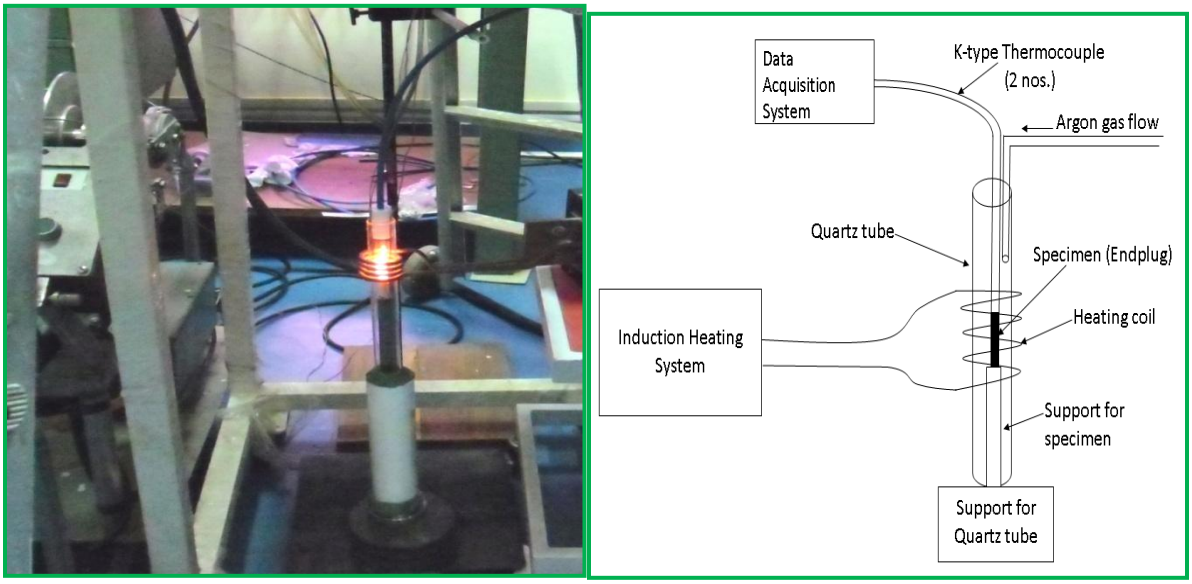

(a) (b)

Figure 4-6 (a) Photograph and (b) Sketch of the arrangement for the development of high-temperature brazed joints using induction heating in an argon gas environment,

A number of trials were carried out to optimize the brazing parameters such as current, peak temperature, duration (time) at peak temperature, argon flow rate etc. Parameters recorded during one of the high-temperature brazing operation during heating and cooling cycle are given in Table 4-4.

Table 4-4: Parameters recorded during heating and cooling

S. No.	Time (min)	Current (A)	Power (W)	Frequency (kHz)	Temperature shown by Thermocouple-1 (^{o}C) (Away from sample)	Temperature shown by Thermocouple-2 (^{o}C) (Near to sample)	Argon gas flow rate (lpm)	Remarks
During heating phase								
1	0	100.7	136	285	28	28	10	Induction heating started
2	2	131.1	253	282	600	620	10	
3	3	131.1	253	282	800	835	10	
4	3	140.6	316	282	800	835	10	
5	5	150.1	362	281	850	900	10	
6	6	150.1	362	281	902	945	10	
7	6	155.8	398	281	902	945	10	
8	7	161.5	442	280	940	984	10	
9	8	169.1	481	280	961	1006	10	
10	10	172.9	516	279	991	1030	10	
11	11	174.8	527	279	991	1032	10	
12	13	174.8	527	279	991	1029	10	
13	14	174.8	527	279	991	1030	10	Induction heating stopped

During cooling phase								
1	0	0	0	0	557	555	10	
2	1	0	0	0	372	357	10	
3	2	0	0	0	254	247	10	
4	3	0	0	0	186	177	10	
5	4	0	0	0	142	134	10	
6	5	0	0	0	110	106	10	
7	6	0	0	0	95	88	10	
8	6	0	0	0	87	82	10	
9	7	0	0	0	80	80	0	Argon gas flow, Stopped

4.8 QUALIFICATION OF NICROBRAZED JOINTS

One of the high-temperature brazed joints (specimen) is shown in Figure. 4-7. Similar specimens have been produced to qualify and characterize the high-temperature brazed joint to be used for instrumented capsule. Samples were examined for leak, and defects like void, porosity, change in hardness compared to the base metal, etc. The instrumented capsule in which this high temperature brazed joint would be used, will be immersed in sodium. Therefore, sodium compatibility test was also carried out and the results obtained are also presented here.

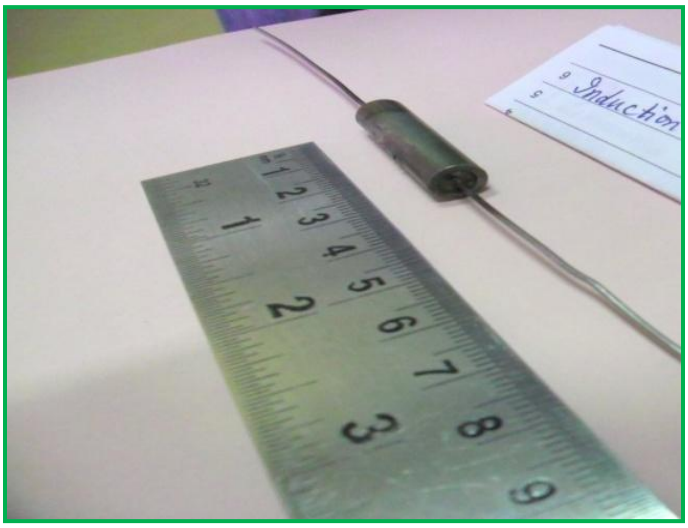

Figure 4-7 High-temperature brazed joint (sample)

4.8.1 HELIUM LEAK TEST

Helium leak detection (HLD) system was used to detect helium leak through the high temperature brazed joints. No observable leak was found during HLD test. The leak rate observed was $3.0*10^{-8}$ mbar.lit/sec.

4.8.2 METALLOGRAPHIC ANALYSIS

Samples were cut circumferentially and moulds were prepared. Grinding and polishing was done using PRESI, MECATECH Z34 machine on the samples. Emery sheet of grade 120 for 12 minute and emery sheet of grade 400 for 3 minute were used for fine grinding. Polishing was done using same machine with the following liquids and lubricants:

PRESI Reflex - 9µ [liquid] for 3 minutes

PRESI Reflex - 3µ [liquid] for 3 minutes

PRESI Reflex - LUB [Lubricant] for 3 minutes

After grinding and polishing, etching was carried out on the samples using electrolytic etching for 10 sec with oxalic acid as electrolyte. Microstructure observed in metallurgical microscope is shown of Figure. 4-8. No cracks have been observed in the high-temperature brazed region.

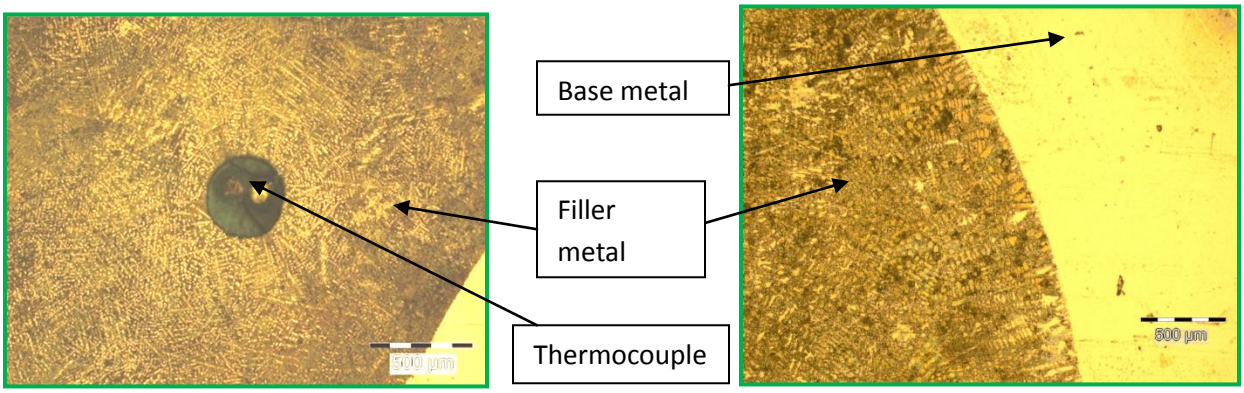

Figure 4-8 Microstructure observed in metallurgical microscope (a) Formation of bond between thermocouple sheath (SS-316) and filler metal (BNi-7), and (b) Formation of bond between base metal (SS-316) and filler metal (BNi-7).

4.8.3 MICRO HARDNESS TEST

Micro hardness test was carried out on the samples by using MATSUZAWA make micro hardness tester. The hardness was measured in the base metal and filler metal region, using test load of 200 gf. Result obtained has been shown in Figure 4-9. Hardness of nicrobrazed region is higher than the base metal because of inter metallic bonds formed in the joint region.

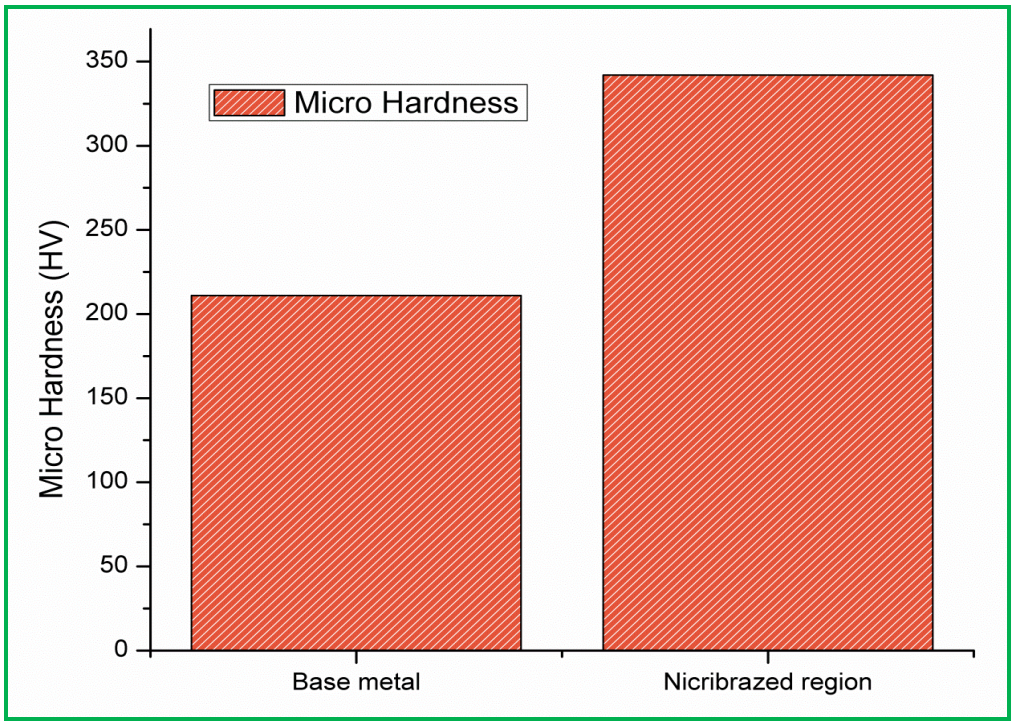

Figure 4-9 Results of micro hardness test

4.8.4 EFFECT OF BRAZING TEMPERATURE ON EMF OF THERMOCOUPLE

The thermocouple, which was passed through the end plug, and on which brazing operation was carried out, was tested in the furnace along with a reference thermocouple to check for deviation in its output (if any). It was observed that there is no change in the output of thermocouple (emf) due to exposure of high temperature (1303 K) for a short duration during brazing.

4.8.5 SODIUM COMPATIBILITY TEST

Nicrobrazed specimens and blanks (SS-316L) were considered in the sodium compatibility test. Two numbers of blanks (SS-316L) along with the two number of nicrobrazed specimens were used to verify that element leached out (if any) in the liquid sodium is from base metal (SS-316L) or from filler metal (BNi-7). They were concentrically placed in four numbers of alumina

crucibles (27 mm ID and 47 mm height). Sodium was filled in the alumina crucibles up to the height of 35 mm. A nickel foil (10 mm width, 50 mm long and 100 μm thicknesses) was kept in the alumina crucible containing sodium to estimate the carbon content of sodium by foil equilibration technique. The crucibles were subsequently covered with stainless steel foil (100 μm) to prevent loss of sodium by evaporation and were placed in four numbers of separate stainless steel vessels fitted with CF 40 flanges. The leak tightness of the vessels was achieved using annealed copper gasket. Thereafter the stainless steel vessels were placed in resistance furnaces and equilibrated at 873 K for a period of 100 h. After cooling, vessels were removed from the furnaces and transferred to an argon filled glove box to retrieve the specimens.

Table 4-5 Observed change in weight due to exposure of sodium

Sl. No.	Sample Identification	Temperature and time of sodium exposure	Weight before Sodium exposure (as-brazed) (g)	Weight after Sodium exposure (g)	Change in weight (g)	Change in weight (%)	Remarks
1.	Specimen-1	823 K, 100 h	6.1313	6.1354	+0.0041	+0.067	No Significant Change in weight
2.	Specimen-2		6.7139	6.7337	+0.0198	+0.294	
3.	Blank-1		5.5209	5.5216	+0.0007	+0.012	
4.	Blank-2		5.5756	5.5760	+0.0004	+0.007	

Specimens were weighed using a semi microbalance (Mettler Toledo, AT-201), before the equilibrium experiment. After completing the equilibrium experiment, the specimens were recovered and thoroughly cleaned with isopropyl alcohol. They were weighed and compared to the earlier weight measurements to determine if there were any significant weight changes. The results are shown in the Table 4-5. It was observed that there is no significant change in weight due to exposure of sodium on the high temperature brazed joints (Specimen 1 & 2).

4.9 COMPARATIVE STUDY ON JOINTS DEVELOPED BY HIGH TEMPERATURE NICROBRAZING, LASER AND GTAW JOINING PROCESSES

In the previous sections, the procedure of development of high temperature brazed joints and their qualification tests have been discussed. Since high temperature brazing, laser welding, or gas tungsten arc welding are three different processes available for the fabrication of instrumented irradiation capsules, a comparative study of these three types of joints was carried out. A comparative study has been performed on these joining methods to identify the best suitable method for our application. Figure 4-10 shows a typical end plug- tube joint configuration, and the same joint configuration was maintained for all the joining methods. Tube and end plug joints were made by GTAW, Laser and Nicrobrazing joining processes. A gap of 50 microns was provided for filling brazing filler metal in the nicrobrazing technique. Gap of 30 microns to 80 microns has been reported in the literature [46 and 47]. No filler metal was used in GTAW and laser methods.

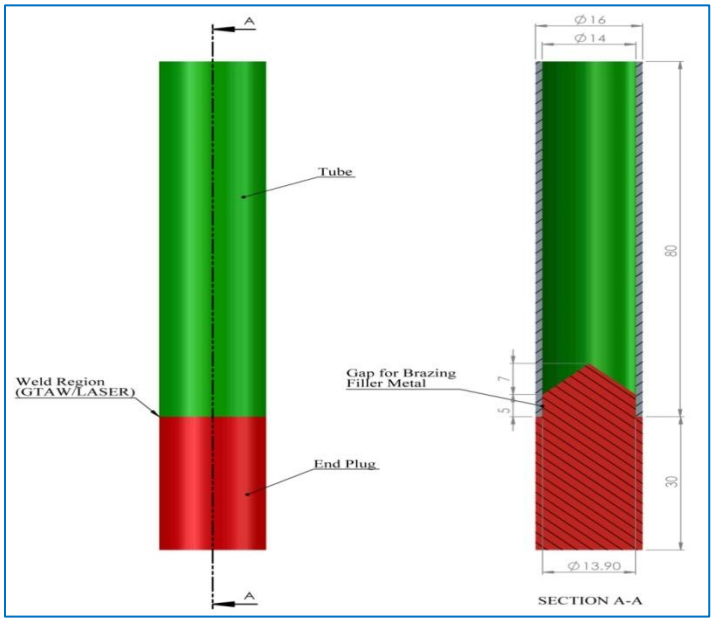

Figure 4-10 Schematic of parent metal geometry

4.9.1 CHEMICAL COMPOSITION OF MATERIALS

Table 4-6. Chemical composition of materials used (Wt. %)

Material	C	Mn	Si	P	Mo	B	Cr	Ni	Fe
Tube (SS 316)	0.067	1.27	0.37	0.041	2.10	-	16.94	10.04	Balance
End plug (SS 316L)	0.03	1.27	0.4	0.03	2.36	0.001	17	13	Balance
Brazing Filler metal (BNi-7)	0.03	-	-	10	-	-	14	Balance	-

4.9.2 JOINT BY HIGH TEMPERATURE NICROBRAZING TECHNIQUE

Nicrobrazed joints were prepared by furnace exposure method. The sample was placed inside the quartz tube, which in turn was placed inside the isothermal zone of electrical furnace. Argon gas flow was directed on the component from the height of around 170 mm inside the quartz tube so that at brazing temperature (eg. 990°C), oxidation can be avoided and at the same time brazing alloy which is in the form of powder is not disturbed. Arrangement for the development of high-temperature brazed joints using furnace heating in an argon gas environment is shown in Figure 4-11. A number of trials were carried out to optimize the brazing parameters such as peak temperature, duration (time) at peak temperature, argon flow rate etc. Parameters recorded during one of the high-temperature brazing operation during heating and cooling is given in the Table 4-7.

Figure 4-11 Arrangement for the development of high-temperature brazed joints using furnace heating in an argon gas environment

Table 4-7 Optimized parameters for high temperature furnace brazing

S.No	Peak Temperature(°C)	Duration/Time(min)	Argon gas flow rate (lpm)
During Heating phase			
1	30	0	10
2	340	5	10
3	501	10	10
4	623	15	10
5	891	20	10
6	990	25	10
7	990	30	10
During Cooling phase			
1	990	0	10

2	810	5	10
3	630	10	10
4	400	15	10
5	220	20	10
6	105	25	10
7	Temperature drop up to 50	30	10, stopped @ 50 ^{O}C

4.9.3 GAS TUNGSTEN ARC WELDING (GTAW)

Figure 4-12 shows the arrangement of GTAW setup. Gas tungsten arc welding process is based on the electric arc established between a non-consumable electrode of tungsten and the work-pieces to be joined. Part of the heat generated by the electric arc is added to the work-pieces, promoting the formation of a weld pool. The weld pool is protected from air contamination by a stream of an inert gas argon [48 and 49]. The process allows a precise control of heat addiction and the production of superior quality welds with low distortion and free of spatter. It is less economical than other consumable electrode arc welding processes, due to its lower deposition rate, and it is sensitive to windy environment because of the difficulty in shielding the weld pool. Besides it shows low tolerance to contaminants on filler or base metals.

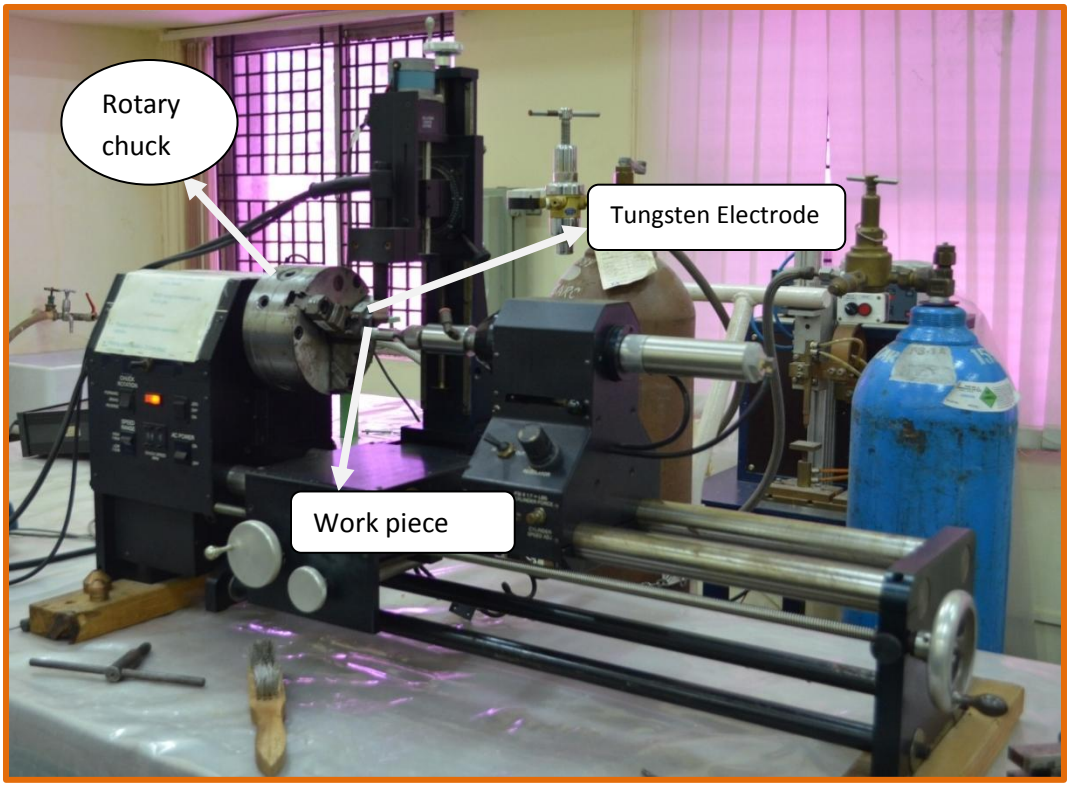

Figure 4-12 GTAW setup arrangement

Figure 4-13 shows the GTA welding operation. The welding machine is of semi- automatic type, which can handle work pieces of 5 mm to 100 mm diameter and 300 mm long. Current has direct influence on weld bead shape, welding speed and quality of the weld. Most GTAW welds employ direct current on electrode negative (DCEN) (straight polarity) because it produces higher weld penetration and higher travel speed than on electrode positive (DCEP) (reverse polarity). Besides, reverse polarity produces rapid heating and degradation of the electrode tip, because anode is more heated than cathode in gas tungsten electric arc [50].

Figure 4-13 GTAW operation

4.9.3.1 PROCESS PARAMETERS

The process parameters used during GTAW process are:

Weld current = 40 Amps

Voltage = 8 Volts

Traverse speed = $\frac{distance}{time}$ (mm/sec)

Traverse speed = 1.0048 mm/sec

Shielding gas(argon) flow rate = 10 lpm

Efficiency of GTAW process is taken as 80% [51]

Heat input can be determined as follows:

Heat input $_{GTAW}$ (J/mm) = {Current × Voltage/ Traverse speed} × Process efficiency

Heat input $_{GTAW}$ (J/mm) = {40 × 8/ 1.0048} × 0.8

Heat input $_{GTAW}$ = 254.77 J/mm

4.9.4 PULSED ND: YAG LASER WELDING

The most popular lasers for welding are the solid-state lasers of neodymium-doped yttrium aluminum garnet (Nd:YAG), generally pulsed wave, and the gas lasers of continuous-wave carbon dioxide (CO_2), whose lasing medium is a mixture of carbon dioxide, nitrogen and helium. Power density of laser welding (10^9-10^{11} Wm^{-2}) is significantly higher than that of arc welding processes (10^6-10^8 Wm^{-2}), though somewhat lower than electron beam welding (10^{11}-10^{13} Wm^{-2}) [52]. The beam energy delivered to the work-piece will be dissipated by reflection and absorption. Work-piece material is heated to a very high temperature, melted and may even vaporize due to very high power density concentrated in the focus of laser beam. Two modes of laser welding can be obtained, the heat conduction mode and the deep-penetration mode, depending on the power density in use [53].

Figure 4-14 CNC Laser work stage

Figure 4-14 shows the solid-state laser of Nd:YAG type, (average power of 530 W) made of a solid yttrium aluminum garnet rod doped with neodymium. Excitation of electrons in neodymium is done with high-power xenon flash lamps.

4.9.4.1 PROCESS PARAMETERS

The process parameters used in our experiments are discussed below.

Peak power = 2500 W

Pulse duration = 8 milli sec

Pulse energy, (J) = Peak power (W) * Pulse duration (sec)

Pulse energy = $2500^* (8^*10^{-3})$

Pulse energy = 20 Joules

Mean power (W) = Pulse energy (J) * Frequency

Frequency = 15 pps

Mean power = 20 * 15 = 300 W

Heat input $_{Laser}$ (J/mm) = {Mean Power/ Traverse speed} * Energy transfer efficiency

Efficiency of Nd: YAG laser is assumed to be 65% [54 and 55].

Traverse speed = 2 mm/sec

Heat input $_{Laser}$ (J/mm) = {300/ 2}* 0.65

Heat input $_{Laser}$ (J/mm) = 97.5

If percentage of over lapping factor is more than 70% , the welds are leak tight. This factor is verified for the process parameter

Over lapping factor (Q_f) = $\left[1 - \frac{V.t_f}{d_s + V.t_p}\right] * 100$

where, for our experiments

V = weld speed/traverse speed (mm/sec) = 2

t_f = 1/frequency = 1/15 = 0.066

d_s = spot diameter (mm) = 0.6

t_p = pulse duration (sec) = $8*10^{-3}$

$Q_f = \left[1 - \frac{2*(\frac{1}{15})}{0.6+(2*8*10^{-3})}\right] *100$

Q_f = 78.357 %

Now Q_f > 70%

Since Q_f is greater than 70% the welds are leak tight.

Table 4-8 Process Parameters of Pulsed Laser, GTAW and Nicrobrazing Processes

Parameters	Pulsed Laser	GTAW	Nicrobrazing
Peak power, KW	2.5	---	
Pulse duration, ms	8	---	
Frequency, pps	15	---	---
Pulse energy, J	20	---	
Mean power, W	300	---	
Heat Input, J/mm	97.5	254.77	

Arc current, A Voltage, V	-- --	40 8	--- ---
Temperature, °C Time, min	--- ---	--- ---	990 30
Defocusing distance, mm Spot diameter, mm Electrode diameter, mm Arc gap, mm	0 0.6 -- --	-- -- 2.4 1.5	---
Shielding gas Flow rate, lpm	99.99% Pure Argon 10	10	10
Traverse speed, mm/s	2	1.0048	---

4.9.5 RESULTS AND DISCUSSION

Process parameters of all the three joining processes are shown in Table 4-8.

4.9.5.1 HELIUM LEAK TEST

Helium leak detection (HLD) test was carried out to detect helium leakage (if any) through the high temperature nicrobrazed joints, GTAW and Laser welds. No observable leak was found during HLD test at $3.3*10^{-9}$ mbar.lit/sec. Figure 4-15 shows the samples of all the joining processes.

Figure 4-15 Samples of all the joining processes

4.9.5.2 METALLOGRAPHIC ANALYSIS

Metallographic analysis was carried out using the procedure discussed in section 4.8.2

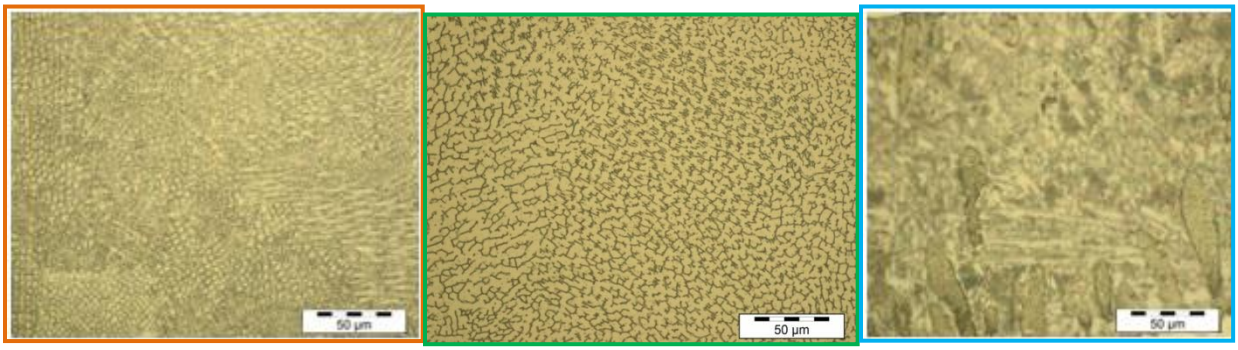

(a) Laser (b) GTAW (c) Brazing

Figure 4-16 Micro structures of weld joints at its centre

No cracks have been observed in the joint regions made by Laser, GTAW and brazing processes. Figure 4-16 and Figure 4-17 show the microstructures at centre of the weld joints. In laser weld, we noticed that two different size grains (fine grains and elongated grains) were formed due to solidification. In other two processes we could not observe any major difference in grain shape. Figure 4-17(a) shows the fine grains of equiaxed structure/phase and no inter metallic compounds formation in the joint region of laser weld, due to this we can expect more strength and ductility. Presence of fine equiaxed grains at weld region is reported to enhance strength and ductility of welds [55]. Figure 4-17(b) shows the elongated grains of columnar structure/phase and no formation of inter metallic compounds in the joint region of GTAW, but the strength of the joint will be lesser than the laser joint because of its grain size and shape. Figure 4-17(c) shows the martensentic structure of joint region. The brazing operation has been carried out at 950°C. The inter metallic compounds (eg: nickle chromite, ferric chromite) have been formed in the brazed joint region. Due to the presence of these compounds the strength of the joint will be

very less and the hardness will be more at the joint area. There are many factors on which strength of the brazed joint depends [56] eg. geometry and surface condition of the joint, size of the joint gap, properties of filler metal selected, heat source, brazing temperature, rate of heating, microstructure etc.

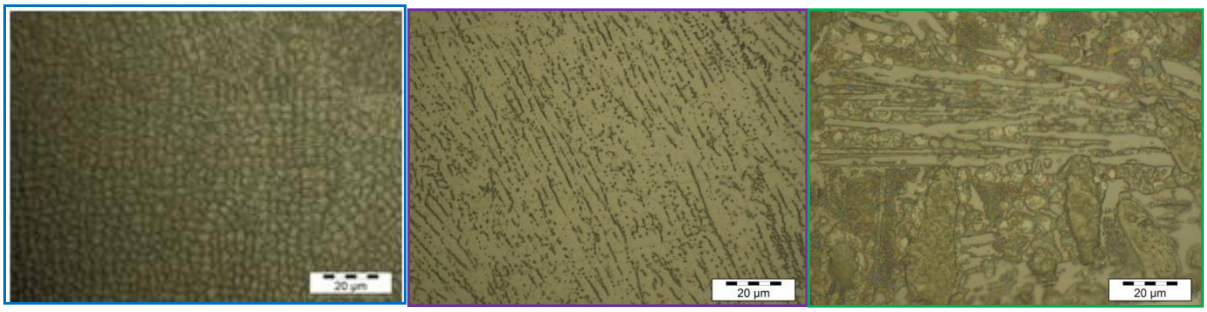

(a) Laser (b) GTAW (c) Brazing

Figure 4-17 Micro structures of weld joints at higher magnification

4.9.5.3 MICRO HARDNESS TEST

Micro hardness test on joint regions of all the three joining processes was carried out, using MATSUZAWA make micro hardness tester, and with a test load of 0.2Kg and dwell time of 10 seconds. We have noticed the difference in hardness values of all the three joining process. High temperature nicrobrazing joints have more hardness value than other two joining(Laser and GTAW) processes. Figure 4-18 shows the hardness values obtained by all the three joining processes.

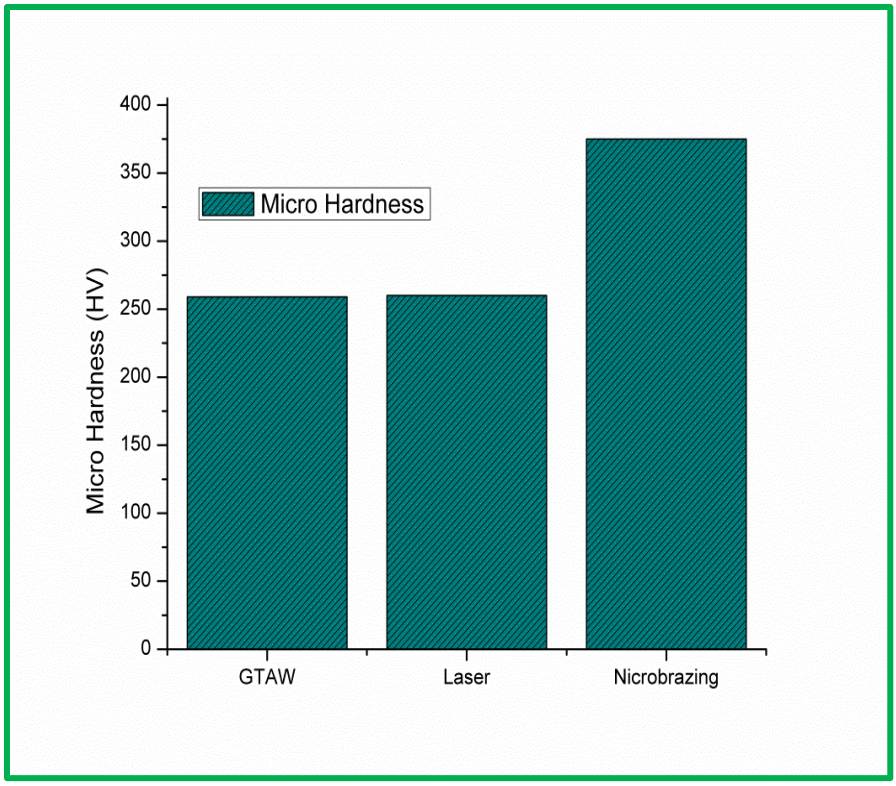

Figure 4-18 Micro hardness values obtained by all the three joining processes

- **Summary**

High temperature nicrobrazing procedure has been established successfully and joints have been tested and qualified. High-temperature brazed joints have been developed using induction heating in an argon gas environment for instrumented capsules to be used for fast reactor applications. Brazed joint formed between the base metal (SS-316L) and filler metal (BNi-7) is leak tight and is compatible with sodium at 873 K upto 100 h. This experimental result will be useful in the development of instrumented irradiation capsules.

High temperature nicrobrazing of AISI 316 stainless steels has been studied by comparing with pulsed laser and gas tungsten arc welding processes. Welds have been analyzed on the

aspects of helium leak detection (HLD), microstructures and micro hardness. It is observed that, no observable leak was found during HLD. Microstructures of welds are noticed to have variation in solidification morphology due to differences in material- heat source interaction and no cracks were noticed. Nicrobrazed joints are harder than GTAW and Laser weld joints.

CHAPTER - 5

5

DESIGN AND DEVELOPMENT OF OUT-OF-PILE VERSION OF INSTRUMENTED CAPSULE FOR ONLINE DETERMINATION OF UNIAXIAL CREEP BEHAVIOR IN STRUCTURAL SPECIMEN

The chapter starts with a brief introduction about the irradiation capsule, bellows and its specifications, tests performed on the bellows and LVDTs. Discussion has been made on experiments carried out on irradiation capsule to test the bellows performance. Design, assembly and out-of-pile experiments carried out on irradiation capsule with special thermocouple attachment have been cleared explained. Finally experimental results obtained are comparison with literature results.

5.1 INTRODUCTION

Irradiation capsule is a device designed to carry out irradiation of any fuel, structural material, and shielding material specimens in a reactor. Diameteral increase of fuel pins due to thermal and irradiation creep, apart from irradiation swelling, reduces the coolant flow area around the fuel pins affecting the effective removal of heat generated in the fuel pins. Such changes due to creep can be determined by material irradiation tests. There is an increasing interest in the use of instrumented irradiation tests for creep measurements. In instrumented irradiation tests, parameters such as specimen temperature, the load exerted on the specimen, specimen elongation etc, are monitored and/or controlled using suitable instruments (extensometer, linear variable differential transformer [LVDT], bellows, thermocouples, etc). Tests with in-pile measurement during irradiation are able to offer more control over experimental variables, more detailed

results associated with the phenomena of interest, and improved accuracy relative to non-instrumented irradiation tests. The resulting data are relatively easy to analyze and apply to design. Such benefits provide motivation for ongoing efforts to measure creep behavior during in-pile irradiation [28].

Irradiation creep property is of primary importance for assessing the integrity of core components of reactors, and therefore irradiation creep has been widely studied for core materials. Creep test rigs have been used for many reactor programs all over the world in the past [6, 18, 22, 23 and 27] to detect the deformation of tensile and creep specimens with bellows to apply a load on the specimen and LVDTs to detect the growth of the specimen. Out-of-pile version of instrumented irradiation capsule has been developed in this work for determination of online creep deformation in a tensile specimen. Details of the design, development, assembly and the tests carried out in the furnace for the out-of-pile version of instrumented irradiation capsule are discussed in this chapter.

5.2 SELECTION OF BELLOWS

Figure 5-1 Special bellow assembly

Bellows (Figure 5-1) have been fabricated in the industry using Inconel 625 material to withstand the high temperature and pressures.

5.2.1 SPECIFICATIONS OF BELLOWS

Specifications of bellows is given in table 5.1.

Table 5-1. Specifications of bellows

Bellows ID (mm)	**8**
Bellows OD (mm)	13.4
Thickness (mm)	0.25
No. of ply	2
Convolutions	6
Conv. Length (mm)	18
Bellows outer tube OD (mm)	16
Bellows outer tube ID (mm)	14
Bellows inner tube OD (mm)	6
Bellows inner tube ID (mm)	4
Total length (mm)	94

5.2.2 CHEMICAL COMPOSITION OF MATERIALS USED IN THE CAPSULE

Table 5-2. Chemical composition of materials used (Wt. %)

Material	C	Mn	Si	P	S	Cr	Mo	Fe	Ni
Inconel 625 (Bellows)	0.03	0.02	0.13	0.005	<0.001	20.60	8.63	4.03	Bal
SS 316 (Bellows end plugs and central tube)	0.067	1.27	0.37	0.041	0.029	16.94	2.10	Bal	10.04
SS 316L Specimen	0.03	1.27	0.4	0.03	-	17	2.36	Bal	13

5.2.3 TESTS PERFORMED ON BELLOWS AFTER FABRICATION

Table 5-3 Tests performed on bellows after fabrication

Type of test	**Experimental parameter**	**Results**
Pressure Test	**at 42 MPa**	**No leak**
Mass spectrometer leak test	$1.5*10^{-8}$ mbar.lit/sec	No leak
Cycle life test	at 29 MPa	> 299 cycles

5.3 COMPONENTS OF INSTRUMENTED IRRADIATION CAPSULE

Figure 5-2 shows the schematic of instrumented irradiation capsule, and Figures 5.3 to 5-6 shows the detailed drawings of components required for instrumented capsule to measure the instantaneous elongation of structural specimen.

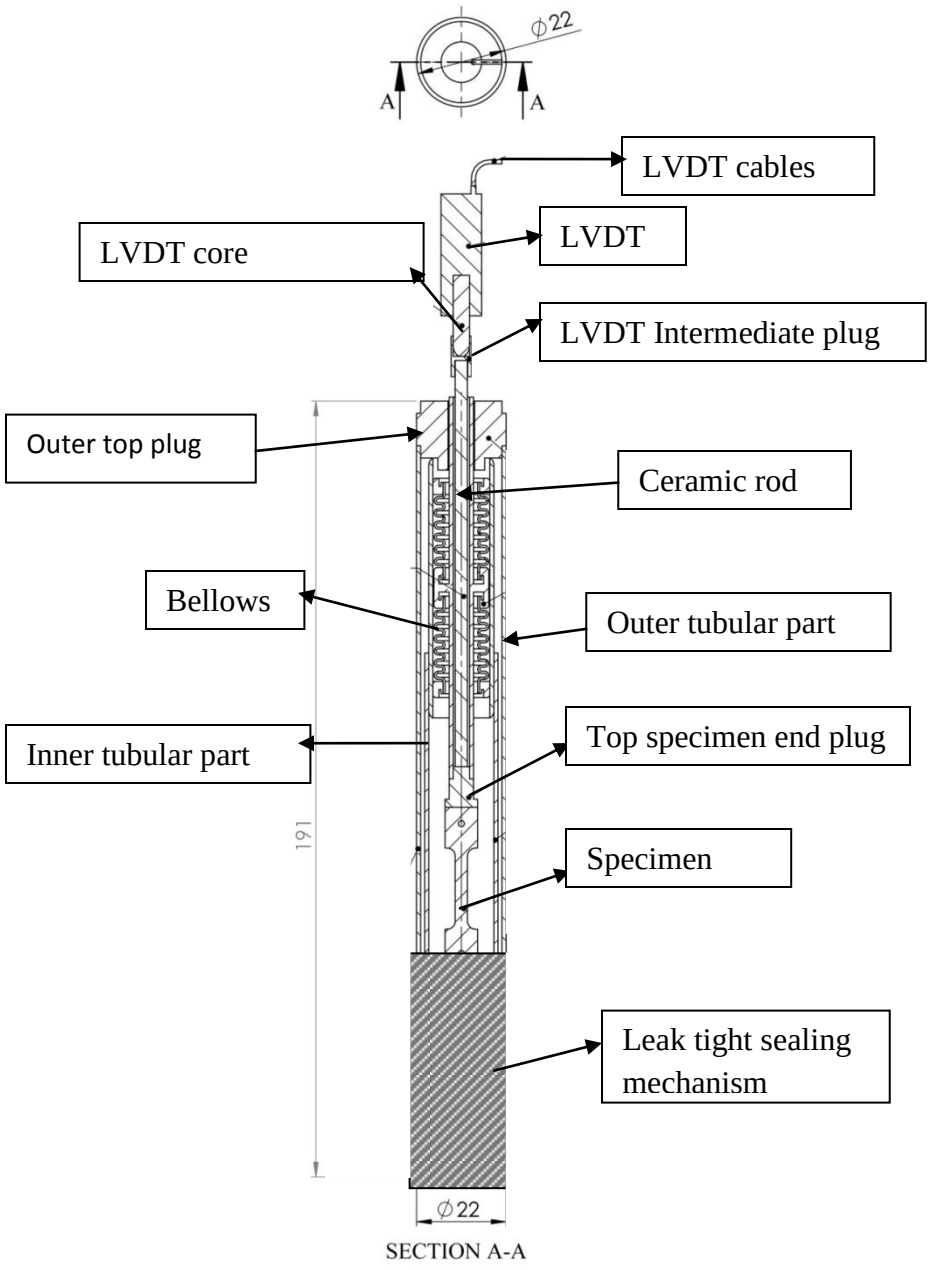

Figure 5-2 Schematic of instrumented irradiation capsule

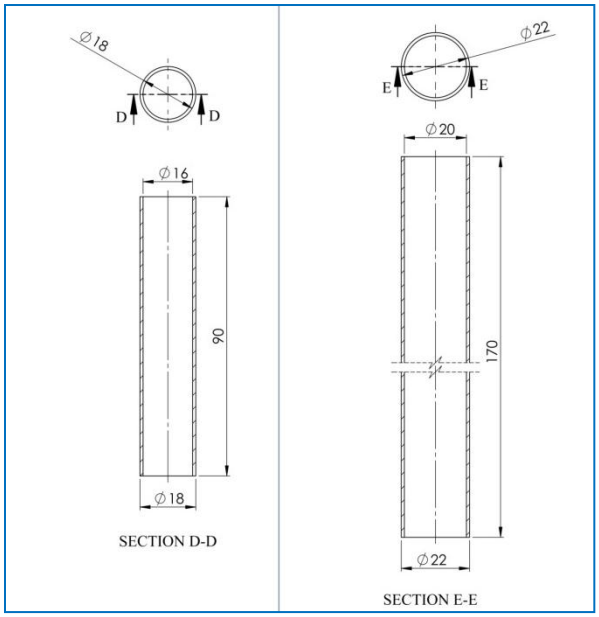

(a) (b)

Figure 5-3 (a) Inner tubular part (b) Outer tubular part

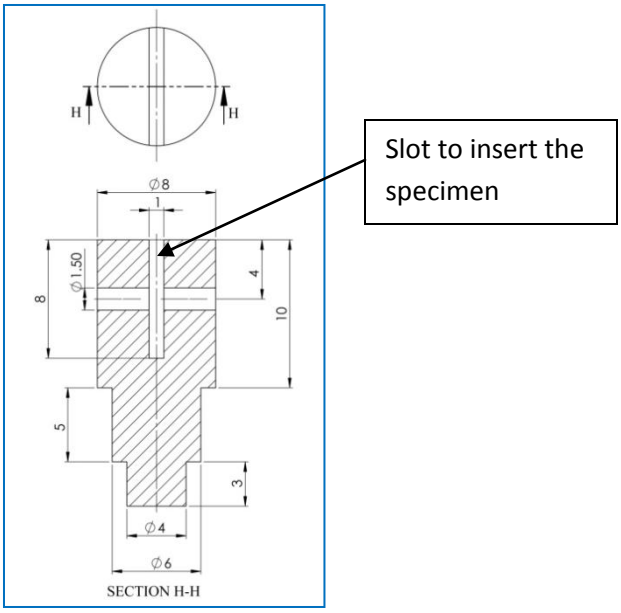

Figure 5-4 Top specimen end plug

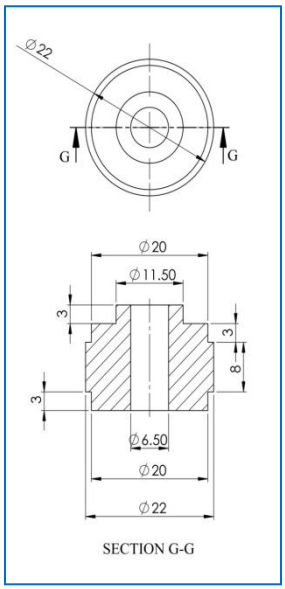

Figure 5-5 Outer top plug

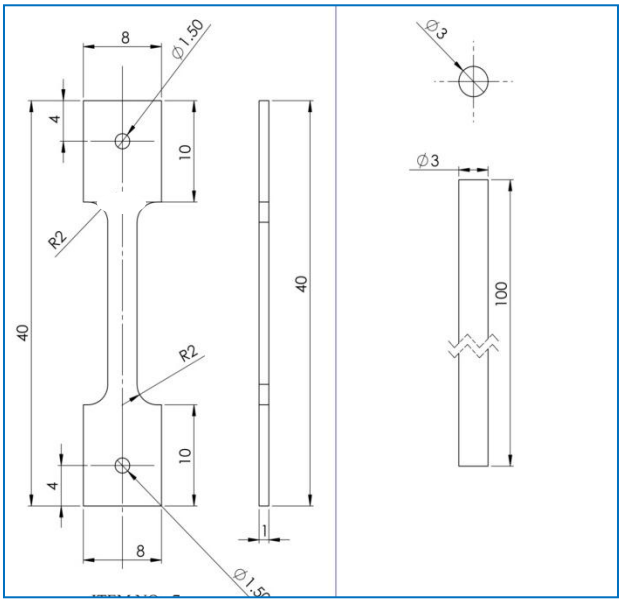

(a) (b)

Figure 5-6 (a) Tensile specimen (b) Ceramic rod

5.3.1 DESIGN AND ASSEMBLY OF AN INSTRUMENTED CAPSULE

Figure 5-7 shows a schematic design of the instrumented irradiation capsule. In the bottom zone, one end of the specimen (40 mm length x 8 mm shoulder width x 1 mm thick) is fixed to the bottom portion of the capsule holder and the other end is connected to the connecting plug. In the middle zone two bellows are interconnected by circumferential welding, with the tube passing through the center of the bellows. In the top zone, a LVDT is placed with its cable connected to the data recorder. The LVDT core is extended to touch the plug connected to the specimen to measure the elongation of the specimen.

The bellows movement is created by the pressure of the argon gas. This gas occupies the bottom bellow of the capsule. The capsule is loaded in electric furnace and the temperature of the furnace is raised. Due to increase of temperature, pressure of gas filled in the capsule raises. The pressure generated forces the bottom bellow to expand and the top bellow to compress. The central tube is welded at its middle portion with the bellows. Due to this bellows movement, tensile load will act on the structural specimen by the central tube. The specimen will elongate axially and the specimen elongation can be measured by the LVDT.

5.3.1.1 LOAD APPLIED ON SPECIMEN AND ELONGATION

The specimen elongation will depend on gas pressure at test temperature (load) and temperature of specimen (thermal elongation). The load applied and the thermal elongation of the specimen can be calculated by the following analytical relations [25].

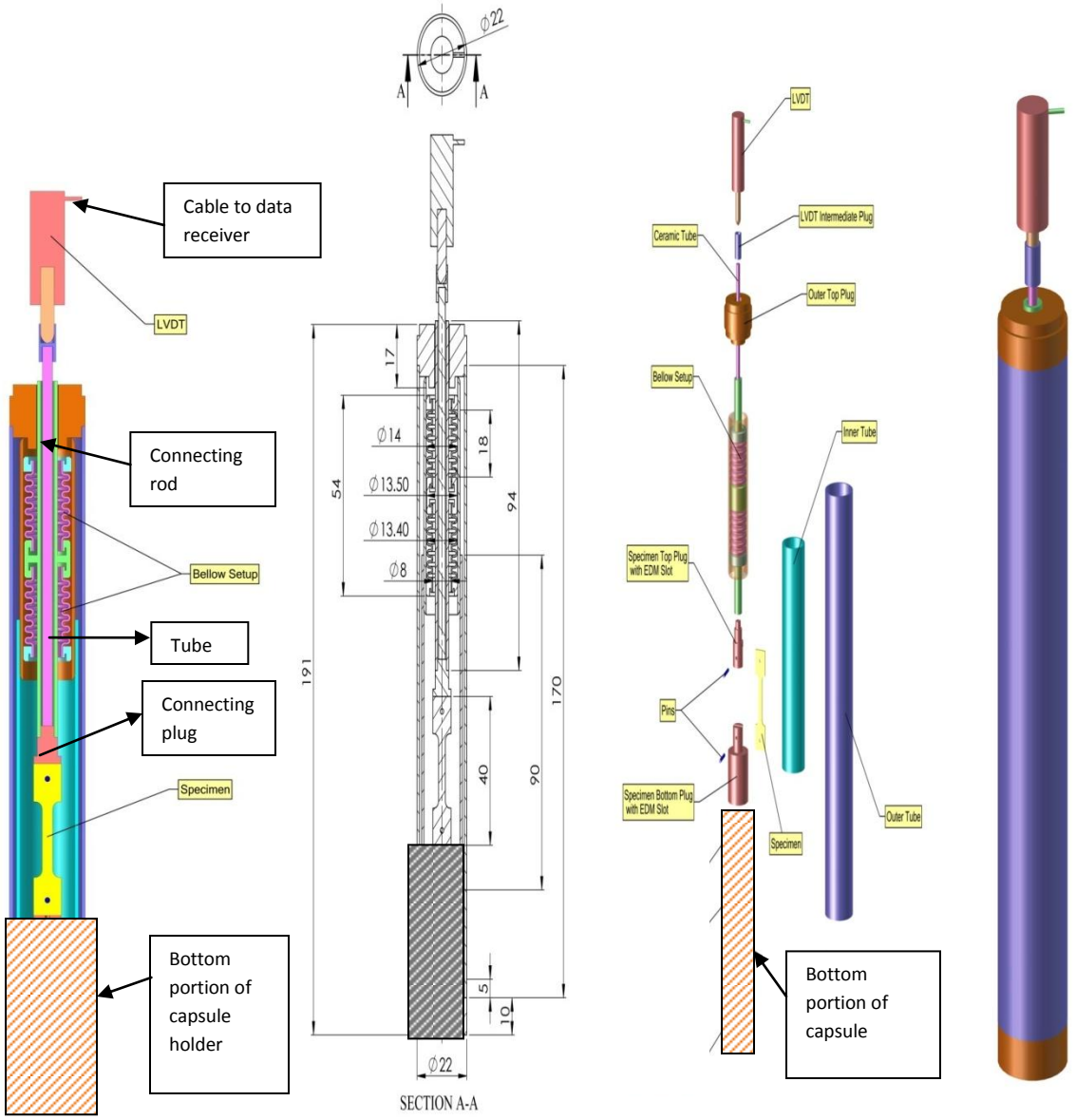

(a) (b)

Figure 5-7 Out-of-pile version of instrumented capsule (a) Schematic view and sketch with dimensions (b) Schematic view of individual components and full assembly

5.3.1.1.1 CALCULATION OF THRUST FORCE AND APPLIED STRESS

To calculate the net thrust force exerted on the specimen, the following needs to be taken into account.

$$p(T) = p_o * \frac{T}{T_0} \quad \text{..... (5.1)}$$

where,

$p(T)$ = Test pressure (MPa)

p_o = Gas pressure at room temperature (MPa)

T = Test temperature (K)

T_o = Room temperature (K)

The force is generated by gas pressure, spring force (from the elastic deformation of bellows wall) and friction force in the system. Here negligible friction force is assumed since the surfaces are smooth. The force exerted by high pressure gas and the spring force are in opposite directions. The gas pressure induced force needs to be the major component for the tensile loading of the specimen and the net force exerted on the tensile specimen is calculated by [25].

$$F_{sp} = A_{eff} \cdot p(T) - F_s - F\mu \text{ ..... (5.2)}$$

where the parameters are defined as:

F_{sp} = Net force acting on the specimen

A_{eff} (effective cross sectional area) = $\frac{\pi}{4}\left[\frac{d_i + d_0}{2}\right]^2$ (mm^2)

d_i and d_o = Inner and outer diameters of the convolutions (mm)

F_s = Force required to elongate the bellow (N)

F_s = Axial spring rate (N/mm)* Axial movement of convolutions (mm)

Fμ = Frictional force (N)

The force generated by gas pressure is transmitted to the specimen through bellows. The stress applied to the specimen can be obtained by dividing the force (F_{sp}) by the cross-sectional area of specimen in the gauge section (A_{sp}).

The axial stress on the specimen is given by;

$$\boldsymbol{\sigma} = F_{sp}/ A_{sp} \text{ .....} \quad \text{.....(5.3)}$$

5.3.1.1.2 CALCULATION OF STRAIN AND ELONGATION OF SPECIMEN

$$\text{Strain, } e = \frac{\sigma}{E} \text{ .....} \quad (5.4)$$

where,

σ = Applied stress (MPa)

E = Youngs modulus of elasticity of the specimen material (MPa)

$$\text{Elongation, } \Delta l = e * l \text{ .....} \quad (5.5)$$

where l = length of the specimen (mm)

5.3.1.1.3 CALCULATION OF THERMAL ELONGATION [57]

$$dL = \alpha * L * (\Delta T) \quad \text{.....(5.6)}$$

dL = Elongation of the specimen due to rise in temperature (mm)

α = Co-efficent of thermal expansion (10^{-6}/ K)

L = Original length of the specimen (mm)

ΔT = Rise in temperature (K)

5.3.2 STEPS IN ASSEMBLY OF AN INSTRUMENTED CAPSULE

Figure 5-8 shows the steps involved in the assembly of the instrumented capsule. The instrumented capsule has three different zones located one over the other. Specimen (fig.5-8(a)) has been located between the top and bottom plugs (figure 5-8 (b)). Figure 5-8(c) shows the bellows set up. The bottom plug has been fitted with leak tight gas filling mechanism (figure 5-8 (d)). The top plug has been welded (GTAW) to the bellows central tube. The inner tube has been welded to the bellows set up (figure 5-8 (e)).

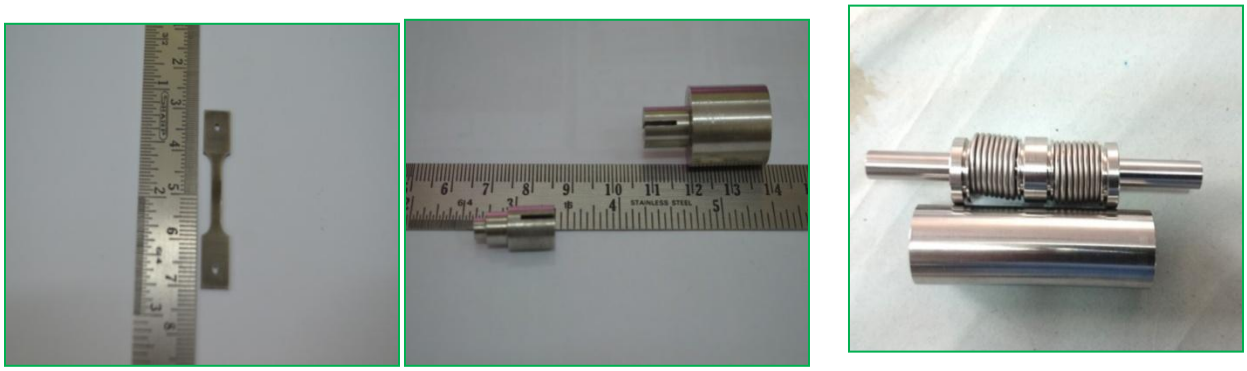

(a) (b) (c)

(d)

(e)

(f)

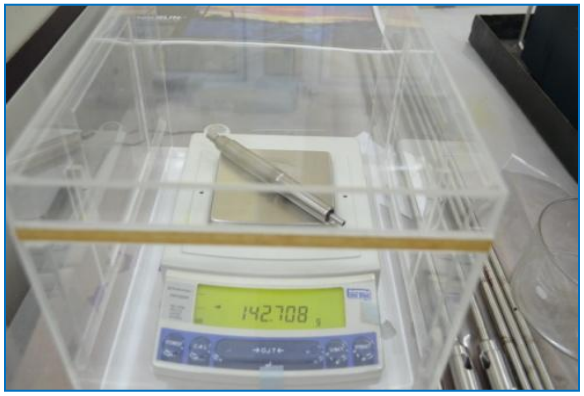

(g)

(h)

Figure 5-8 Components of instrumented capsule: (a) Tensile specimen (b) Top and bottom plugs to hold the specimen (c) Bellows set up (d) Specimen connected to the bellows central tube (e) Inner tube welded to the bellows set up (f) Gas filling operation (g) Weight measurement after gas filled in the capsule (h) Full assembly of capsule.

Argon gas filling at 6 MPa is shown in Figure 5-8 (f). The weight of the capsule has been measured before filling the gas, and after filling of gas (figure 5-8 (g)) to know the mass of gas filled in. We have noticed a mass difference of the order of 1355 mg in the capsule. Finally the outer tube has been welded to the top and bottom end plugs (figure 5-8 (h)). In the top most zone

of the capsule, the LVDT is placed and its core joined with a ceramic rod is passing through the central tube.

5.3.3 OUT-OF-PILE EXPERIMENTAL SET UP

The out-of-pile version of instrumented capsule was fabricated and tested in electrical furnace as shown in Figure 5-9. Two numbers of k-type thermocouples have been fixed around the instrumented capsule (one in specimen zone and another in bellows zone) to measure the temperature. The LVDT has been positioned over the furnace by using a structural support. The ceramic rod has been joined between the end point of the LVDT and the top plug connected to the specimen to measure the elongation of the structural specimen (figure 5-9). The LVDT cables are connected to the displacement indicator and YOKOGAWA make data logger to measure and record the data. The temperature of furnace was varied from 100-330°C. The pressure of gas increased due to the raise in temperature, applying load on the specimen. The elongation was noticed in the LVDT sensor.

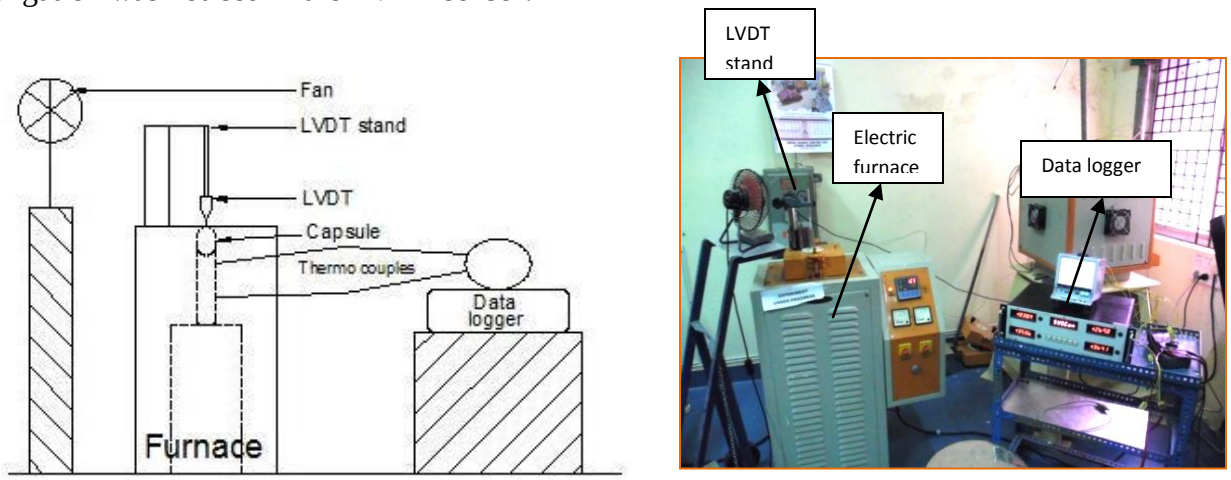

(a) (b)

Figure 5-9 (a) Schematic diagram (b) Out-of-pile experimental set up arrangement with capsule loaded in electric furnace

5.3.4 EXPERIMENTAL ANALYSIS

The experiment was carried out at two different temperatures (130°C and 330°C). The results indicating the temperature of the gas with time, and the elongation of the tensile specimen with time due to increased pressure of gas as indicated by LVDT are shown in Figure 5-10 (a). This elongation is (i) due to thermal expansion of specimen and (ii) due to load applied by the gas pressure on the specimen. The elongation of specimen due to temperature and due to the load caused by pressure of gas are shown in Figure 5-10 (b).

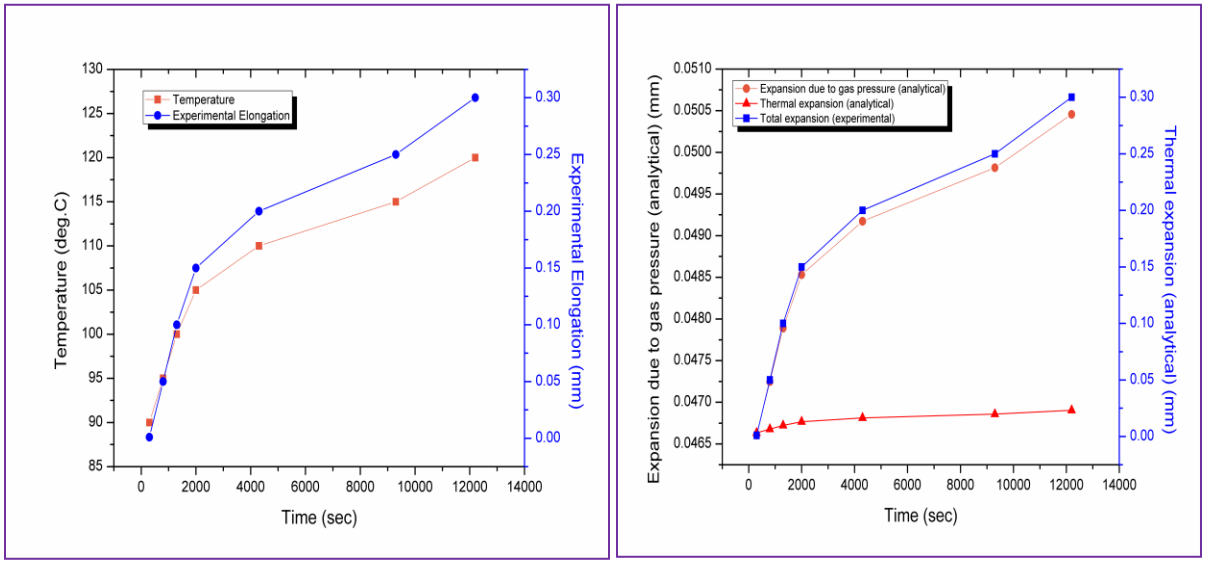

(a) (b)

Figure 5-10 (a) Temperature and elongation of the specimen with time up to 130°C (b) Components of elongation

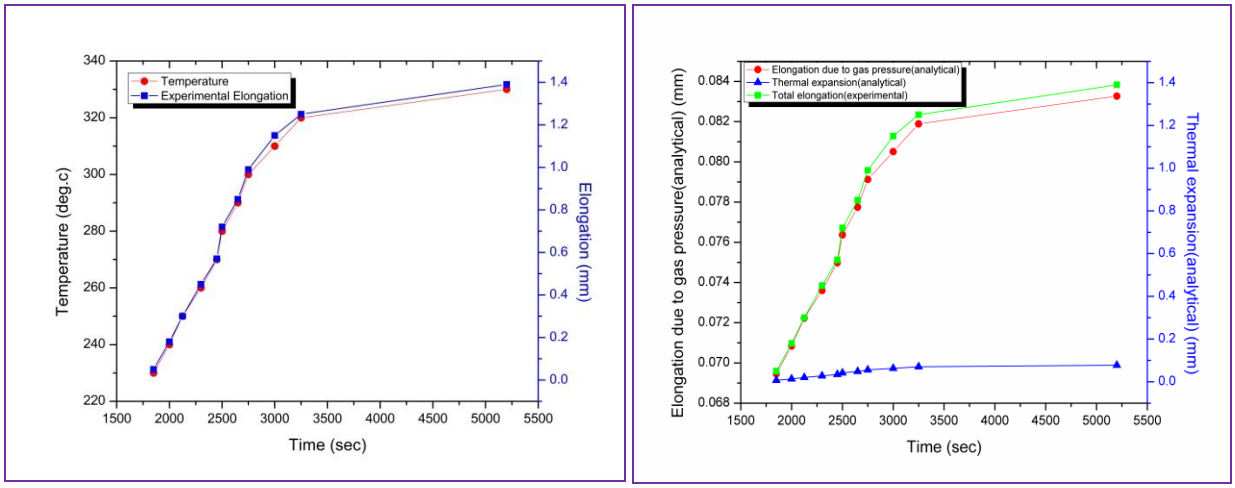

(a) (b)

Figure 5-11 (a) Temperature and elongation of the specimen with time up to 330°C (b) Component of elongation

The thermal elongation seems to be very less, and most of the elongation is due to force induced by the gas pressure. Similar experimental results for a test temperature of up to 330°C are shown in Figure 5-11 (a) and 5-11 (b).

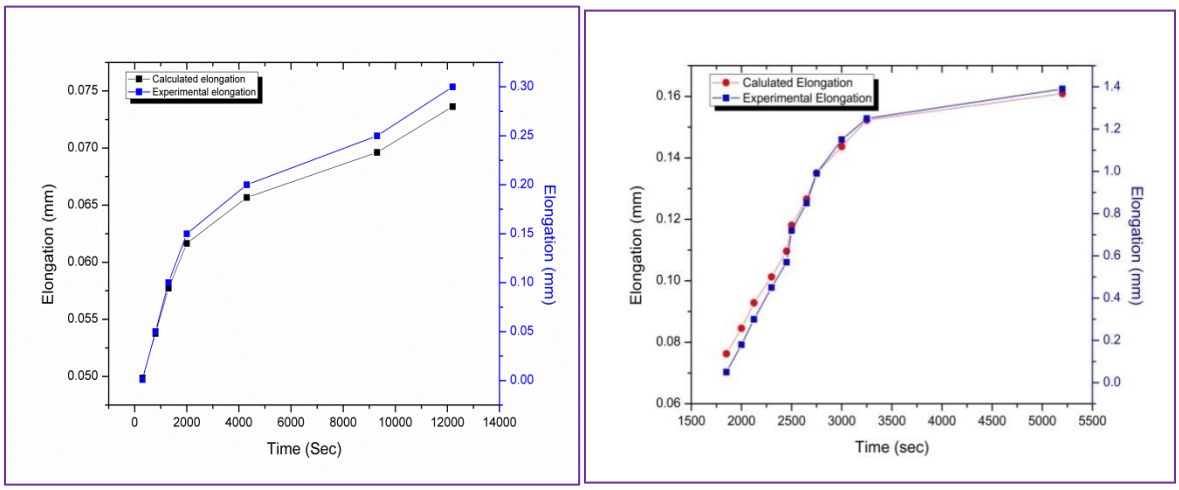

(a) (b)

Figure 5-12 Comparison of results (a) at temperature 130°C (b) at temperature 330°C

Elongation of the specimen as calculated theoretically (section 5.3.1.1.2) and measured experimentally (section 5.3.4) are compared in Figure 5-12 for the temperatures of 130°C and 330°C. It can be seen that both results match closely.

5.4 OUT- OF- PILE EXPERIMENT FOR ONLINE DETERMINATION OF UNIAXIAL CREEP BEHAVIOR IN STRUCTURAL SPECIMEN

Figure 5-13 shows the schematic of instrumented capsule with thermocouple attachment at the specimen to measure the temperature of the specimen directly. This is the modified version of earlier capsule for online determination of uniaxial creep behavior in structural specimen. In this set up, pressurization has been done using argon gas at room temperature , filled at 6 MPa. At the temperature of testing of 550°C, the pressure increases to 16 MPa. With the application of pressure, the bottom bellow expands and the top bellow gets compressed. During this expansion of the bottom bellow, tensile load is applied on the specimen. The elongation of the specimen is measured by the movement of the core of the LVDT. The details of assembly of experimental set up and experimental result of the out-of-pile version of instrumented capsule for determination of online creep deformation are discussed. The experimental results have been compared with the literature results [58] and design concepts are validated.

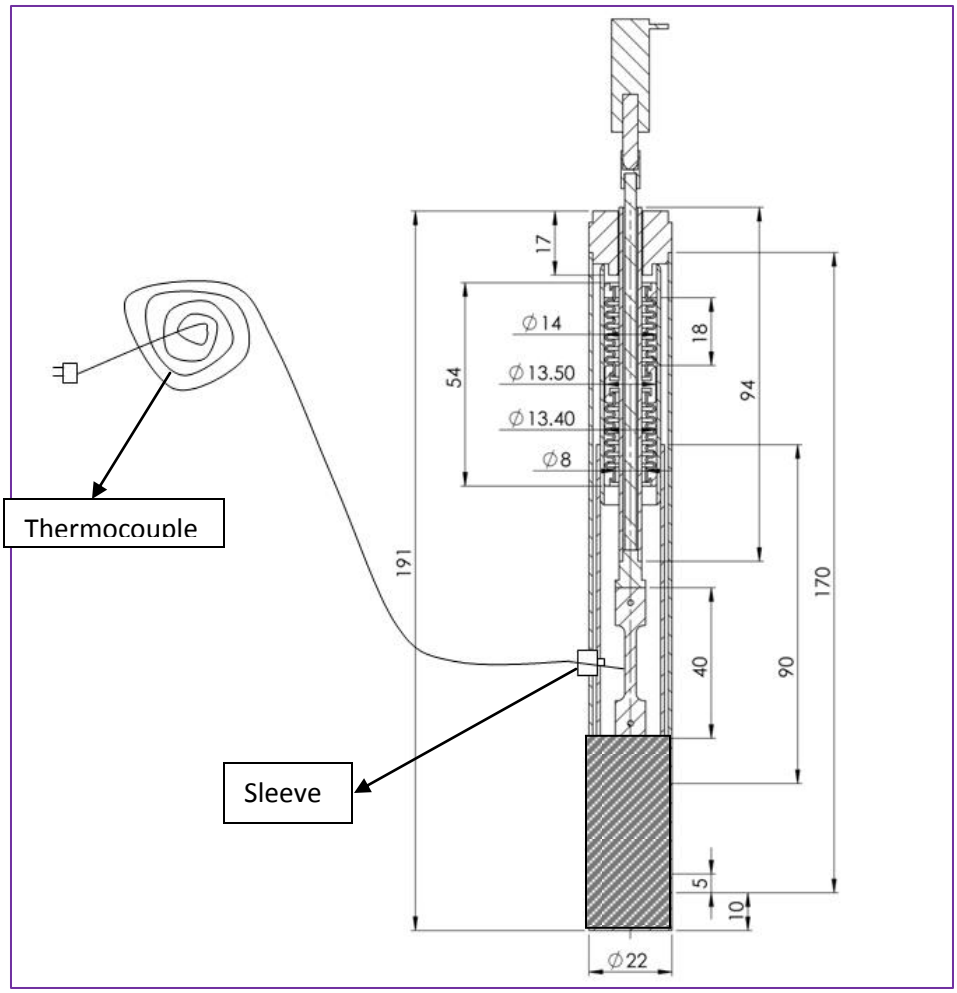

Figure 5-13 Schematic of instrumented capsule with thermocouple attachment

5.4.1 MODIFICATIONS CARRIED OUT

Figure 5-13 shows a schematic design of the instrumented irradiation capsule with thermocouple attachment. This capsule is the modified version of the capsule shown in figure 5-2. In the bottom zone one end of the specimen (40 mm length x 8 mm shoulder width x 1 mm thick) is fixed to the bottom portion of the capsule holder and the other end is connected to the connecting plug. Thermocouple of 1 mm diameter has been attached in the middle of the specimen to measure the exact temperature of the specimen. Due to this uncertainty in the temperature can be avoided.

5.4.2 ASSEMBLY OF EXPERIMENTAL SET UP

Thermocouple has been attached in the middle of the specimen by a laser welded sleeve arrangement shown in Figure 5-14.

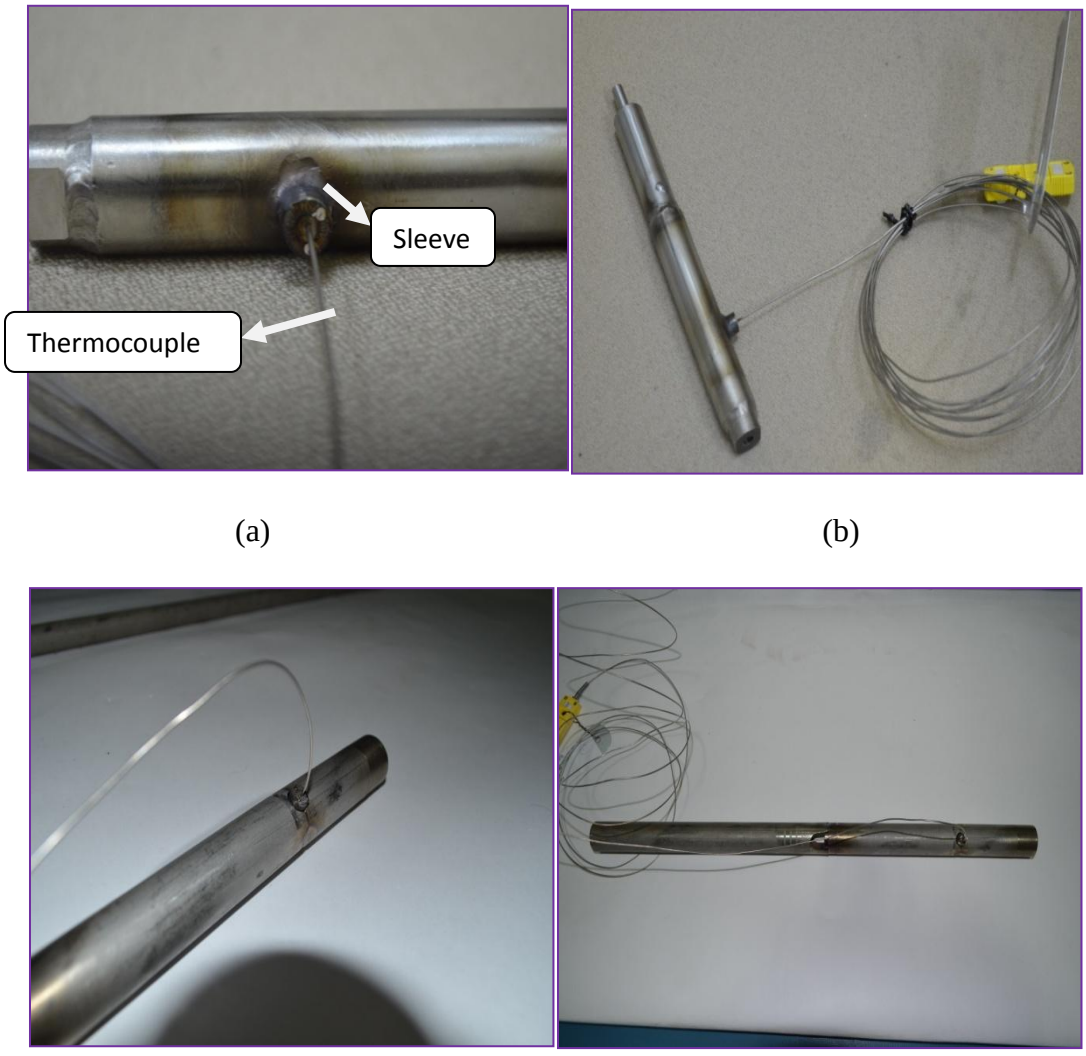

Figure 5-14 Steps involved in instrumented capsule experimental set up assembly: (a) and (b) Thermocouple attachment at the specimen zone, (c) and (d) Full assembly of instrumented capsule to load into the electric furnace.

5.4.3 OUT-OF-PILE EXPERIMENT

The assembled instrumented capsule has been placed in the electrical furnace with two thermocouples, one attached at middle of the specimen and other one at around the capsule in the specimen zone to measure the temperature of furnace. The LVDT has been positioned over the furnace as explained earlier. The LVDT cables are connected to the displacement indicator and YOKOGAWA make data logger to measure and record the data. Figure 5-15 (c) shows the experimental set up arranged in our laboratory to perform the uniaxial creep experiments. The creep experiments are usually carried out between 100 hours to 1000 hours at high temperatures and high stresses [59-60]. The uniaxial creep tests were carried out with a temperatures of 450, 500 and 550°C at related stresses. Each experiment was carried out under constant stress at specified temperature for 200 hours of time. The results have been recorded in the data logger.

(a) (b)

(c)

Figure 5-15 Out-of-Pile experimental set up (a) LVDT positioned over the furnace by a stand arrangement (b) Displacement indicator and Data logger (c) Uniaxial creep experimental set up made in laboratory

5.4.4 RESULTS AND DISCUSSION

The experiment has been carried out at three different temperatures and three different stresses (269 MPa at 450°C , 287 MPa at 500°C and 306 MPa at 550°C). Initially the capsule has been filled with pre-pressurized argon gas at 6 MPa at room temperature. Electric furnace temperature was set to obtain 450°C in the specimen zone of the capsule. At this temperature 269 MPa of stress would apply on the specimen. The temperature and stress values are kept constant for 200 hours to get the secondary creep in the specimen. The same procedure has been followed for the remaining temperatures and stresses. The elongation of the specimen was measured by LVDT. These results are shown in Figure 5-16.

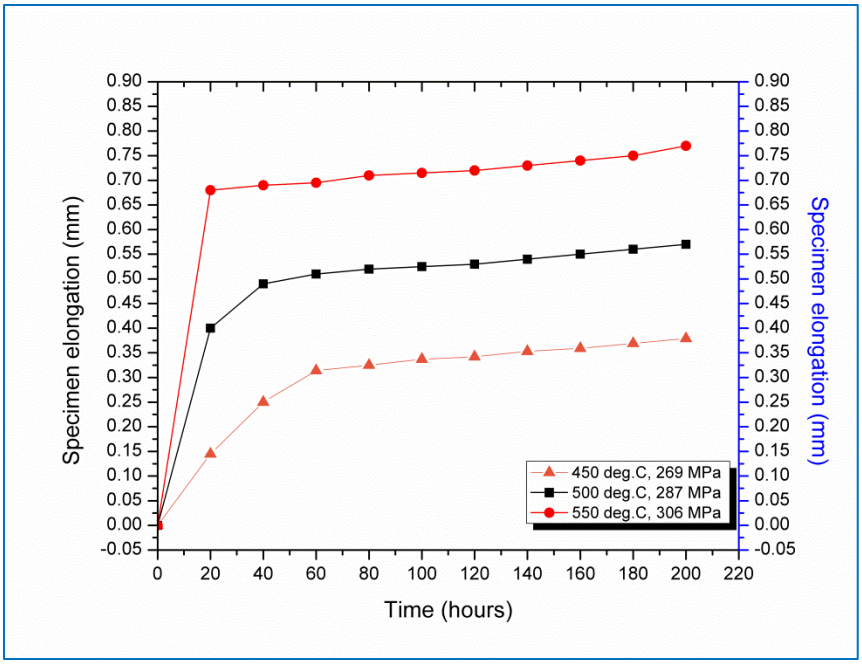

Figure 5-16 Out-of-pile experimental results

At 450°C with 269 MPa of stress, the secondary creep has started after 65 hours and continued steadily. At 500°C with 287 MPa of stress, after 50 hours secondary creep has started. Finally at 550°C with 306 MPa of stress, after 20 hours itself the secondary creep region has commenced.

5.4.4.1 DETAILED ANALYSIS

The capsule has been pre-pressurized with argon gas of 6 MPa at RT. The pressure of the argon will increase with the rise in temperature of the furnace. Due to this the bellow will expand and load will act on the specimen. The load generated in the capsule depends on: (i) Argon gas pressure at the test temperature and (ii) Effective cross-sectional area of the bellow.

$$F = P(T) * A_{eff} \quad \text{.....(5.7)}$$

where,

F = Total load (N)

P(T) = Pressure at test temperature (MPa)

A_{eff} = Effective cross-sectional area of bellow (mm^2)

The load exerted by the bellow depends on the geometrical property of the material like stiffness and material property like young's modulus. The stiffness of the bellow can be calculated by equation (5.8) [61].

$$k_{bellow} = 1.7 * \left(\frac{D_m.E_b.t_p^3.n}{w^3.c_f}\right) \quad \text{..... (5.8)}$$

where,

k_{bellow} = Stiffness of the bellow (N/mm)

D_m = Mean diameter of bellow (mm)

E_b = Young's modulus (MPa)

t_p = Thickness of ply (mm)

n = Number of ply's

w = Convolution depth (mm)

C_f = Anderson factor

The stiffness of the specimen can be calculated as

$$k_s = \frac{A.E}{L} \quad \text{.....(5.9)}$$

where,

k_s = Stiffness of specimen (N/mm)

A = Gauge area of specimen (mm^2)

E = Young's modulus of SS (MPa)

L = Length of the specimen (mm)

By using the above relations, stiffness of bellow and specimen can be calculated. The stiffness value depends on the geometry of the bellow and young's modulus, and these values are changing with the temperature. Figure 5-17 shows the detailed information about the stiffness and young's modulus of the materials with respect to temperature. The graphs have been plotted between temperature Vs Young's modulus and temperature Vs stiffness of the materials. As the temperature increases, the Young's modulus of elasticity decreases. Similarly the stiffness of the material is also decreasing with increasing temperature. The stiffness and young's modulus are indirectly proportional to the temperature. The bellows stiffness value is very less compared to specimen stiffness. Due to this reason the maximum amount of load will be applied on the specimen and very less amount of load will act on the bellows at same elongation.

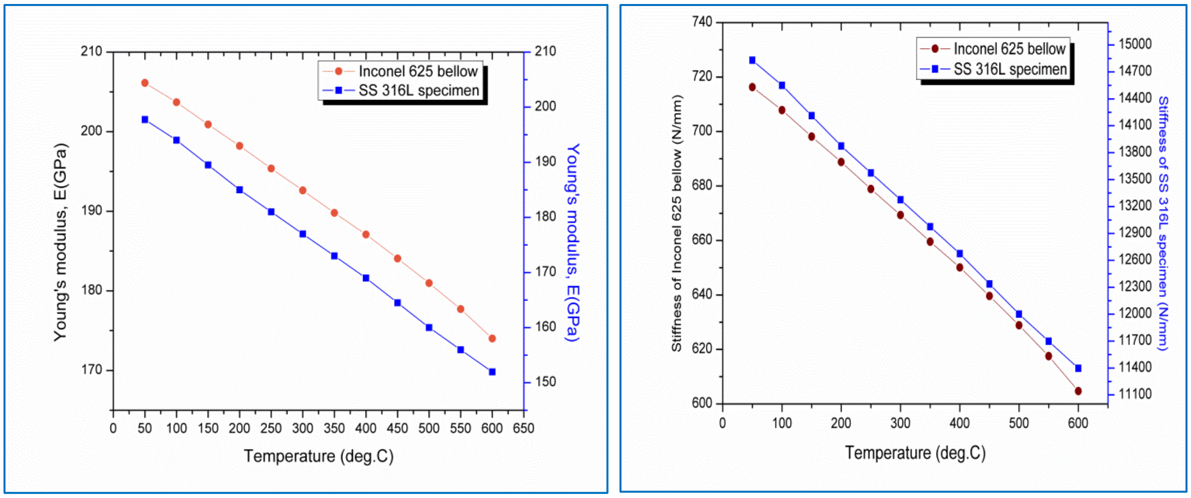

(a) (b)

Figure 5-17 (a) Temperature Vs Young's modulus (b) Temperature Vs Stiffness of Inconel 625 and SS 316L

The net force/load acting on the specimen can be calculated by using following relation. During application of load by gas pressure, elongation in both the specimen and bellow materials is same i.e. strains are equal.

$$F = F_1 + F_2 \ldots\ldots\ldots\ldots\ldots\ldots\ldots\ldots\ldots\ldots\ldots\ldots\ldots\ldots\ldots\ldots\ldots\ldots(5.10)$$

F = Total force = $(k_b.\delta_1) + (k_s.\delta_2)$

$\delta_1 = \delta_2$ (elongations are equal)

$F = (k_b + k_s).\delta$

$\delta = \frac{F}{k_b + k_s}$

where,

F_1 = Load on bellow (N)

F_2 = Load on specimen (N)

δ_1 = Elongation of the bellow (mm)

δ_2 = Elongation of the specimen (mm)

δ = Elongation of bellow/ specimen (mm)

The above relations are useful to calculate the elongation in the system, and by using this elongation we can calculate the actual load acting on the specimen and bellows.

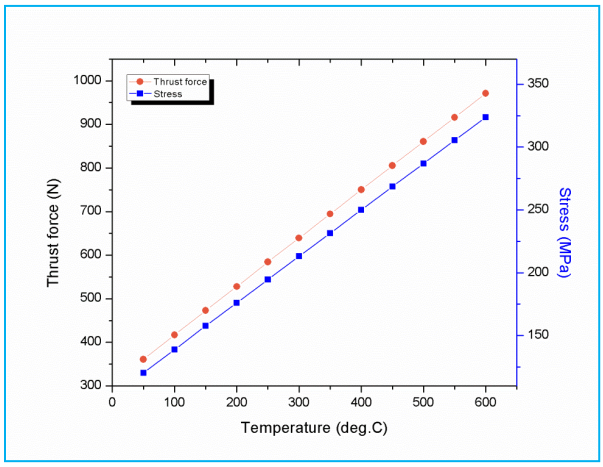

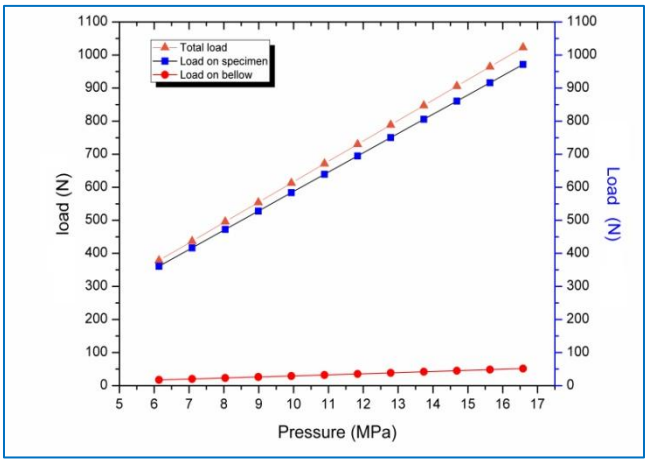

Figure 5-18 Thrust force and Stress Vs Temperature Figure 5-19 Pressure Vs Total load, specimen load and load on bellow

Figures 5-18 and 5-19 show the Thrust force vs and temperature stress, and elongation with respect to total load, and the load acting on the specimen/ bellow. The load depends on the pressure of the gas. Figure 5-19 shows the load acting on the specimen and bellow when pressure of the gas is varied. It can be seen that a large load is acting on the specimen but a very less amount of load is only taken by bellows. From the above analysis, it can be found out that 95% of the load is taken by specimen and only 5% of the load is acting on the bellow.

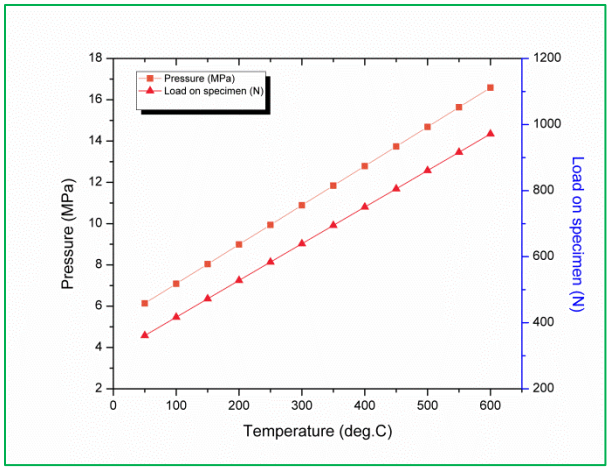

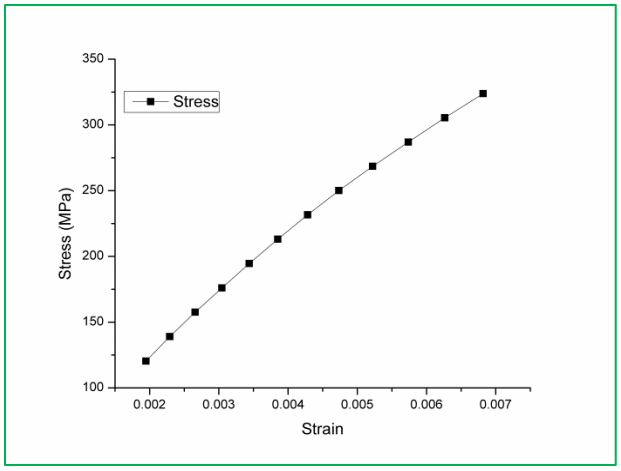

(a) (b)

Figure 5-20 (a) Temperature Vs Pressure and Specimen load (b) Stress Vs Strain

Figure 5-20 (a) shows that as the temperature increases, the pressure of the gas increases which in turn increases the load acting on the specimen. Figure 5-20 (b) shows the stress-strain relation. This stress and strains can be calculated by using the following relations.

Load acting on the specimen = F_2

$$\delta = \frac{F_2.L}{A.E} \quad \text{.....(5.11)}$$

where,

δ = Elongation of specimen (mm)

L = Length of specimen (mm)

A = Cross-sectional area of specimen (mm^2)

E = Young's modulus elasticity at temperature T

$\boldsymbol{\sigma}$ = Stress

$F_2 = (\delta.A.E)/(L)$

Stress, $\boldsymbol{\sigma} = \frac{F_2}{A}$

Strain, $e = \delta/L$

The above relations have been used to calculate the stress values acting on the uniaxial creep specimens in the irradiation capsule at test temperatures. Experimental results have been compared with the results available in literature [58]. It is found that the experimental creep strain rate values match with the strain rate values reported in literature at the specified temperature and stress values.

5.4.4.2 COMPARISON OF RESULTS

Creep deformation is highly dependent on test temperature and stress level. Creep tests were performed using the instrumented capsule on uniaxial specimen at 450, 500 and 550°C under 269, 287 and 306 MPa stress level. Creep strain rate can be determined by using power law (Norton law) relationship [59 and 60].

$$\dot{\varepsilon} = A\sigma^n \quad \text{.....(5.12)}$$

Where, $\dot{\varepsilon}$ is strain rate (/hr), $\boldsymbol{\sigma}$ (MPa) is applied stress, A is the material constant and *n* is the stress exponent. The following experimental strain rates are taken from the Figure 5-16.

$\dot{\varepsilon}_1 = 2.0*10^{-6}$ /hr at 450°C and 269 MPa

$\dot{\varepsilon}_2 = 3.0*10^{-6}$ /hr at 500°C and 287 MPa

$\dot{\varepsilon}_3 = 4.5*10^{-6}$ /hr at 550°C and 306 MPa

Stress co-efficient value can be calculated from the nortons law by using the following relations

$$\frac{\dot{\varepsilon}_1}{\dot{\varepsilon}_2} = \frac{A\sigma_1^{n_1} \exp\left(-\frac{Q}{RT_1}\right)}{A\sigma_2^{n_2} \exp\left(-\frac{Q}{RT_2}\right)} \quad \text{..... (5.13)}$$

$$\frac{\dot{\varepsilon}_2}{\dot{\varepsilon}_3} = \frac{A\sigma_2^{n_2} \exp\left(-\frac{Q}{RT_2}\right)}{A\sigma_3^{n_3} \exp\left(-\frac{Q}{RT_3}\right)} \quad \text{.....(5.14)}$$

and $$\frac{\dot{\varepsilon}_3}{\dot{\varepsilon}_1} = \frac{A\sigma_3^{n_3} \exp\left(-\frac{Q}{RT_3}\right)}{A\sigma_1^{n_1} \exp\left(-\frac{Q}{RT_1}\right)} \quad \text{.....(5.15)}$$

From the above three relations, the stress exponent values are n_1 = 6.28

n_2 = 6.28

n_3 = 6.40

The average value has been taken, n_{avg} = 6.32.

Creep tests have been conducted at National University of Malaysia [58] using Zwick/ Roell 030 machine according to the ASTM E139-00 standard procedure for conducting creep test of metallic materials using constant load. The specimen elongation was measured using a rod-in-tube extensometer where ceramic extension arms were attached to the gage length area of the specimen. The axial creep strain was recorded with the help of an arm ceramics touched to the gage length specimen. The furnace of creep machine has a maximum temperature rating of 1200 °C. Temperature for creep tests was maintained with three zone resistance furnace which was capable of maintaining the temperatures within ±2°C of the test temperature using thermocouples.

The following relationship has been reported from the above experimental work [58] at 565°C.

$$\dot{\varepsilon} = 3 * E - 25\sigma^{7.159} \text{.....(5.16)}$$

$\dot{\varepsilon} = Strain\ rate/sec$

$\dot{\varepsilon}_{l1}$ = 7.41* 10^{-8} /sec = 2.67 *10^{-4} /hr at 269 MPa

$\dot{\varepsilon}_{l2}$ = 1.18* 10^{-7} /sec = 4.25*10^{-4} /hr at 287 MPa

$\dot{\varepsilon}_{l3}$ = 1.87 * 10^{-7} /sec = 6.74*10^{-4} /hr at 306 MPa

The above strain rates are at a temperature of 565°C.

The strain rates at 450, 500 and 550°C under 269, 287 and 306 MPa stress levels are calculated using the above literature results and the equation 5-17, and the calculated values are given in the table 3-4.

$$\frac{\dot{\varepsilon}_1}{\dot{\varepsilon}_l} = \frac{A\sigma_1^{n_{avg}} \exp\left(-\frac{Q}{RT_1}\right)}{A\sigma_l^{n_l} \exp\left(-\frac{Q}{RT_l}\right)} \quad \text{.....(5.17)}$$

where,

$\dot{\varepsilon}_1$ = Strain rate (/hr) at stress σ_1

$\dot{\varepsilon}_l$ = Strain rate (/hr) at stress σ_l

$\sigma_1 = \sigma_l$ = Applied stress (MPa)

A and Q are considered as same in temperature range of 450 to 600°C

n_l = 7.159 (at 565°C, from ref [58]), n_{avg} = 6.32 (calculated value [60])

T_1 = Test temperature (K) (450°C, 500°C, 550°C) [723 K, 773 K, 823 K]

T_l = Temperature value in literature (K) (565°C) [838 K]

Table 5-4 Comparison of results

S.No	Test Temperature (°C)	Applied Stress, $\boldsymbol{\sigma}$ (MPa)	Strain rate as derived from literature data $\dot{\varepsilon}_{lit}$ (/hr)	Strain rate from the present experimental work $\dot{\varepsilon}_{Exp}$ (/hr)	Comparison (%)
1	450	269	2.44*10^{-6}	2.0*10^{-6}	81.96
2	500	287	3.68*10^{-6}	3.0*10^{-6}	81.52
3	550	306	5.53*10^{-6}	4.5*10^{-6}	81.37

It can be seen from Table 3.4 that both strain rates from the present experimental and as obtained through literature data are closely matching. The experimental results have been compared with the reference results in, the Figure 5-21. The test temperatures are taken on x-coordinate and strain rates have been taken on y-coordinate. It can be seen that both results are matching closely.

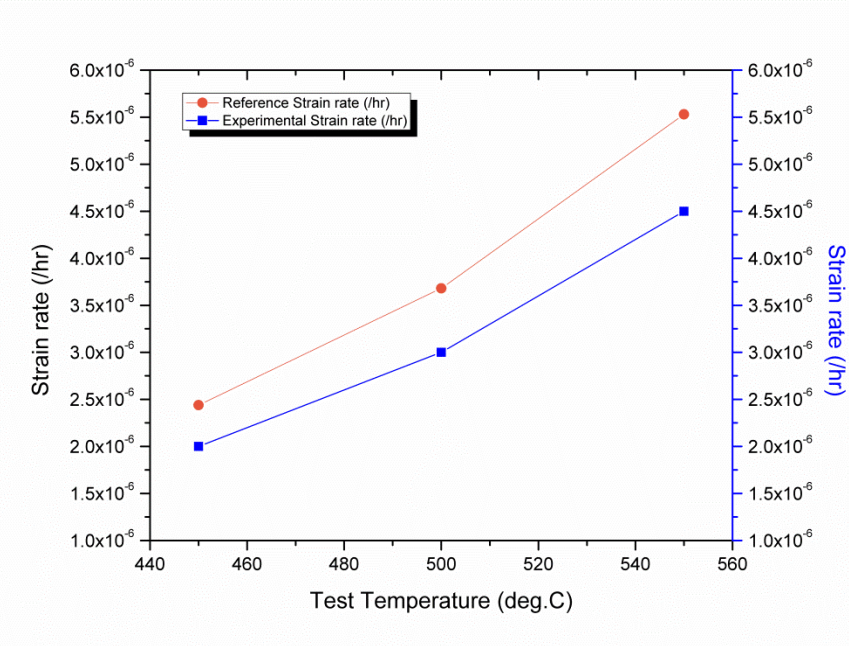

Figure 5-21 Comparison of strain rates

5.4.5 Summary

- Out-of-pile version of instrumented capsule has been designed and developed for online determination of uniaxial creep behavior in structural specimen.
- Force/ load due to argon gas pressure is the major component for the tensile loading of the specimen.
- 95% of the total load is acting on the specimen and remaining 5% load only is acting on the bellow.
- Experimental results (steady state creep values) have been compared with the literature results, and found to be closely matching .

- Design concept of instrumented capsule for uniaxial creep measurement has been validated.
- The design of instrumented capsule is directly applicable for in-reactor experiments of a fast reactor.

CHAPTER - 6

6

SUMMARY AND SUGGESTIONS FOR FUTURE WORK

This chapter summarizes the research works carried out towards design and development of instrumented capsule for on-line measurement of uniaxial creep behavior in structural specimen and the out-of-pile experiment for validation design concepts. Also, it provides suggestions to be carried out in future in this field.

This work has been motivated by a need to develop an instrumented irradiation capsule for Indian Fast Breeder Test Reactor (FBTR) to determine the uniaxial creep behavior in structural specimen. According to the literature, before attempting in-pile testing it is always preferred to do out-of pile experiment to verify the design and experimental concepts and ensure satisfactory performance of all the subsystems involved. The objective of this work is design and development of out-of-pile version of instrumented capsule for online determination of uniaxial creep behavior in structural specimen. The summary of the thesis is given below.

The general background and introduction about the irradiation capsules and experimental methods, explanation to creep phenomenon, short description of Fast Breeder Test Reactor (FBTR) and Prototype Fast Breeder Reactor (PFBR) core configurations and their flow systems are given in chapter 1.

Literature review on various topics of irradiation creep measurements and international developments of design and analysis of irradiation capsules are discussed in the literature review chapter. The motivation drawn out of the literature review and scope of the research work are also discussed in this chapter.

In Chapter 3, a brief`` discussion on heat transfer analysis of irradiation capsule by analytical and simulation techniques has been given. In one of the types of irradiation capsules, the specimens are kept in four to five separate sealed compartments of the capsule located one over the other. Helium/ Argon gas or mixture of these gases will be filled around the specimens in these compartments. Liquid sodium, which is the coolant in the fast reactor, will be flowing around the irradiation capsule. The temperature of specimens has been determined with various types of gases (helium/ argon/ helium-argon mixture) filled in the compartment and the results are presented in this chapter. Variable properties of gases have been used and iterative method has been employed to calculate the temperatures. Using the results obtained, we can select the type of gas mixture required to attain a specific higher temperature in the specimens during irradiation. The results have been compared with the results obtained through the use of a computer code COMSOL. Similar analysis will be required in all types of irradiation capsules, whether non- instrumented or instrumented.

The establishment of high temperature nicrobrazing procedure under argon gas atmosphere which is required in the fabrication of instrumented irradiation capsule has been discussed in the subsequent chapter.

Fabrication of instrumented capsule requires the development of thin-walled joints capable of withstanding high temperatures. High-temperature brazing method has an advantage of joining multiple metal-sheathed cables such as thermocouples through a solid stainless steel plug in a single operation. High-temperature nicrobrazed joints under argon atmosphere have been developed as part of the research work. An induction heating technique has been used for this development. Protective atmosphere is required for high-temperature brazing to prevent oxidation of the base metal and the filler metal during the brazing operation. Commercial grade

argon gas (99.996% pure) has been used and brazed joints have been developed. Brazing procedure has been established and development of high temperature nicrobrazed joints using induction heating system in an argon gas environment has been carried out. Helium leak test, metallographic, micro hardness tests, and sodium compatibility test have been carried out on the brazed samples to qualify the joints.

The fabrication of an instrumented capsule also requires joints with tube-to-tube and tube-to-end plug configurations. Optimization of the parameters of available joining methods and qualification of the joints according to the standards have been carried out. Helium leak test, metallographic and micro hardness tests have been carried out on the joints made by laser, GTAW(Gas Tungsten Arc Welding) and high temperature nicrobrazing joining processes. Common joint area has been provided for all the joining processes to measure and compare the merits and demerits of each joint.

Design and analysis of instrumented capsule for online determination of uniaxial creep behavior in structural specimen has been presented in chapter 5. Fabrication of an out-of-pile version of instrumented capsule and testing of it in a vertical electrical furnace for validation of design concepts has been carried out. The overall diameter of this instrumented capsule is 22 mm and operative portion is 170 mm. This capsule has three different zones located one over the other. In the bottom zone of the capsule the tensile specimen (40 mm length x 8 mm shoulder width x 1 mm thick) is located, with one end fixed to the bottom portion of capsule and the other end connected to a central tube through a connecting plug; in the middle zone two bellows are arranged back to back by circumferential welding, with the tube passing through the centre of the bellows. The middle portion of the central tube is welded to the bellows circumferentially. In the top zone a LVDT is placed and its core is passing through the central tube. The end point of the

LVDT core touches the plug connected to the specimen to measure the elongation of the structural specimen. In this capsule setup, bellows are used to apply a tensile load on the structural specimen with the use of pressurized argon gas. The elongation of the structural specimen will be measured by the movement of the core of the LVDT. Bellows setup has been fabricated through the industry. These bellows have been tested under cyclic load and found to be performing satisfactorily. In the experimental setup, pressurization has been done in the bottom bellow using argon gas at room temperature filled at a pressure of 6 MPa. At the temperature of testing of 550 °C, the pressure increases to about 16 MPa resulting in a tensile stress of ~306 MPa in the gauge portion of the tensile specimen. The fabricated instrumented capsule has been placed in the electric furnace with two thermocouples, one positioned at middle of the specimen and other one positioned on the capsule at nearly the same plane to measure the temperatures at these two points. The LVDT has been positioned out of the furnace using an vertical stand arrangement. The LVDT cables are connected to the displacement indicator and YOKOGAWA make data logger to measure and record the data.

The experiment has been carried out by using the above set up arranged in our laboratory to perform the uniaxial creep experiments. The experiment has been carried out at three different stresses and temperatures (269 MPa at 450°C, 287 MPa at 500°C and 306 MPa at 550°C). This condition has been kept constant for 200 hours to get the secondary creep data in the specimen secondary creep rate obtained for experiments have been compared with those values reported in literature, and found to be closely matching.

In short, this thesis is a dedicated research work on development of theoretical models to achieve desired temperature of irradiation in irradiation capsules, development of high temperature nicrobrazing joints under argon gas atmosphere in laboratory conditions, comparison of different

types of capsules (High Temperature Brazing, GTAW, and laser welding) to access them before choosing them for application in development of this capsule and finally to design and develop an instrumented capsule for online determination of uniaxial creep behavior in structural specimen in a fast reactor environment and out-of-pile (laboratory scale) validation of the design concepts. This instrumented capsule design will be directly useful for in-pile creep experiment on core structural materials in fast test reactors.

Scope for future work

This research work contributes to the detailed design, development and experimental procedures of out-of-pile type of instrumented capsule for online measurement of uniaxial creep behavior in structural specimen. Establishment of high temperature nicrobrazing procedure under argon gas atmosphere and optimization of its process parameters and qualification of these joints by standard methods has been carried out. The following are suggested future works.

- Design and fabrication of in-pile version of instrumented irradiation capsule for online determination of uniaxial creep behavior in structural specimen.
- Design and development of instrumented irradiation capsule by using high-temperature LVDTs.
- Design and development of instrumented capsule for online measurement of creep strain under compressive load.
- Design of instrumented irradiation capsule under biaxial loading conditions.

References

[1] K V. Suresh Kumar, R P. Kapoor, P V. Ramalingam, B. Rajendran, G. Srinivasan and K V. Kasiviswanathan, Fast Breeder Test Reactor. 15 Years of Operating Experience, Technical Meeting on Operational and Decommissioning Experience with Fast Reactors, **2002**, 15-27 IAEA-TM-25332, IAEA.

[2] G. Srinivasan, K V. Suresh Kumar, B. Rajendran and P V. Ramalingam, *Nuclear Engineering and Design*, 236, **2006**, 796-811.

[3] K V. Suresh Kumar and G. Srinivasan, A brief Description of FBTR, *Indian Nuclear Society News*, 7, **2010**, 5-11.

[4] S. Raghupathy, O P. Singh, S. Govindrajan, S C. Chetal and S B. Bhoje. Design of 500 MWe Prototype Fast Breeder Reactor, *Indira Gandhi Center for Atomic Research, Department of Atomic Energy*, **2003**, 1-9.

http://www.dae.gov.in/ni/nimar04/design.pdf

[5] Design of Prototype Fast Breeder Reactor, *Indira Gandhi Center for Atomic Research, Department of Atomic Energy, Kalpakkam* **2003**, 1-6.

http://www.igcar.ernet.in/brochure/design.pdf

[6] B G. Kim, J L. Rempe, D L. Knudson, K G. Condie and B H. Sencer, "In-Situ Creep Testing Capability Development for Advanced Test Reactor", Idaho Falls, ID Idaho National Laboratory, **2010**, INL/ EXT-10-17779.

[7] K L. Davis, D L. Knudson, J L. Rempe, and K G. Condie, "A Variable Load LVDT-Based Creep Test Rig for Use in ATR Loop 2A", Idaho Falls, ID Idaho National Laboratory, **2013**, INL/EXT-13-29551.

[8] Moilanen, P S. Tähtinen, B N. Singh, and P. Jacquet, “In-Situ Investigation of the Mechanical Performance and Life Time of Copper: Final report on design, construction, and calibration of test module for in-reactor tensile tests in BR-2 reactor”, 27 October **2004**, VTT Report BTUO 76-031127.

[9] N. Singh, S. Tähtinen, P. Moilanen, P. Jacquet, and J. Dekeyser, “In-reactor uniaxial tensile testing of pure copper at a constant strain rate at 90°C,” *Journal of Nuclear Materials*, 320, **2003**, 299–304.

[10] R V. Nieuwenhove and S. Solstad, In-core fuel performance and material characterization in the Halden reactor, *ANIMMA International Conference*, 7-10 June **2009**, Marseille, France.

[11] S. Solstad and R V. Nieuwenhove, Instrument Capabilities and Developments at the Halden Reactor Project, *Sixth American Nuclear Society International Topical Meeting on Nuclear Plant Instrumentation, Control, and Human-Machine Interface Technologies* NPIC&HMIT 2009, Knoxville, Tennessee, 5-9 April, **2009**, American Nuclear Society, LaGrange Park.

[12] W. Wiesenack, "Status and outlook for irradiation testing from a Halden Reactor perspective", Presented at *International Conference on the Physics of Reactors “Nuclear Power: A Sustainable Resource”* Casino-Kursaal Conference Centre, 14-19 September, **2008**, Interlaken, Switzerland.

[13] W. Wiesenack and T. Tverberg, The OECD Halden reactor project fuels testing programme: methods, selected results and plans, *Nuclear Engineering and Design* 207, **2001**, 189–197.

[14] T M. Karlsen, Achievements and further plans for the OECD Halden, reactor project materials programme, *Nuclear Engineering and Design* 207, **2001**, 199–206.

[15] J F. Villard, “State-of-the-art and improvement of online measurements in present and future French research reactors,” September **2009**, presentation at the Idaho National Laboratory.

[16] J L. Rempe, D L. Knudson, K G. Condie, J E. Daw, and S C. Taylor, “Instrumentation to Enhance Advanced Test Reactor Irradiations,” September **2009**, INL/EXT-08-13985.

[17] P. Bennett and T. Karlsen, "In-core corrosion monitoring in the Halden test reactor", *Energy Materials: Materials Science and Engineering for Energy Systems*, Volume 3(2), June **2008**, 81-90(10).

[18] D L. Knudson, J L. Rempe, and J E. Daw, “Evaluation of Candidate Linear Variable Displacement Transducers for High Temperature Irradiations in the Advanced Test Reactor”, September **2009**, Idaho National Laboratory, INL/EXT-09-16972.

[19] F. Øwre and M. McGrath, "Present Status and Future Plans of the Halden Reactor", presented at *12th IGORR*, 28-31 October **2009**, Beijing, China.

[20] Y. Kurata, Y. Itabashi, H. Mimura, T. Kikuchi, H. Amezawa, S. Shimakawa, H. Tsujiand and M. Shindo, “In-pile and post-irradiation creep of type 304 stainless steel under different neutron spectra”, *Journal of Nuclear Materials*, 283-287, **2000**, 386-390.

[21] L E. Rehn, “Production of freely-migrating defects”, *Journal of Nuclear Materials*, 174, **1990**, 144-150.

[22] W. Schule. and H. Hausen, “Neutron irradiation creep in stainless steel alloys,” *Journal of Nuclear Materials*, 212-215, **1994**, 388-392.

[23] B G. Kim, et al., “Status and Perspective of Material Irradiation Tests in the HANARO", *paper and presentation from the 1st International Symposium on Materials Testing Reactors*, JAEA-Oarai, July **2008**, Japan.

[24] B G. Kim, K N Choo, J M. Sohn, S J. Park, Y K. Kim and Y J. Kim, “Instrumentations for Materials Irradiation Tests in HANARO,” *Proceedings of the ANS NPIC HMIT 2009 Topical*

Meeting on Nuclear Plant Instrumentation, Controls, and Human Machine Interface Technology, April **2009**, Knoxville, TN.

[25] B G. Kim, K N. Choo, Y K. Kim and J J. Ha, "Irradiation and Instrumentation Technology in HANARO", Presented at *2nd International Symposium on Material Test Reactors,* 28 September-1 October, **2009**, Idaho Falls, Idaho, USA.

[26] H. Hausen and W. Schule, "Neutron irradiation creep at 100°C on 316L AMCR, welded 316L stainless steel alloys". Proc. 18th Int. Symp. on Effects of radiation on materials, Hyannis, MA, USA, ASTP STP, 25–27 June, **1996**, 1325, 830 – 49.

[27] B G. Kim, "In-situ creep testing capability development for the advanced test reactor", Idaho Falls, ID Idaho National Laboratory, **2010**, INL/ EXT-10-17779.

[28] D L Knudson and J L. Rempe, "Linear variable differential transformer (LVDT)-based elongation measurements in advanced test reactor for high temperature irradiation testing". Meas. Sci. Technol, 23, **2012**, 1–7.

[29] D. Knudson, J. Rempe and K. Condie, "*Application of LVDTs for Creep Testing in the Advanced Test Reactor",* Idaho Falls, ID Idaho National Laboratory, **2011**, INL/EXT-11-23281.

[30] T S. Byun, M. Li, L L. Snead, Y. Katoh, T D. Burchell and J L. McDuffee, " Principles and practice of a bellows-loaded compact irradiation vehicle", *Journal of Nuclear Materials,* 439**, 2013**, 108-116.

[31] Metal Bellows Manual published by Witzenmann GmbH (1999) or The Manual of Expansion Joint Technology by the same company, **2010**.

[32] L L. Snead, T S. Byun, M. Li, Y. Katoh and J L. McDuffee, "Irradiation Creep Behaviors of Nuclear Graphite", *J. Nucl. Mater*., in press.

[33] G S. Sawhney, *Heat and Mass Transfer*, Second edition, I K International Publishing house Pvt Ltd, New Delhi, **2010**, 53.

[34] www.mace.manchester.ac.UK/stainlesssteel/thermal properties.html.

[35] V S. Yamnikov and L L. Malanchanko, "*Variation of thermal conductivity of a gas mixture under the fuel-element jacket during burn-up*", Soviet Atomic Energy Volume 42, **1977**.

[36] G F. Naterer, "*Heat transfer in single and multiphase systems*", ISBN 9780849310324 - CAT#1032, CRC-Press, **2002**, 586-587.

[37] D S. Gelles, "Effects of radiation on materials 17th International Symposium ASTM committee on Nuclear Technology and Applications"- Google books.htm.

[38] M. Schwartz Mel , "*Fundamentals of Brazing*" , Sikorsky Air craft, Volume 6, ASM **1993**, 114-125.

[39] M. Melvin Schwartz, "*Introduction to Brazing and Soldering*" Sikorsky Air craft, ASM, Volume 6, **1993**, 109-113.

[40] ASM Hand Book of "*Welding, Brazing and Soldering"*. Volume 6, **1993**.

[41] Johnson Matthey, "*Technical brochure of High Temperature Brazing Alloys"*.

[42] M. Schwartz Mel, "*Brazing for the Engineering Technologists"*. **1995**.

[43] M/S Wall Colmonoy corporation, Madison heights, USA, *Nicrobraze Technical Data Sheet.*

[44] P K. Chaurasia, K. Chandran, Sadu Venkatesu, S. Murugan, S. Anthonysamy, S. Venugopal and T. Jayakumar, "*Developement of High-Temperature Brazed Joints and its Compatibility test with High Temperature Sodium"*, National Welding Seminar, Delhi, **2015**, 5.

[45] P K. Chaurasia, S. Murugan and S. Venugopal, "*Development of Brazed Joints Using Induction Heating System for High Temperature Nuclear Applications"*, NWS, **2009**, 31.

[46] Sadu Venkatesu, P K. Chaurasia , S. Murugan, S. Venugopal and T. Jayakumar, "*Development of High-Temperature Nicrobrazed joints using Induction heating in an Argon gas Environment"*, National Weld Meet, Kelakarai, **2014**, 38.

[47] H E. Pattee, "*High-Temperature Brazing*", Source book of Brazing and Brazing Technology, ASM, **1980**.

[48] K L. Narayana, S V. Ramana and P. Vamsi Krishna "*Production Technology"*, Second edition, I K International Publishing House Pvt Ltd, New Delhi, **2010**, 94-95.

[49] P J. Norberto, L. Altino and B. Gunnar, "*Welding Robots*", Springer publishers, **2005**.

[50] P W. Fuerschbach and G A. Knorovsky, "A Study of Melting Efficiency in Plasma Arc and Gas Tungsten Arc Welding", *Welding Journal*, **1991**, 287_s-297_s.

[51] J. Norrish, "*Advanced welding processes*", Institute of Physics Publishing, **1992**.

[52] J. Mazumder, "*Laser beam welding*", Handbook, 4 ASM, **1993**, 263-269.

[53] M. Vedani, "Microstructural evolution of tool steels after Nd-YAG laser repair welding", *Journal of Materials Science*, 39, **2004**, 241 – 249.

[54] T. Kim, C E. Albright and S. Chiang, "The energy transfer efficiency in laser welding process", *Journal of Laser Applications*, Volume 2(1), **1990**, 23-28.

[55] AWS Welding Handbook, 8th Edition, Volume 1, **1987**.

[56] H R. Brooker and E V. Beatson, "*Industrial Brazing*", ISBN: 0408001720.

[57] R K. Bansal, "*Strength of Materials*", 4th edition, Laxmi publications pvt. ltd, New Delhi, **2007**, 42.

[58] K A. Mohammad, E S. Zainudin, M S. Salit, N I. Zahari and A. Ali. "Experimental determination of the fatigue behavior of austenitic 316L stainless steel under fatigue and creep-fatigue tests at high temperature". *International Journal of Metal and Steel Research Technology*, Volume 1(1), July **2013**, 1- 11.

[59] M N. Shetty, "Dislocations and mechanical behavior of materials", 2nd edition, PHI Learning pvt. ltd, **2013**.

[60] G E. Dieter, "Mechanical metallurgy", 3rd edition, , McGraw-Hill book Co. **1988**.

[61] Standards of the Expansion Joint Manufacturers Association, (EJMA) 9th edition, **2008**.